Electromagnetic Science
vol. 2, no. 2, 0060521, June 2024
https://doi.org/10.23919/emsci.2023.0052

Review

Antenna Design for Modern Mobile Phones: A Review

Yan Wang[1], Libin Sun[2], Zhengwei Du[3], and Zhijun Zhang[3]

1. *Key Laboratory for Information Science of Electromagnetic Waves* (*MoE*), *School of Information Science and Technology*, *Fudan University*, *Shanghai 200433*, *China*
2. *Shanghai Huawei Technologies*, *Ltd.*, *Shanghai 201206*, *China*
3. *Beijing National Research Center for Information Science and Technology*, *Department of Electronic Engineering*, *Tsinghua University*, *Beijing 100084*, *China*

Corresponding authors: Libin Sun, Email: sunlibin0624@163.com; Zhijun Zhang, zjzh@tsinghua.edu.cn.
Received January 2, 2024; Accepted March 8, 2024; Published Online May 28, 2024.

Abstract — Due to limited antenna space, high communication requirements, and strict regulatory constraints, the design of antennas for modern mobile phones has become an exceedingly challenging task. In recent years, numerous studies have been conducted in this area, leading to significant advancements. This review paper comprehensively summarizes recent progress made in antenna design for modern mobile phones. Firstly, the challenges faced in antenna design for modern mobile phones are described, including bandwidth enhancement, integration and decoupling techniques, mm-wave array antennas, satellite communication antennas, as well as interactions between mobile antennas and the human body. Secondly, the basic antenna types (such as inverted-F, slot, loop, and planar inverted-F antennas) commonly used in modern metal-bezel mobile phones along with their key characteristics are briefly summarized. Thirdly, the commonly exployed methods used in practical applications for designing wideband antennas within compact sizes and achieving decoupling among multiple antennas with wide bandwidths are collected. Fourthly, recent advances in the design of compact, wideband, and wide-angle scanning mm-wave arrays for modern mobile phones are summarized. Fifthly, recent progress made in satellite communication antenna designs for modern mobile phones, including broadside and end-fire radiation patterns, is presented. Sixthly, recent studies on the interaction between mobile antennas and the human body are briefly concluded. Finally, the future challenge of antenna design for mobile phones is briefly discussed. It is our hope that this comprehensive review will provide readers with a systematic understanding of antenna design principles applicable to modern mobile phones.

Keywords — Mobile antenna, Bandwidth, Decoupling, mm-Wave antenna, Satellite communication antenna, Specific absorption rate.

Citation — Yan Wang, Libin Sun, Zhengwei Du, *et al*., "Antenna design for modern mobile phones: a review," *Electromagnetic Science*, vol. 2, no. 2, article no. 0060521, 2024. doi: 10.23919/emsci.2023.0052.

I. Introduction

Mobile phones, which are capable of performing a wide range of functions, such as phone calls, video calls, navigation, Internet searches, social media apps, banking, and car control, have become essential tools in people's daily lives. Furthermore, mobile phones are an emerging trend in science and technology with 75% of the world's population projected to have mobile connectivity by 2030 [1]. As illustrated in Figure 1, the number of worldwide mobile phone shipments is forecasted by the International Data Corporation (IDC) to exceed 1200 million per year for the next five years [2]. Currently, each person on Earth possesses more than one mobile phone on average.

The antenna, being an essential component of mobile phones, significantly impacts the user's experience. Since the invention of mobile phones in the 1980s, antennas for mobile phones have been extensively studied by the academic and industrial communities. The mobile antenna has evolved from an external sleeve dipole antenna (such as the mobile antenna in the Motorola DynaTAC 8000X phone [3]), to an external monopole antenna (such as the mobile antenna in the Motorola MicroTAC9800X phone [4]), to an internal patch antenna (such as mobile antenna in the Nokia 3210 phone [5]), and to the present integrated metal-bezel antenna (such as the mobile antenna in the Apple iPhone 5 phone [6]). The major design requirement of the mobile antenna is to integrate the antenna into a mobile phone which can satisfy the radiation specification, such as frequency coverage, antenna efficiency, radiation pattern, specific absorption rate (SAR), hearing aid compatibility (HAC), electromagnetic compatibility (EMC).

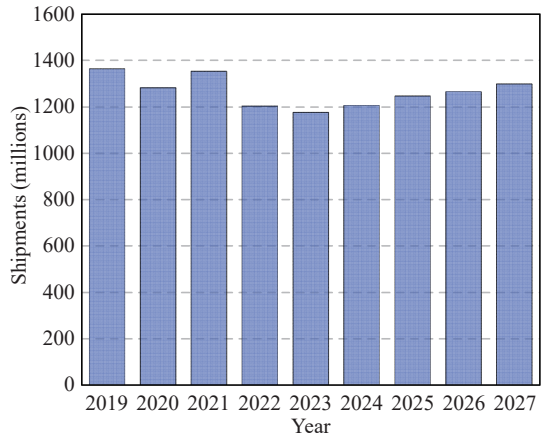

Figure 1 Worldwide mobile phone shipments forecast [2].

To study mobile antennas comprehensively, Reference [7] is a recommended book that presents the history, fundamental theory, key methods, typical designs, MIMO technology, practical applications, passive and active measurements, and regulations of mobile antennas in detail. Additionally, the book chapters in [8], [9] give a generalized description of the mobile antenna. In addition, a review article [10] mainly discusses the design concepts of the external antenna for mobile phones before 2000, such as improving the antenna's performance, making the antenna size small, and reducing the SAR. The review article [11] gives a survey of internal patch antennas in mobile phones from 1997 to 2010 on the antenna types, feeding structures, active antennas, isolation, loading techniques, manufacturing technologies, SAR, etc. Additionally, a review article [12] addresses the internal multi-band antennas from 1997 to 2012, discussing antenna types, multi-band design, bandwidth-enhanced design, MIMO antenna, 4G LTE antenna, industry requirements, etc. The book [7], book chapters in [8], [9], and review articles [10]–[12] provide a comprehensive understanding of the antenna design for the 1G, 2G, 3G, and 4G mobile phones.

Coming to the present 5G era, the mobile antenna design has faced a greater challenge due to the limited antenna space and an increasing number of design specifications. The design environment of the display, cameras, battery, speaker, printed circuit board (PCB), universal serial bus (USB) port, etc., the design requirements of the multiple frequency bands, multiple antennas with high isolation, high efficiency, mutual coupling effect, etc., and the design concepts of antenna types, common mode (CM) and differential mode (DM) theory, 5G NR MIMO antenna design, millimeter-wave antenna-in-package (AiP) module, etc. are briefly stated in [13]. In addition to the design environment, the typical designs of 5G sub-6GHz antennas and 5G mm-wave antennas are briefly sketched in [14]. In this review paper, we provide a comprehensive review of antenna design for modern mobile phones, including design challenges, basic antenna types, key techniques, and future challenges.

This review paper is organized as follows. Section II summarizes the five main design challenges of modern mobile antennas. Section III presents the main characteristics of modern mobile antennas for metal-bezel mobile phones. Section IV discusses the commonly used techniques for designing a wide/multi-band mobile antenna within a compact size. Section V discusses the commonly used techniques for designing a wideband MIMO antenna with high isolation. Section VI summarizes recent advances in the design of mm-wave antenna-in-package (AiP) for modern mobile phones. The design of a satellite communication antennas for modern mobile phones is presented in Section VII. Section VIII briefly describes the recent processes involved in the interaction between mobile antennas and the human body. The future challenge of mobile antenna design is prospected in Section IX. Finally, Section X concludes this review paper.

II. Requirements and Challenges in Antenna Design for Modern Mobile Phones

1. Requirements

The design of mobile antennas requires a comprehensive consideration of industrial design (ID) and architecture, communication specifications, user experience, human body impact, and legal requirements, which constitutes a complicated system engineering process. As shown in Figure 2, these diverse requirements form a triangular relationship, and mobile antenna engineers need to find a balance to achieve an optimal design of products.

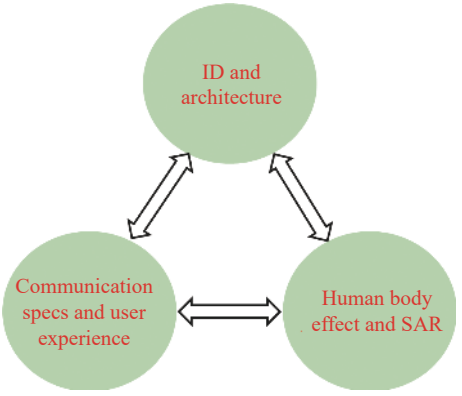

Figure 2 Triangular relationship of antenna design in modern mobile phones.

Currently, with the improvement of communication requirements and the evolution of communication specifications, the number of antennas in smartphones has reached 20–30 (as depicted in Figure 3), including the following antennas:

– Four antennas for LB (low band): 698–960 MHz;

– Four antennas for MHB (mid- and high-band) MIMO operation: 1710–2690 MHz;

– Four antennas for 5G New Radio (NR) band MIMO operation: 3300–4200 MHz & 4400–5000 MHz;

– Two or more dual-band millimeter-wave AiP antennas: 24.25–29.50 GHz and 37.00–43.50 GHz;

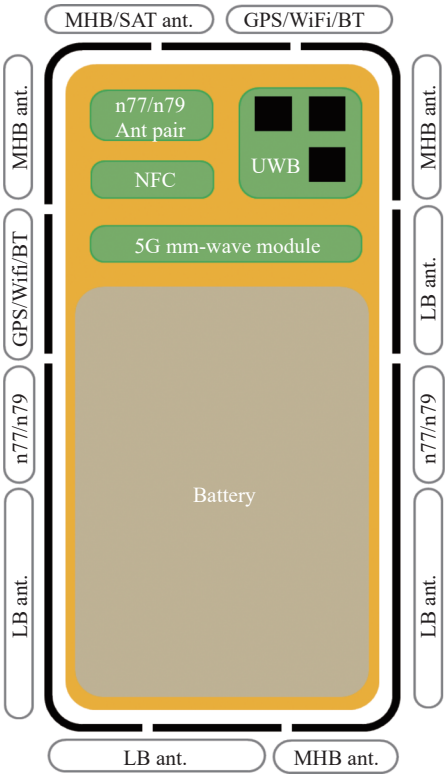

Figure 3 Conceptual diagram of the antennas in modern mobile phones.

– One or more satellite communication antennas: the operating band is the L- or S-band;

– Two GNSS (global navigation satellite system) antennas: GPS L5 at 1176 MHz and GPS L1 at 1575 MHz;

– Two to four tri-band WiFi (wireless fidelity) and BT (Bluetooth) antennas: 2400–2484 MHz, 5150–5350 MHz, and 5725–5825 MHz;

– One NFC (near field communication) antenna: 13.56 MHz;

– Three UWB (ultra-wideband) antennas: 6240–6740 MHz and 7750–8250 MHz.

To fully demonstrate the antenna design requirements, Table 1 summarizes the frequency range, main specifications, key figures, and number of antennas for different communication standards. For the 2G and 3G communication systems, the mobile antenna should cover the 824–960 MHz and 1710–2400 MHz frequency bands. For flagship mobile phones, two 2G/3G antennas are usually selected for the best performance. The key figure of the antenna is its efficiency. High efficiency associated with high communication quality. For the 4G LTE and 5G Sub–6GHz communication systems, the mobile antenna should cover the 704–960 MHz and 1710–2690 MHz frequency bands for 4G LTE operation and 3300–4200 MHz / 4400–5000 MHz frequency bands for 5G sub–6GHz operation. Four antennas are usually deployed on a mobile phone for MIMO operation. In addition to efficiency, the isolation and envelope correlation coefficient (ECC) among each antenna element are also key figures [7]. High isolation and low ECC result in a high system capacity. For the 5G mm-wave, the mobile antenna should cover the 24.25–29.50 GHz / 37.00–43.50 GHz frequency bands. Mobile phones usually contain 2 to 3 mm-wave AiP modules for larger spherical coverage. According to [15] and [16], the spherical coverage is evaluated by the CDF (convolutional distribution function) of the EIRP (effective isotropic radiated power). The EIRP is calculated from the array gain and the RF power. For satellite communication, the mobile antenna should cover the L- and S-bands with the characteristics of high gain and circular polarization [17].

For the GNSS system, the flagship mobile phones usually have two GPS antennas, one for GPS L1 band and the other for GPS L5 band. Despite the efficiency, the upper-hemisphere gain is also a key figure to evaluate GPS antenna performance. The WiFi/BT antenna, should cover the 2.4–2.484 GHz and 5.15–5.875 GHz frequency bands. Two antennas are usually used for MIMO operation. The efficiency, isolation, and ECC are key figures for WiFi antennas. The NFC is a short-range communication standard whose operation frequency is 13.56 MHz. The card reading distance is the key parameter of the NFC antenna. References [18]–[20] proposed three NFC antennas with good performance. UWB positioning technology is a new function of mobile phones that works at the 6240–6740 MHz and 7750–8250 MHz frequency bands. The UWB usually uses a three-element antenna array for the position function. The key figures of the UWB are the efficiency and the phase center. Reference [21] proposed a dual-band circular-polarized microstrip antenna array for UWB applications. In addition to the antenna efficiency, the over-the-air (OTA) per-

Table 1 Frequency range, main specifications, key figures, and the antenna number of the mobile antenna for different communication standards

Communication standards	Frequency range	Main specifications	Key figures	Number of antennas
2G/3G	824–960 MHz / 1710–2400 MHz	Antennas selection	Efficiency	2
4G LTE	704–960 MHz / 1710–2690 MHz	MIMO	Efficiency, ECC, and isolation	4
5G Sub-6GHz	3300–4200 MHz / 4400–5000 MHz	MIMO	Efficiency, ECC, and isolation	4
5G mmW	24.25–29.50 GHz / 37.00–43.50 GHz	AiP module	Coverage, EIRP	2–3
Satellite	L-band / S-band	–	Gain, polarization, coverage	1
GNSS	1.176 GHz / 1.575 GHz	GPS L1&L5	Efficiency, upper-hemisphere gain	2
WiFi/BT	2.4–2.484 GHz / 5.15–5.875 GHz	MIMO	Efficiency, isolation, ECC	2
NFC	13.56 MHz	–	Card reading distance	1
UWB	6240–6740 MHz and 7750–8250 MHz	Antenna array	Efficiency, phase center	3

formance is a system level performance of mobile antennas, including the total radiated power (TRP) and total isotropic sensitivity (TIS) [7]. The TRP, which is used to evaluate a phone's performance when served as a transmitter, is defined as the conductive power plus with the antenna efficiency. The TIS, which is used to evaluate a phone's performance when served as a receiver, is defined as the conductive sensitivity plus with the antenna efficiency.

Because of the constraints of ID and architecture, the design space of mobile antennas is very limited. To achieve more effective power radiation in extremely limited environments, important antennas are generally designed on the metal bezel of mobile phones. Additionally, in practical products, the display, cameras, battery, speaker, printed circuit board (PCB), universal serial bus (USB) port, etc., should also be considered [14]. In [22], a 4G LTE antenna covering the 824–960 MHz and 1710–2690 MHz frequency bands considered all the necessary components, such as the front-facing camera, dual back-facing camera, receiver, screen, and steel sheet. Additionally, the effect of the USB connector, LCD, battery, speaker, camera, and microphone on the antenna performance is studied in [23]–[25].

2. Challenges

For modern mobile phones, under the ID of the metal bezel and full screen, the antenna design has only a small clearance of less than 1 mm, so we need to resolve the contradiction between antenna size and performance. In addition, considering the absorption of the antenna by the human body and the regulatory constraints of the antenna radiation on the human body, the design rule for different antennas will be greatly restricted. Therefore, the main technical challenges facing for the antenna design of modern mobile phones are listed below.

1) Antenna size and bandwidth enhancement

The size and bandwidth of small antennas are fundamentally constrained by the Chu-limit [26], [27] and substantial advancements to overcome these constraints remain elusive. However, for modern mobile phones, space is mainly reserved for large display, large battery, an increasing number of cameras, larger speakers, PCBs, etc., and the space available for antenna design is extremely limited. In addition, the number of antennas is continuously increasing, so as to each antenna could only occupy a small space. Therefore, designing a compact mobile antenna with a wide bandwidth and high efficiency is a large technical challenge.

2) Integration and decoupling of multiple antennas

As mentioned before, the number of antennas in modern mobile phones has reached 20–30 now and will be further increased in the future, and it will be difficult to design so many independent antennas in such a limited mobile phone environment. Consequently, many antennas need to coexist with a small spacing due to system requirements, thus, decoupling between these same-band or adjacent-band antennas is a technical challenge and a must for modern mobile phones. Moreover, how to integrate multiple antennas into one antenna branch is also an important technique that needs to be studied for the miniaturization of modern mobile antennas.

3) Millimeter-wave antenna design

The design of millimeter-wave antennas in mobile phones completely differs from that of traditional sub-6 GHz mobile antennas. It utilizes the phased-array AiP module to achieve high-gain beam scanning. The challenge in designing millimeter-wave mobile phone antennas is to achieve wide-angle scanning across two wide frequency bands (i.e., 24.25–29.50 GHz and 37.00–43.50 GHz) while maintaining compatibility with the ID and architecture of mobile phones.

4) Satellite communication antenna design

To satisfy the communication requirements of areas where network coverage is absent, a growing number of modern mobile phones will accommodate direct satellite-to-handset communication. Given the considerable distance between satellites and the Earth's surface, mobile phones are required to employ high transmission power and high-gain antenna technology to meet the EIRP criteria for effective communication. Furthermore, because all spaceborne antennas utilize circularly-polarized antennas, it is advantageous for mobile antennas to adopt a circularly-polarized configuration to mitigate polarization loss in communication links. Consequently, the design of high-gain circularly polarized antennas represents a new technical challenge for modern mobile antenna engineering.

5) Interaction between antennas and the human body

Unlike other antennas, mobile antennas strongly interact with the human body. The antennas designed in the lower and upper regions of a mobile phone are affected by the hand grip and the head, respectively. Therefore, we need to investigate the human body absorption effect of different antennas to reduce the antenna efficiency drop when the human body is close to the antennas and also reduce the specific absorption rate (SAR) of the antenna to meet the legal requirements.

III. Antenna Type, Basic Geometry, and Main Characteristics

For modern mobile phones, metal-bezel mobile phones have become mainstream. To conform to modern metal-bezel mobile phones, the main antenna types of modern mobile antennas are inverted-F antennas (IFAs), slot antenna, loop antennas, and planar inverted-F antennas (PIFAs). The IFA, slot antenna, and loop antenna can integrate with the metal bezel of the mobile phone while the PIFA is mainly located on the back cover of the mobile phone. The working principle of these antennas has been well analyzed in [7]. Here, we briefly state their major antenna characteristics, including the geometry, impedance, modes, and potential bandwidth.

1. Inverted-F antenna (IFA)

As shown in Figure 4(a), the basic geometry of the IFA has a shorting end at point A and an opening end at point B. The IFA is fed at point C. The branch AC between shorting

point A and feeding point C functions as a shunt-distributed inductor. The branch AB can integrate with the metal bezel of the mobile phone. The distance between branch AB and the ground plane is the antenna clearance G. As shown in Figure 4(b), the three main resonant frequencies within the 0.5–5 GHz frequency band are located at 0.82, 2.65, and 4.50 GHz. In addition, Figure 4(c) depicts that, as the antenna clearance G decreases, the potential −6 dB impedance bandwidth decreases considerably. Additionally, the antenna potential bandwidth is narrow in the lower frequency band. Figure 4(d) shows that, the current distribution at 0.82 GHz, which reaches the maximum value at point A and the minimum value at point B, is the 1/4-wavelength mode of branch AB. Additionally, Figures 4(e)–(f) shows that, the current distributions at 2.65 and 4.50 GHz are the 3/4-wavelength mode and 5/4-wavelength mode of branch AB, respectively. Therefore, an IFA usually has 1/4-, 3/4-, and 5/4-wavelength modes.

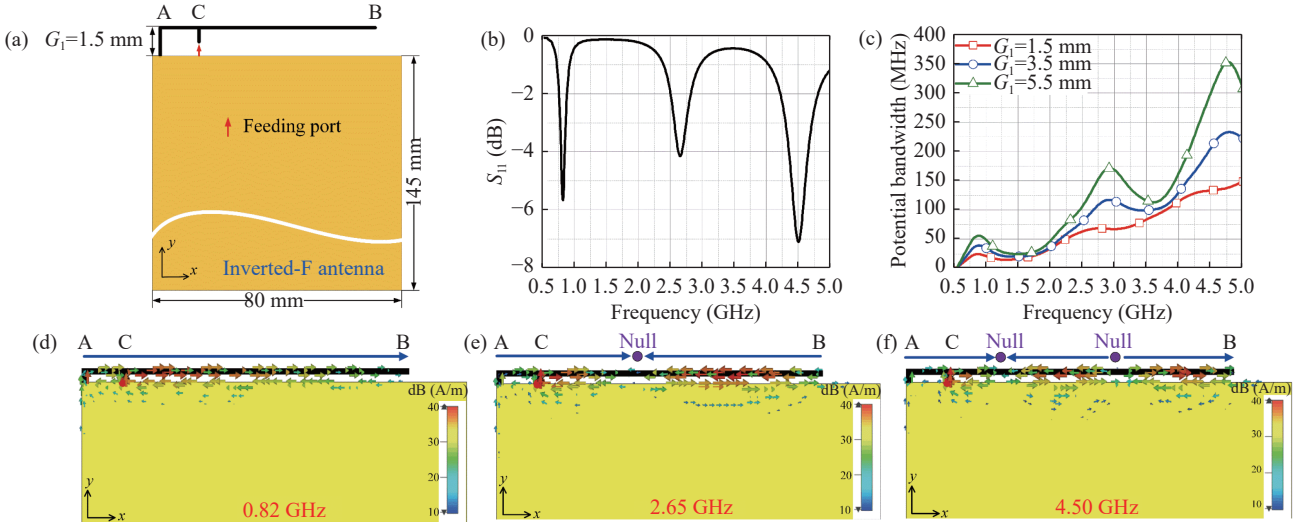

Figure 4 Characteristics of the inverted-F antenna (IFA). (a) Antenna structure; (b) Simulated S_{11}; (c) Simulated potential −6 dB impedance bandwidth with different values of antenna clearance G; (d)–(e) Simulated surface current distributions at (d) 0.82 GHz, (e) 2.65 GHz, and (f) 4.50 GHz.

2. Slot antenna

The two main types of slot antennas are closed slot antennas and opened slot antennas. Their basic geometry is shown in Figure 5(a). The closed slot antenna has two shorting ends at points A and B and is fed at point C. The opened slot antenna, which is fed at point C, has a shorting end at point A and an opening end at point B. Note that, for the modern mobile antenna, the slot antenna is usually deployed at the edge of the main ground for the display. The branch AB can integrate with the metal bezel of the mobile phone. The width of slot G is the antenna clearance. The opened slot antenna, which evolved from a closed slot antenna with a half size, is similar to the IFA antenna. Here, we only present the characteristics of the closed slot anten-

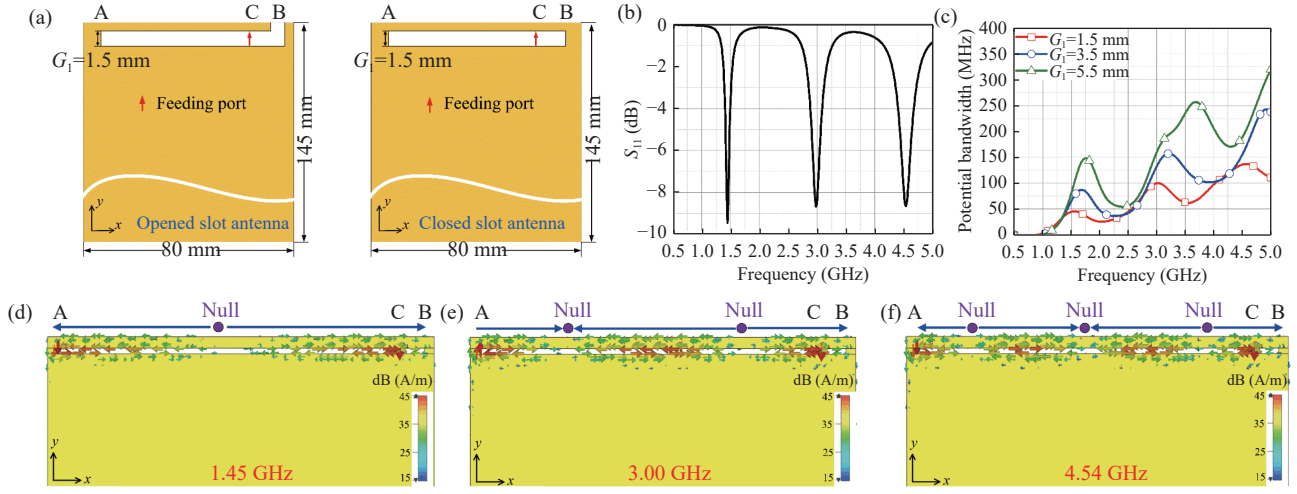

Figure 5 Characteristics of the slot antenna. (a) Antenna structure; (b) Simulated S_{11} of the closed slot antenna; (c) Simulated potential −6 dB impedance bandwidth with different antenna clearance G of the closed slot antenna; (d)–(f) Simulated surface current distributions of closed slot antenna at (d) 1.45 GHz, (e) 3.00 GHz, and (f) 4.54 GHz.

na. As shown in Figure 5(b), the three main resonance frequencies within the 0.5–5 GHz frequency band are located at 1.45, 3.00, and 4.54 GHz. Figure 5(c) shows that the potential −6 dB impedance bandwidth decreases consistently with the decreasing of antenna clearance. Figure 5(d) shows that the current distribution at 1.45 GHz, which reaches the maximum value on the two sides and the minimum value in the middle, is the 1-wavelength slot mode. Additionally, Figures 5(e)–(f) shows that the current distributions at 3.00 and 4.54 GHz are the 2-wavelength and 3-wavelength slot modes, respectively. Therefore, the closed slot antenna has 1-, 2-, and 3-wavelength modes.

3. Loop antennas

The basic geometry of the loop antenna, which is shown in Figure 6(a), has an unbroken branch with a feeding point and a shorting point at points A and B, respectively. The feeding point and shorting point connect to the ground directly. In practical applications, the branch EF can integrate with the metal bezel, and the branches AE and BF can be realized using a flexible printed circuit (FPC) or laser direct structuring (LDS) structure. The distance between the branch EF and the ground is the antenna clearance. As shown in Figure 6(b), the six resonant frequencies within the 0.5–5 GHz frequency band are located at 1.07, 1.51, 1.75, 2.67, 3.92, and 4.53 GHz. Figure 6(c) shows that the potential −6 dB impedance bandwidth of the loop decreases considerably as the antenna clearance decreases. Figure 6(d) shows that the current distributions at 1.07 GHz, which reach the maximum values at the feeding and grounding points and have one minimum value on the branch, are in the 0.5-wavelength loop mode. Additionally, Figures 6(e)–(i) shows that the current distributions at 1.51, 1.75, 2.67, 3.92, and 4.53 GHz are in the 1.0-, 1.5-, 2.0-, 2.5-, and 3.0-wavelength loop modes, respectively. Therefore, the loop antenna has more resonant modes than the IFA and slot. Accordingly, the loop antenna occupies a larger space.

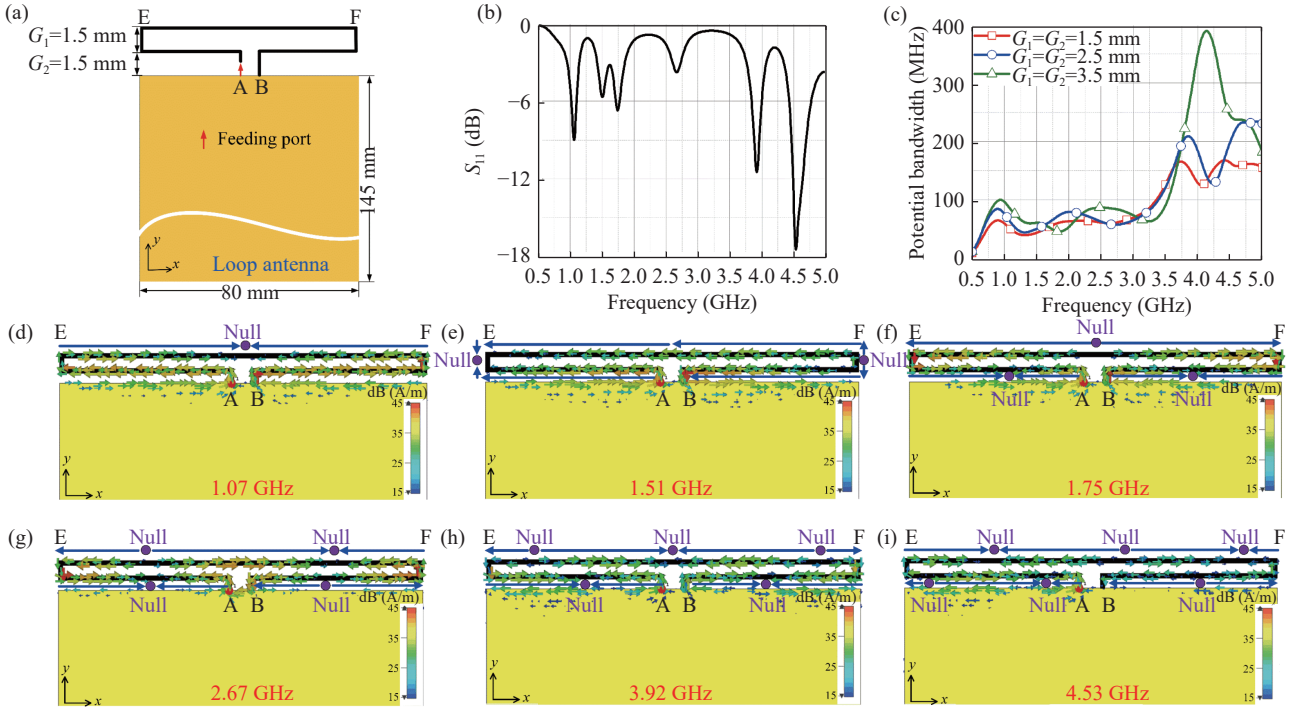

Figure 6 Characteristics of the loop antenna. (a) Antenna structure; (b) Simulated S_{11}; (c) Simulated potential −6 dB impedance bandwidth with antenna clearance G_1 and G_2; (d)–(i) Simulated surface current distributions at (d) 1.07 GHz, (e) 1.51 GHz, (f) 1.75 GHz, (g) 2.67 GHz, (h) 3.92 GHz, and (i) 4.53 GHz.

4. Planar inverted-F antenna (PIFA)

The geometry of a common PIFA is shown in Figure 7(a). The PIFA usually has a patch on a PCB ground with a feeding pin and a grounding pin. The grounding pin functions as a shunt inductor that can be replaced by a lumped inductor. The height G between the patch and the ground greatly affects the antenna performance. The working principle and design method of the PIFA have been well addressed in [7] and [28]. For modern mobile antennas, the PIFA, which is usually located at the back cover of the mobile phone, is mainly applied to work as a 4G LTE MHB or 5G sub-6GHz MIMO antennas because of its inferior efficiency. As illustrated in Figure 7(b), the four resonant frequencies within the 0.5–5 GHz frequency band are located at 0.74, 2.65, 3.31, and 4.57 GHz. Figure 7(c) shows that the potential −6 dB impedance bandwidth of the PIFA also decreases considerably with increasing height. Figures 7(d)–(g) shows that the current distributions at 0.74, 2.65, 3.31, and 4.57 GHz are the 0.25-, 0.5-, 0.75-, and 1.0-wavelength PIFA modes, respectively.

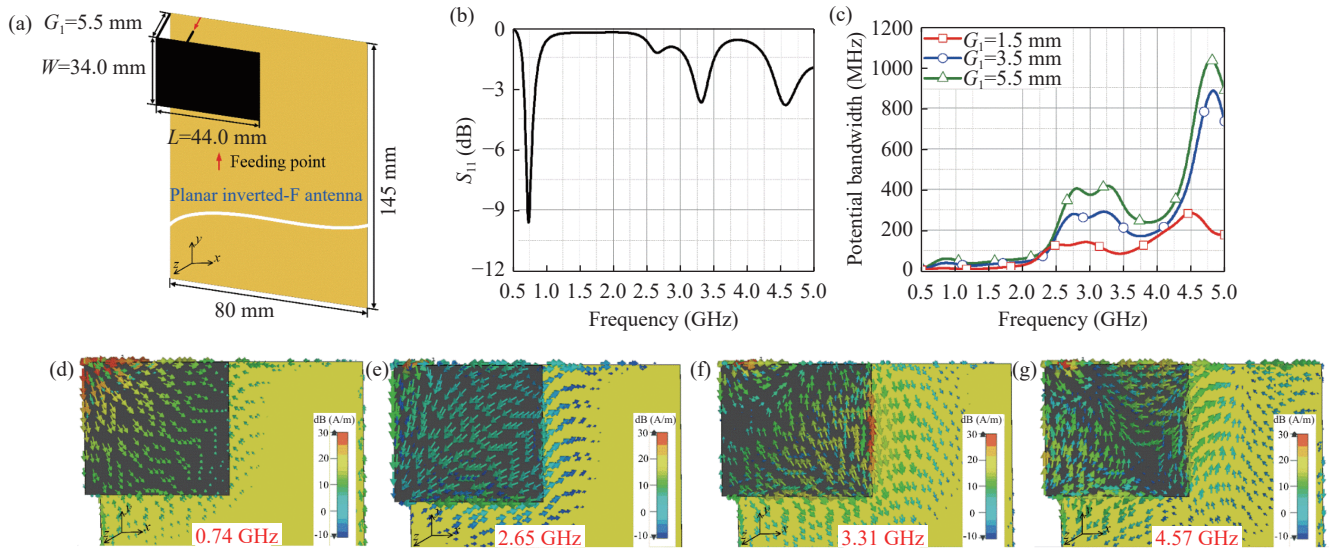

Figure 7 Characteristics of the planar inverted-F antenna (PIFA). (a) Antenna structure; (b) Simulated S_{11}; (c) Simulated potential −6 dB impedance bandwidth with different antenna height G; (d)–(g) Simulated surface current distributions at (d) 0.74 GHz, (e) 2.65 GHz, (f) 3.31 GHz, and (g) 4.57 GHz.

IV. Design of the Compact and Wide/Multi-Band Mobile Antenna

As mentioned before, the antenna space in modern mobile phones is extremely limited. Designing a wideband or multi-band mobile antenna within a compact size is always a challenge for antenna designers. The commonly used methods for reducing the antenna size and widening the antenna bandwidth are briefly summarized as follows.

1. Miniaturization

Antenna miniaturization refers to reducing the antenna size without changing the resonant frequency, or lowering the antenna resonant frequency without changing the antenna size. The commonly used methods for antenna miniaturization are listed below.

1) Loading material with a high permittivity or permeability

An antenna always resonates at a fixed guided wavelength. Therefore, a straightforward method is to use a material with high permittivity or permeability to reduce the guided wavelength [29]–[31]. As shown in Figure 8(a), with the use of a new ceramic material in [29], the antenna size has been reduced by 22%. Additionally, as shown in Figure 8(b) by utilizing the magneto-dielectric material in [30] as the antenna substrate, the antenna size can be reduced. Material loading can effectively reduce the size of the antenna, which has been used in practical commercial mobile phones. However, these new materials are generally more expensive and increase the cost of the antenna.

2) Meander line

As the antenna resonates at a fixed guided wavelength, another effective method is to bend the trace of the antenna branch within a fixed space. Thus, the antenna occupied space is reduced [32], [33]. In Figure 9, a folded loop antenna with a bending trace was proposed to reduce the occupied space [32]. The meander line has the attractive merit of flexibility. It is one of the most commonly used methods for reducing antenna size.

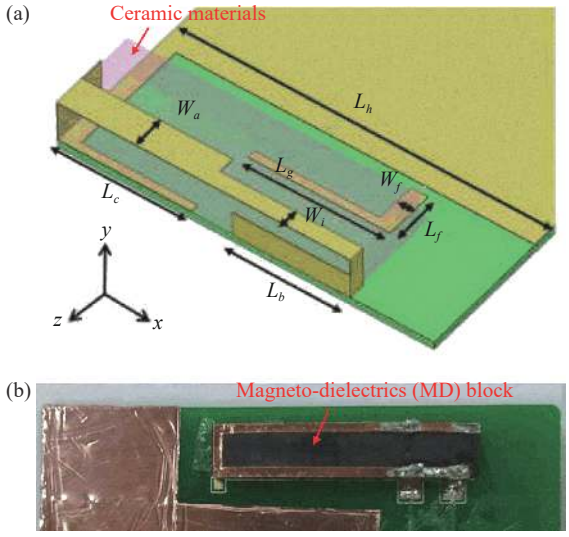

Figure 8 Material loading for miniaturization. (a) Loading ceramic materials with a high permittivity [29]; (b) Loading magneto-dielectrics with a high permittivity and permeability [30].

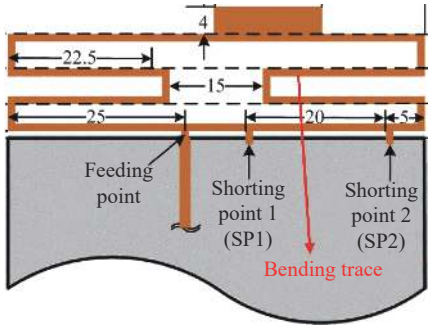

Figure 9 Meander line for miniaturization [32].

3) Loading inductor on the antenna branch

As a common knowledge, the capacitive reactance of

the antenna increases as the antenna size decreases. Therefore, loading inductor can mitigate the increased capacitive reactance for a compact antenna [34]–[36]. As shown in Figure 10(a), the length of the radiating branch of a monopole antenna is reduced from 0.25 to 0.17 wavelengths by loading a lumped inductor on the branch [34]. A distributed inductor can also replace the lumped inductor. As shown in Figure 10(b), with the help of the distributed inductor, the monopole antenna in [35] works well in the 0.17-wavelength mode. In practical design, loading inductor will increase the antenna quality factor and considerably reduce the antenna bandwidth.

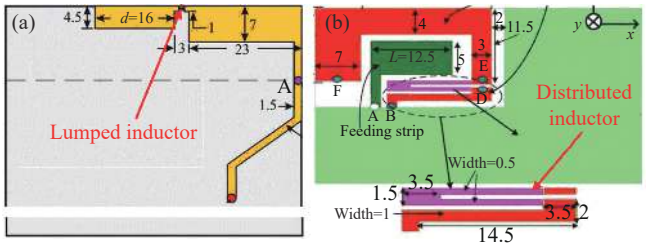

Figure 10 Inductor loading for miniaturization. (a) Lumped inductor loading [34]; (b) Distributed inductor loading [35].

4) Matching circuit

Using a matching circuit to match the antenna impedance at a lower frequency band is also a useful method for reducing the antenna size [37]–[43]. As it is illustrated in Figure 11(a), the resonance has been matched in the lower frequency band by applying a lumped-element matching circuit. Additionally, the lumped element in the matching circuit can be replaced by a distributed element. In [41], as shown in Figure 11(b), an F-shape strip serves as a distributed matching circuit to provide a lower frequency band within a compact size. In practical applications, the matching circuit method is widely used for mobile antenna design. However, lumped-element matching circuits might occupy part of the PCB space and introduce loss.

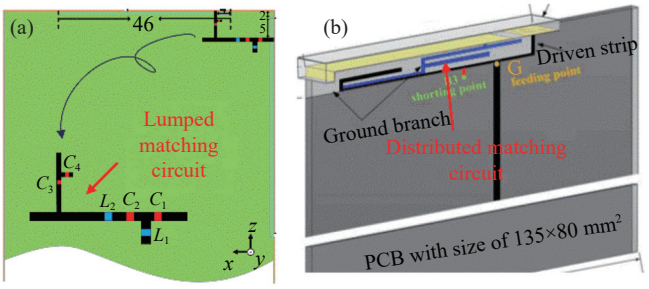

Figure 11 Matching circuit of miniaturization. (a) Lumped matching circuit [37]; (b) Distributed matching circuit [41].

2. Wideband/multi-band coverage

Wideband/multi-band coverage refers to the method of expanding the antennas' bandwidth within a limited space. The commonly used methods for wideband/multi-band coverage in modern mobile phones are listed below.

1) Widening the width of the antenna branch

It is common knowledge that widening the antenna width can smooth the surface currents of the resonant branches and thus reducing the Q factor and increasing the intrinsic bandwidth of the antenna [44], [45]. As shown in Figure 12(a), a folded metal plate is used to extend the width of the radiating branch, which effectively extends the intrinsic bandwidth of the monopole antenna [44]. As shown in Figure 12(b), the bandwidth of the single open-slot antenna in [45] is widened by increasing the slot width. In practical applications, using a metal bezel to design mobile antennas can be considered a method for widening the antenna width.

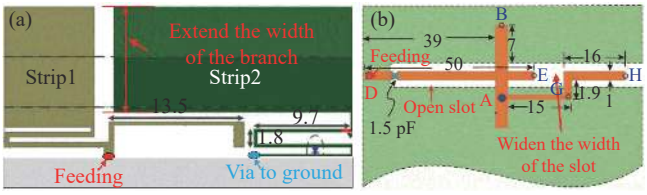

Figure 12 Widen the antenna width for bandwidth enhancement. (a) Widen the width of the branch [44]; (b) Widen the width of the slot [45].

2) Multiple modes and multiple branches

As previously studied, the IFA, slot antenna, loop an-

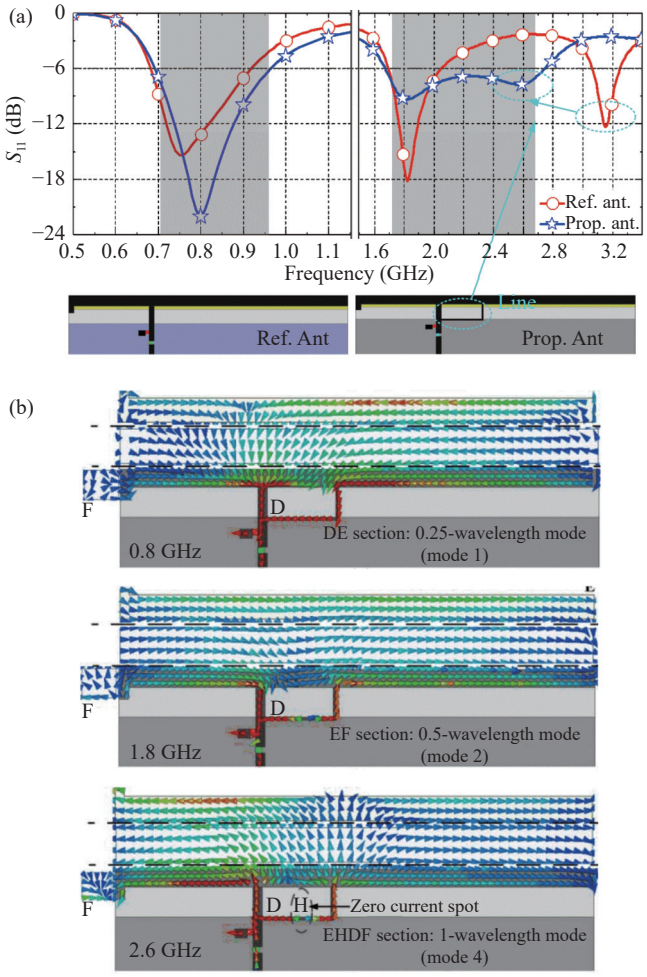

Figure 13 Multiple modes for bandwidth enhancement [46]. (a) Applying multiple modes and tuning line; (b) Simulated surface current distributions.

tenna, and PIFA have multiple modes located at different resonant frequencies. However, these resonant frequencies are usually outside the desired frequency band. In the open literature, many methods have been proposed to change the resonant frequency of one mode while keeping those of other modes unchanged [46]–[51]. As shown in Figure 13(a), a line is applied to change the resonant frequency of the third resonant mode while slightly affecting the resonant frequencies of the first two modes [46]. This phenomenon occurs because the line is located at the E-field minimum value of the third mode while the E-filed maximum value of the first two modes as shown in Figure 13(b). In practical applications, the method of controlling the resonant frequencies of some modes while keeping those of others unchanged is one of the most effective ways to cover the desired frequency band. The multiple modes method is widely used in commercial mobile phones.

As the antenna modes of one branch are limited, using multiple branches to cover multiple frequency bands is another effective method [52]–[58]. When multiple frequency bands are close together, wideband coverage is achieved. If multiple frequency bands are far apart, multi-band coverage is realized. As shown in Figures 14(a) and (b) in [53], by adding antenna branch CD to antenna branch AB, two resonant frequencies at 1.9 and 2.44 GHz are achieved, which can widen the antenna bandwidth. However, as shown in Figure 14(b), the added branch CD usually introduces a radiation efficiency local minimum, which greatly affects antenna performance. In [53], the method of using two different feeding phases on the two branches is applied to mitigate the radiation efficiency local minimum and enhance the antenna efficiency by 2.31 dB, as shown in Figure 14(c). Multiple branches method is also widely used in commercial mobile phones.

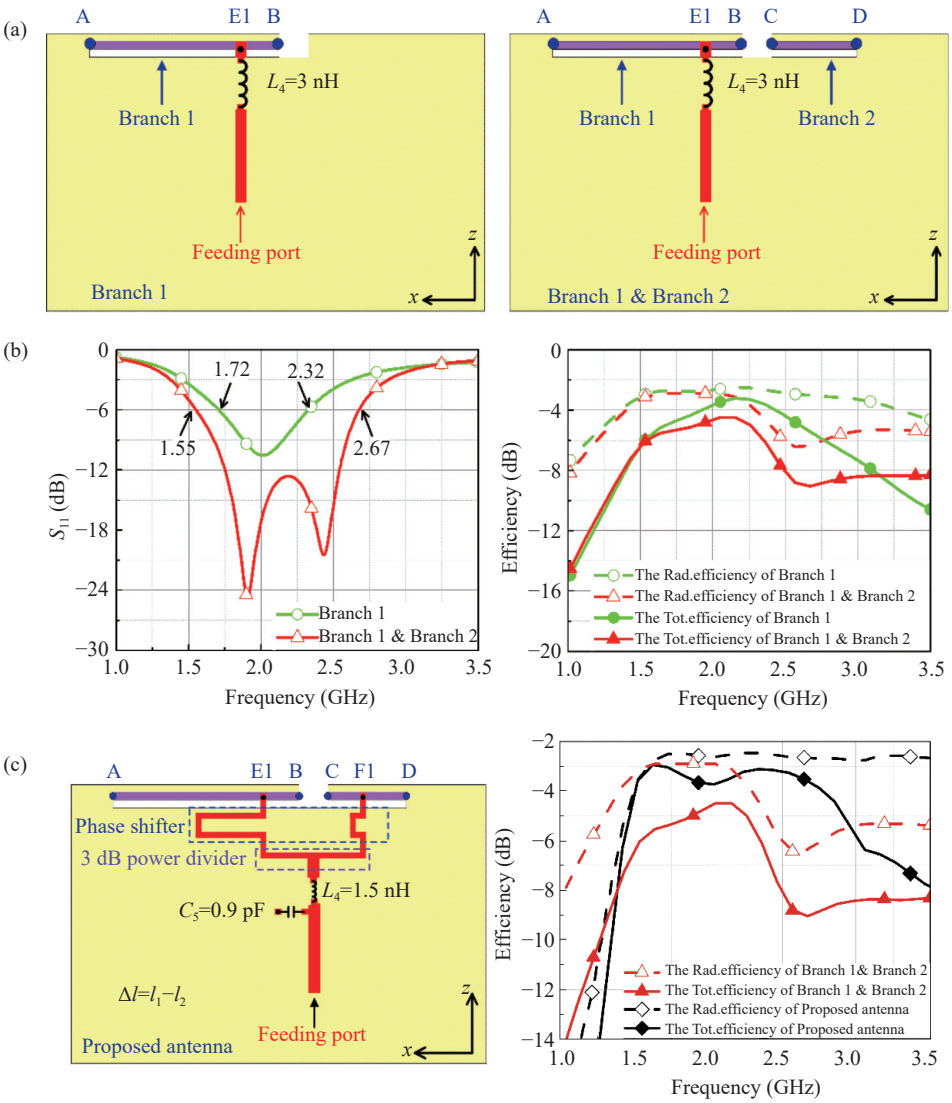

Figure 14 Multiple branches for bandwidth enhancement [53]. (a) Appling multiple branches; (b) The simulated S_{11} and efficiency[53]; (c) The method to improve the antenna efficiency.

3) Matching circuit

The matching circuit is another effective method for bandwidth enhancement. The desired impedance matching can be achieved with a matching circuit [59]–[64]. As

shown in Figure 15(a), the matching circuit with a lumped element is used to generate new resonant modes at 950 MHz, which effectively extends the bandwidth of the antenna in combination with the original antenna structure's resonant mode at 730 and 1030 MHz in [59]. As shown in Figure 15(b), the monopole antenna in [60] operates at 0.75 wavelength at 1740 and 2420 MHz. To broaden the antenna bandwidth, a short branch is used as a distributed inductor matching circuit to excite a new resonant mode at 2890 MHz. Matching circuits, which can simultaneously reduce the antenna size and extend the antenna bandwidth, are commonly used in practical designs.

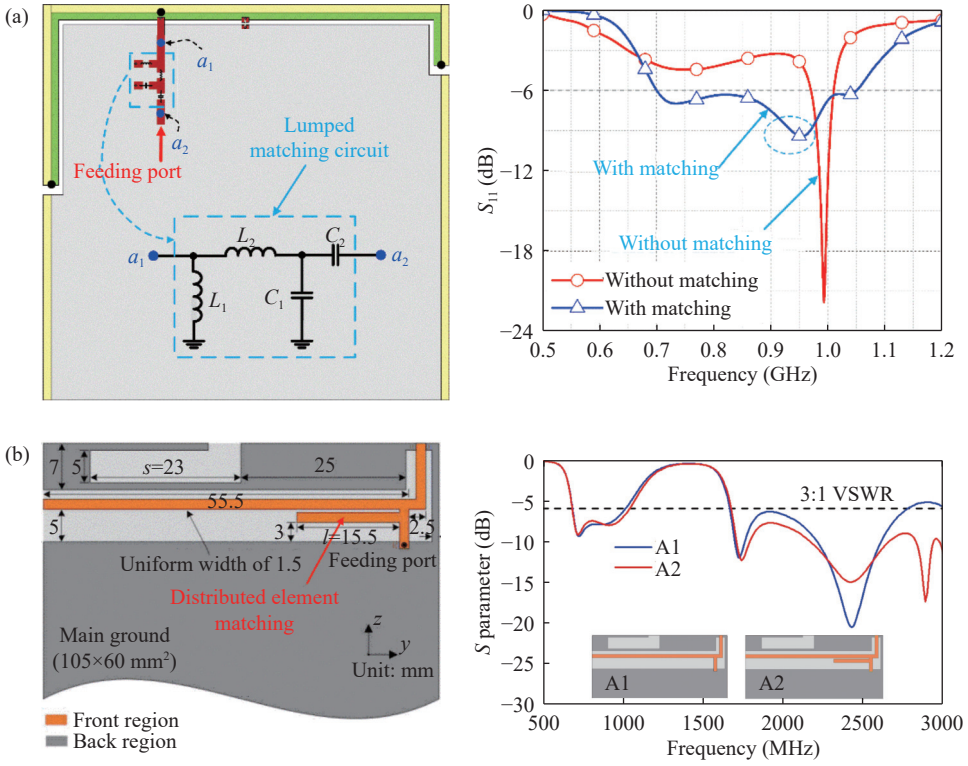

Figure 15 Matching circuit for wideband operation. (a) Matching circuit with lumped element [59]; (b) Matching circuit with distributed element [60].

4) The reconfigurable method

The reconfigurable method mainly uses PIN diodes, varactor diodes, 4 × single-pole-single-throw (4 × SPST) , and single-pole-four-throw (SP4T) switches, etc., to change the resonant frequency of each mode at different states [65]–[70]. Thus, although the intrinsic bandwidth is narrow, different frequency bands can be covered separately.

As shown in Figure 16(a) [65], the PIN diode is applied on the radiated branch. When the PIN diode is in the "OFF" state, the antenna operates in loop mode covering the 790–870 MHz and 1490–2225 MHz bands. When the PIN diode is in the "ON" state, the antenna operates in two IFA modes covering the 845–980 MHz and 2240–2565 MHz bands. Thus, multiple bands are covered. In [66], as shown in Figure 16(b), the resonant frequencies of the slot branch can be tuned by varying the capacitor of varactor diodes. Consequently, a wide frequency band can be covered separately. As shown in Figure 16(c), the reconfigurable antenna in [67] uses a 4 × SPST switch to provide three inductor states with different values for different paths, and changes the resonant frequency. Thus, the monopole antenna operating in 0.25-wavelength mode can cover the 704–960 MHz frequency bands with these three states. However, utilizing an RF switch usually introduces loss from the switch. To improve the antenna efficiency, an analysis of the RF switch and methods to reduce the loss of antenna efficiency were proposed in [67]. By applying the series inductor L_3 and shunt inductor L_6, the average efficiency within the 80 MHz band can be improved by 6%. In practical applications, the SP4T switch and the 4 × SPST switch are widely used, while PIN diodes are rarely applied. The SP4T switch and the 4 × SPST switch connect to the antenna branch with the inductor or the capacitor to tune different resonant paths or switch multiple modes of the same antenna structure. The design method of the switch and the method for reducing the loss from the switch are similar to [67] in Figure 16(c). Commercial flagship mobile phones might have 4–8 switches to cover different frequency bands.

V. Design of the Wideband High-Isolation MIMO Antenna

As mentioned before, MIMO technology has been widely adopted in modern mobile phones. The function and working principle of MIMO technology are well addressed in [7] and [71]. However, as the available space for modern mo-

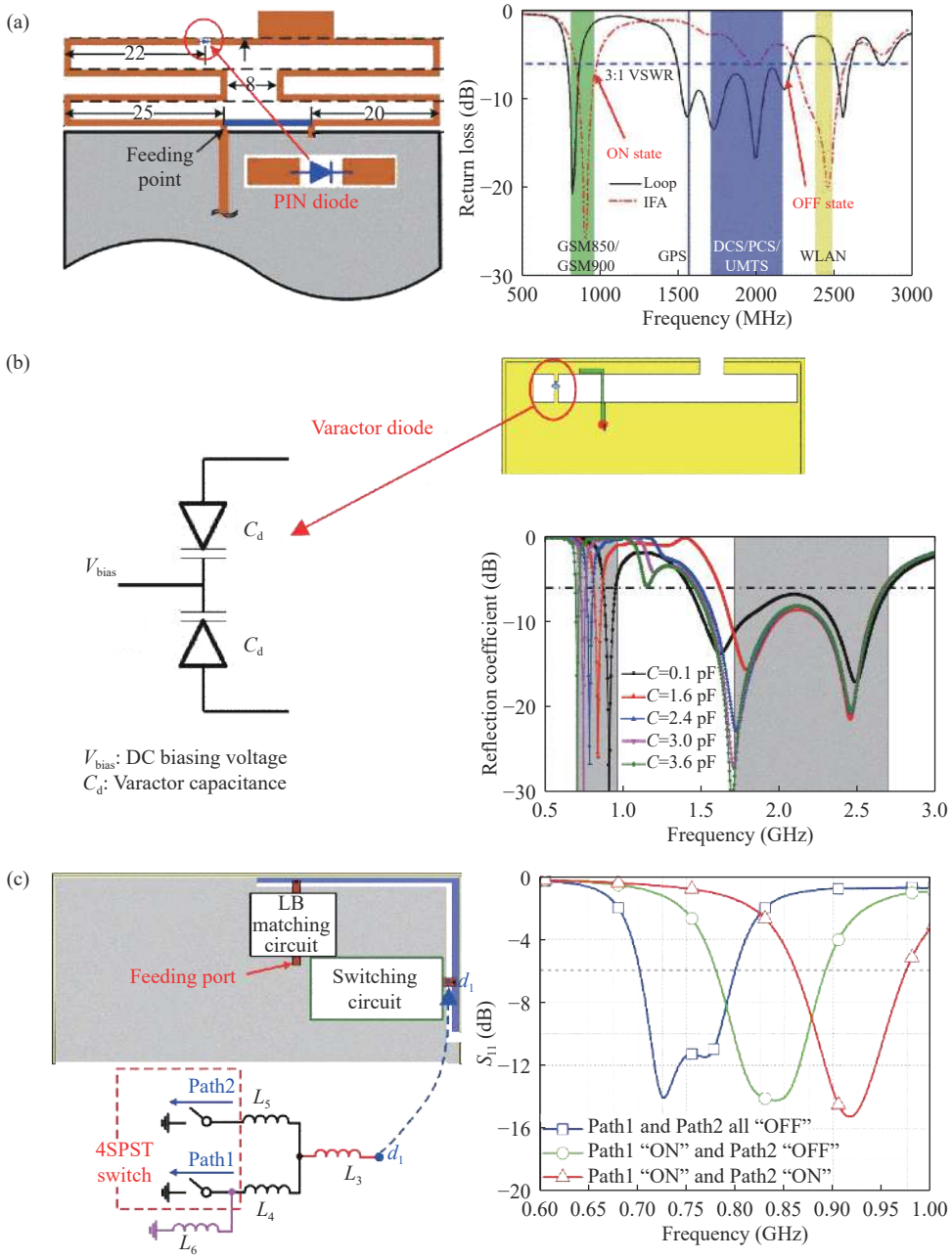

Figure 16 The reconfigurable method for bandwidth enhancement. (a) Loading PIN diodes [65]; (b) Loading varactor diode [66]; (c) Loading RF switches [67].

bile antennas becomes extremely limited and the number of antennas in mobile phones continues to increase, the spacing among each antenna element in modern mobile phones is continuously decreasing. Thus, the mutual coupling between each antenna is strong which results in poor antenna performance. Recently, many efficient techniques have been proposed to reduce mutual coupling, which is summarized below.

1. Spatial layout

The simplest method for achieving high isolation among two antenna elements is to increase their distance [72]–[74]. A larger distance usually results in greater isolation. As shown in Figure 17(a), eight antenna elements working at 3.5 GHz have a spacing of more than 19 mm. Thus, a high isolation of more than 17.5 dB is achieved. Another effective method is to select the element deployment that has the highest isolation [75], [76]. As shown in Figure 17(b), the orientations of the four elements are rotated to achieve better isolation. Additionally, high isolation is achievable if one antenna element (Ant 2) is located at the E-field null of another element (Ant 1) as shown in Figure 17(c) [77]. In practical applications, the deployment of mobile antennas is usually restricted by the system architectures of the mobile phones and the choice of the antenna position based on the antenna performance is not always available.

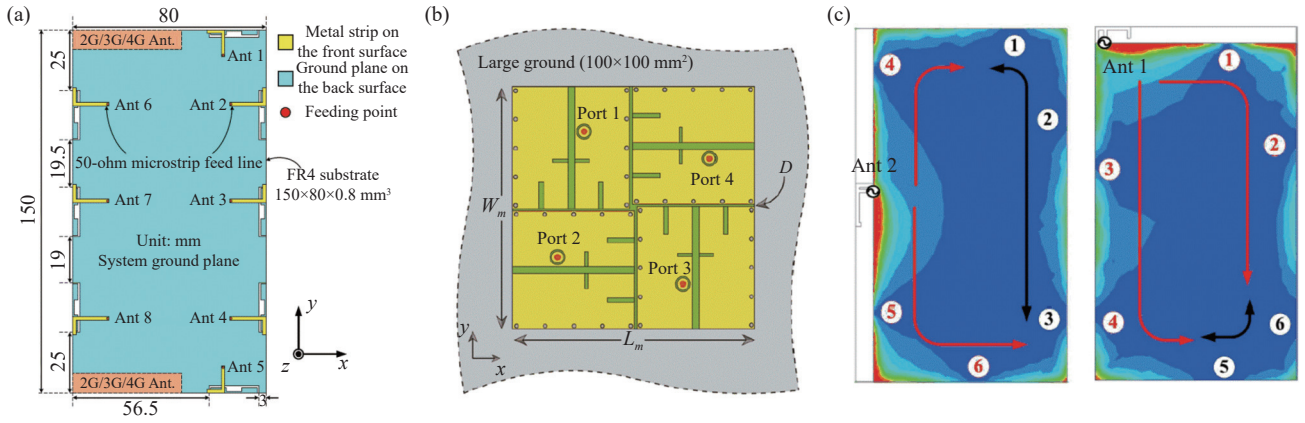

Figure 17 Decoupling method of spatial layout. (a) Enlarging the element distance [74]; (b) Rotating the element orientation [76]; (c) Putting one element (Ant 2) at the E-filed null of another element (Ant 1) [77].

2. Orthogonal mode

Two orthogonal modes are naturally irrelevant. If two antennas can excite two orthogonal modes, they will have high isolation. To the best of the authors' knowledge, reference [78] is the first open article that uses two orthogonal modes to design a high-isolation MIMO antenna for mobile phones. As shown in Figure 18(a), the two orthogonal polarizations and patterns are realized by the monopole antenna and the dipole antenna. In [79], two antenna elements (Ant 1 and Ant 2) can radiate two orthogonal radiation patterns, thus, a high isolation of 20 dB is achieved, as shown in Figure 18(b). Additionally, using two orthogonal chassis modes can also achieve high-isolation MIMO antennas [80]–[82]. As shown in Figure 18(c), two feeding ports excite two orthogonal chassis modes along the length and width directions, thus, an isolation of 7.5 dB is achieved within the LB band. Another effective method, which is shown in Figure 18(d), is to use two higher-order modes. The two higher-order modes can achieve high isolation by properly designing the in-phase and out-of-phase currents on the antenna. In engineering design, because of the small size of mobile phones, two wideband orthogonal modes are difficult to find at the lower frequency band.

3. Parasitic elements

A parasitic element, which is usually located between two exciting elements, can introduce a new mutual coupling to mitigate the original mutual coupling [84]–[86]. Thus, high isolation is achieved. To achieve good performance, the parasitic element should be resonant at the desired frequency band. Additionally, using multiple parasitic elements can achieve wideband isolation. For example, in [85], two parasitic elements can achieve a high isolation of 15 dB within the 1.7–2.7 GHz frequency band, as shown in Figure 19(a). To better control the original coupling and newly introduced coupling, the lumped element can be integrated into the parasitic element [87], [88], as shown in Figure 19(b). In addition to the two-element MIMO antenna, in [89], the parasitic element can also be applied to decouple the four-element array. As shown in Figure 19(c), the cross-line parasitic element can reduce the mutual coupling of a four-element array to −11 dB within the 3.3–5.0 GHz frequency band. Additionally, the parasitic element can work in the lower frequency band [90]–[92]. In [92], a folded dual inverted-shaped parasitic element is applied to decouple the two-element MIMO antenna to lower than −10 dB within the 698–974 MHz frequency band, as shown in Figure 19(d). Another interesting advantage of the parasitic element is that it can reduce the mutual coupling and widen the bandwidth simultaneously [85]. Because of the versatile functions of simultaneous decoupling and bandwidth enhancement, parasitic elements have been widely used in modern mobile antenna design for practical applications.

4. Decoupling network

A decoupling network, which is usually located at a PCB, comprises a decoupling unit and a matching unit [93]–[95].

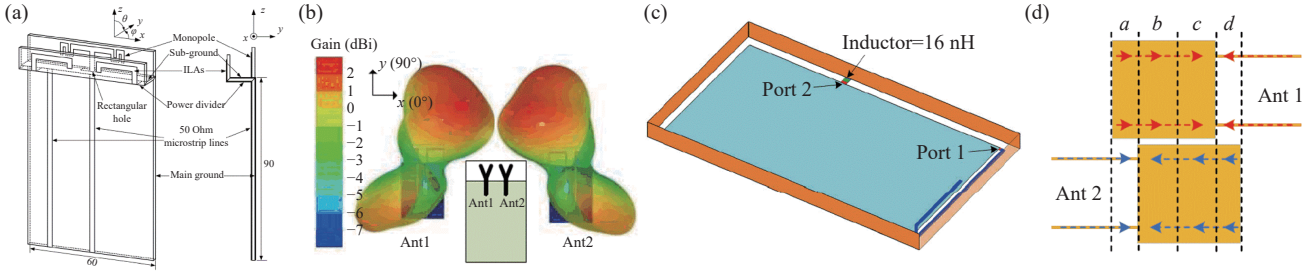

Figure 18 Decoupling method of an orthogonal mode. (a) Orthogonal polarizations and patterns [78]; (b) Orthogonal radiation patterns [79]; (c) Orthogonal chassis modes [82]; (d) Two higher-order modes [83].

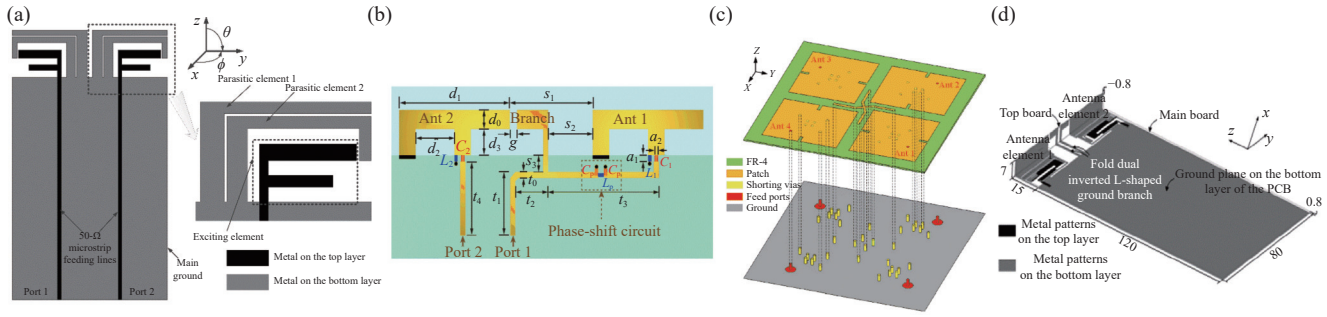

Figure 19 Decoupling method of parasitic element. (a) Two parasitic elements to achieve a wideband decoupling [85]; (b) Parasitic element with lumped element [88]; (c) Parasitic element for four-element MIMO antenna [89]; (d) Parasitic element works at the lower frequency band [92].

The decoupling unit, which connects the feeding line of the two elements, introduces a new mutual coupling to mitigate the original coupling. The matching unit can match the antenna well after decoupling. A typical decoupling network where a transmission line connects two antenna elements is shown in Figure 20(a) [95]. In addition to the direct connection between two elements, new mutual coupling can be introduced by the resonator [96] and coupler [97]. As shown in Figure 20(b), the decoupling network comprises directional couplers, a transmission line, and a parallel resonant circuit [97]. Additionally, the decoupling network can be used to decouple dual-band [98] or circularly polarized MIMO antennas [99]. Figure 20(c) is a dual-band decoupling network with two resonant circuits [98]. An attractive advantage of the decoupling network is that the MIMO antenna and the decoupling network can be designed separately. The decoupling network does not occupy the antenna space.

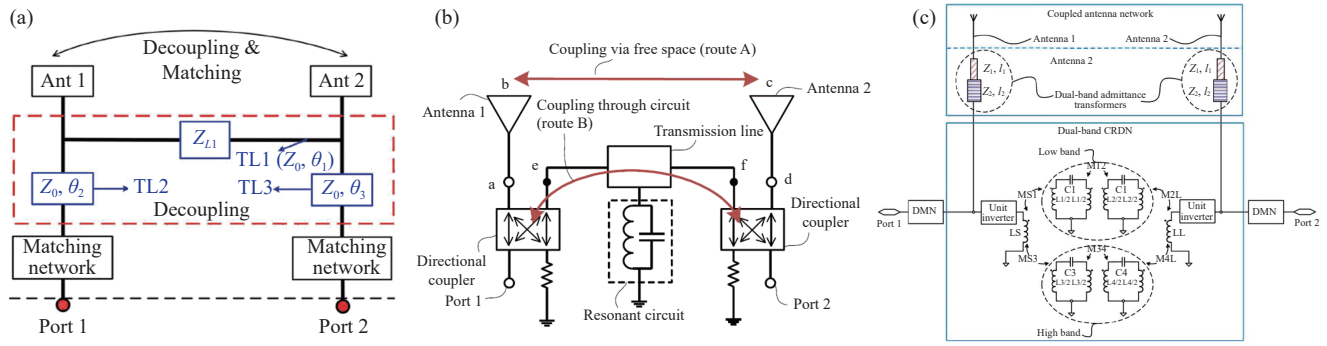

Figure 20 Decoupling method for a decoupling network. (a) Typical decoupling network [95]; (b) Coupled decoupling network [97]; (c) Dual-band decoupling network [98].

5. Neutralization line

The neutralization line, which is realized by connecting two antenna elements with one or more connecting lines, introduces a new mutual coupling to mitigate the original mutual coupling [100]–[102]. A single line usually decouples the MIMO antenna at a single frequency with a narrow decoupling bandwidth. Using multiple neutralization lines can decouple the MIMO antenna at multiple frequencies with a wide bandwidth [102]. As shown in Figure 21(a), [102] uses three neutralization lines to introduce three new mutual coupling currents (b_1, b_2, and b_3) to mitigate the original coupling current (a) within a wide frequency band. Thus, decoupling within the 1.62–2.84 GHz frequency band with mutual coupling lower than −15 dB is achieved. Using a long neutralization line or loading the lumped inductor on the neutralization line can decouple the MIMO antenna at the lower frequency band [103]–[105]. Figure 21(b) shows that, as the lumped inductor is integrated into the neutralization line, the neutralization line can decouple the MIMO antenna at the 704–960 MHz frequency band and slightly affects on the mutual coupling at the 1710–2690 MHz frequency band [105]. Additionally, the neutralization line can decouple the four-element MIMO antenna, as shown in Figure 21(c) [106]. An attractive advantage of the neutralization line is its small occupied space, which is highly important for mobile antenna design. Some commercial flagship mobile phones, such as Samsung S20 and Huawei P20, have adopted neutralization lines to design high-isolation MIMO antennas.

6. Common mode and differential mode theory

Physical orthogonality can be used to design integrated yet decoupled antenna pairs, thereby realizing natural high isolation for closely spaced antenna elements [107]–[116]. This approach often requires a clever antenna design and balanced feeding design to achieve good orthogonality and high isolation within a compact antenna size. As shown in Figure 22, a set of tightly-arranged orthogonal monopole and dipole antenna pairs is proposed [107], and a high iso-

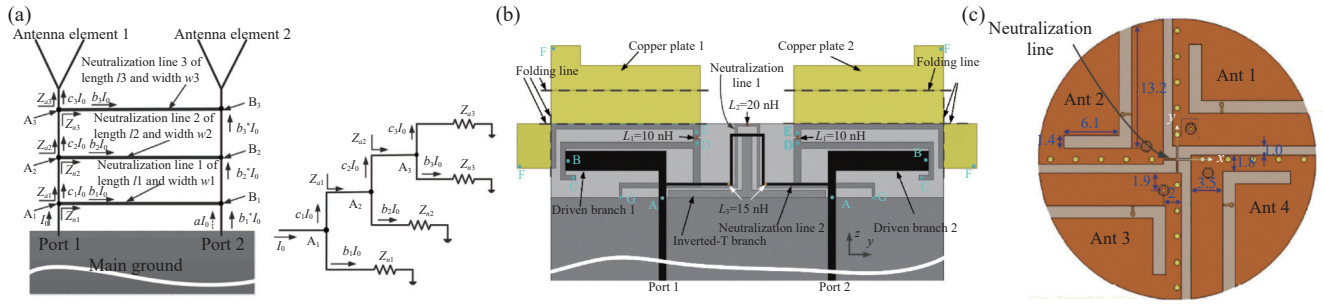

Figure 21 Decoupling method of a neutralization line. (a) Wideband decoupling by three neutralization lines [102]; (b) Decoupling at the lower frequency band with a lumped inductor [105]; (c) Decoupling for a four-element MIMO antenna [106].

lation of more than 20 dB can be realized according to a balanced feeding method for the dipole antenna. In [111], as shown in Figure 23, an open-slot structure is proposed that incorporates orthogonal in-phase current and slot modes, and a high isolation of more than 20 dB is also realized for the metal-bezel mobile phone application. Furthermore, the bandwidth of the orthogonal-mode antenna pair can be substantially enhanced by employing a unique combination of two sets of orthogonal modes in different frequency bands [116]. This approach is illustrated in Figure 24, where the combination of orthogonal monopole and dipole modes with orthogonal slot and open-slot modes can be strategically engineered into a single antenna structure for wideband orthogonal mode design. The proposed design can cover the entire 5G NR frequency band of 3.3–5.0 GHz with a high isolation of more than 20 dB.

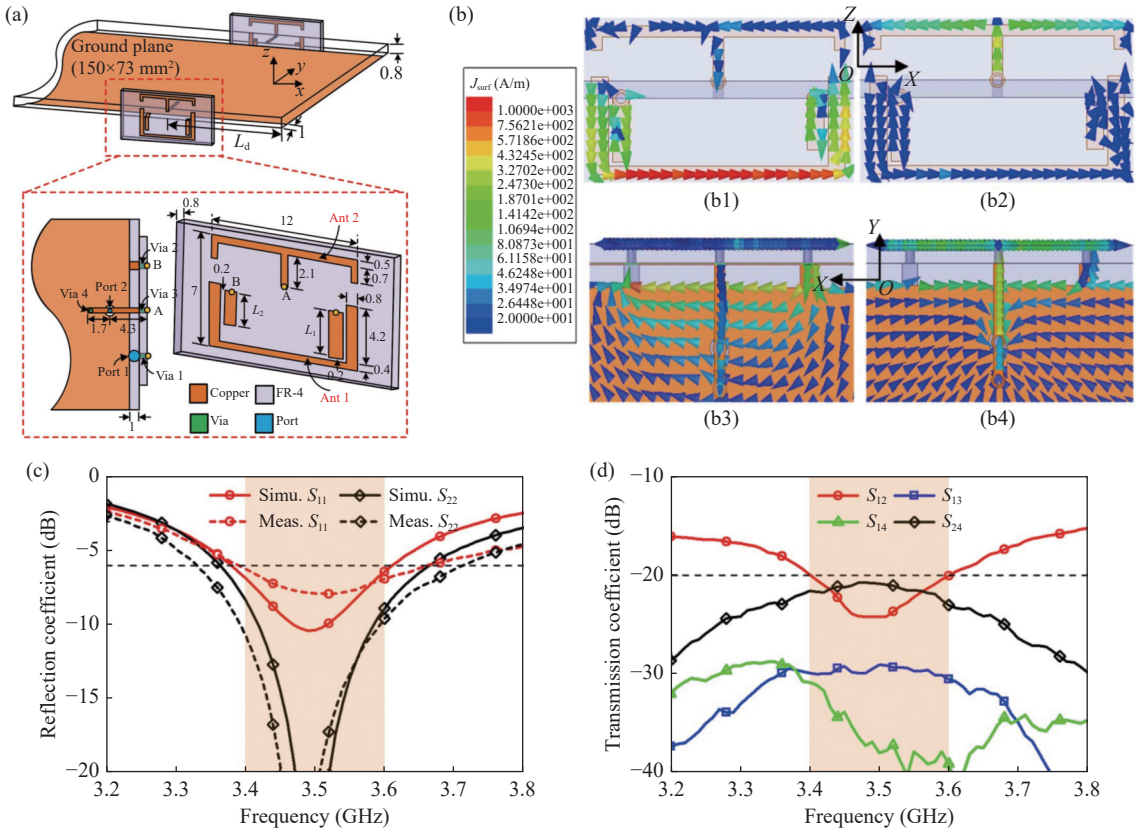

Figure 22 Orthogonal-mode antenna pair designed with dipole and T-monopole modes [107]. (a) Antenna configuration; (b) Operating modes; (c) *S* parameters; (d) Isolation.

Although the orthogonal mode method offers promising results in terms of achieving high antenna isolation, it often requires complex balanced feeding techniques and its application in the design of array antennas is often limited. Consequently, a simplified antenna decoupling methodology based on common mode (CM) and differential mode (DM) cancellation, referred to as the mode cancellation method (MCM), has been proposed [117]–[125]. This methodology aims to eliminate the mutual coupling between two antenna elements by strategically implementing CM and DM cancellation. As illustrated in Figure 25, theoretical analysis confirmed that the mutual coupling be-

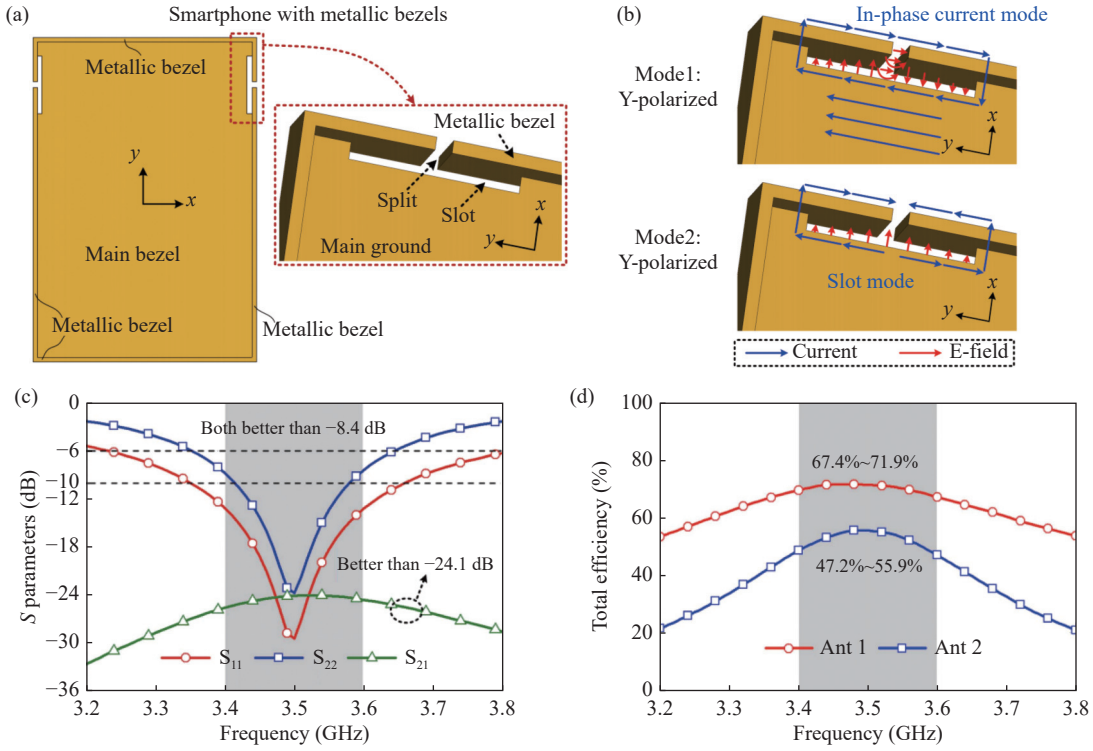

Figure 23 Orthogonal-mode antenna pair designed with in-phase current and slot modes [111]. (a) Antenna configuration; (b) Operating modes; (c) *S* parameters; (d) Total efficiency.

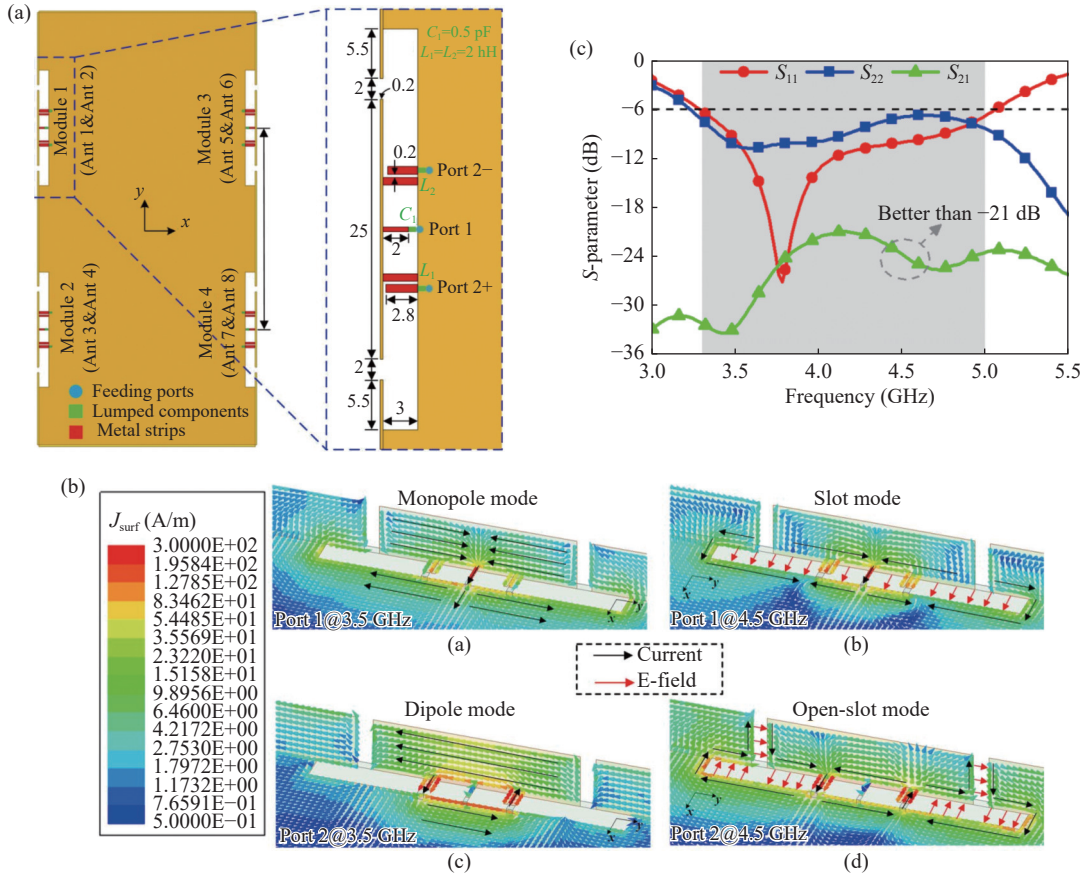

Figure 24 Wideband orthogonal-mode antenna pair designed with two pairs of orthogonal modes [116]. (a) Antenna configuration; (b) Operating modes; (c) *S* parameters.

tween two antenna elements can be eliminated when the corresponding CM and DM impedances are identical [117], [118]. This conclusion could offer a new perspective on antenna decoupling and enable independent tuning of CM and DM impedances by strategically exploiting the orthogonal properties of these modes. As a demonstration, a self-decoupled antenna pair with a shared aperture is illustrated in Figure 26, demonstrating the practicality of the proposed methodology [117]. The current mode fed through Port 1 can be equivalent to the superposition of the CM and DM current modes, thus, the current mode on the passive port can be completely canceled when the CM and DM impedances are identical. As shown in Figure 26(c), we can tune the impedances of the CM and DM by adjusting the distance of the feeding ports. A good isolation of more than 10 dB across a wide bandwidth can be realized when the impedances of the CM and DM are in the optimal similarity. In [125], the self-multipath counteraction method was proposed to isolate more than 20 dB within the 3.3–5.0 GHz frequency band.

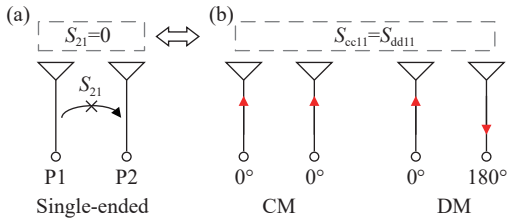

Figure 25 Decoupling conditions for an arbitrary dual-antenna system from two different perspectives [117], [118]. (a) Single-ended model and the corresponding decoupling condition. (b) CM and DM models and the corresponding decoupling condition.

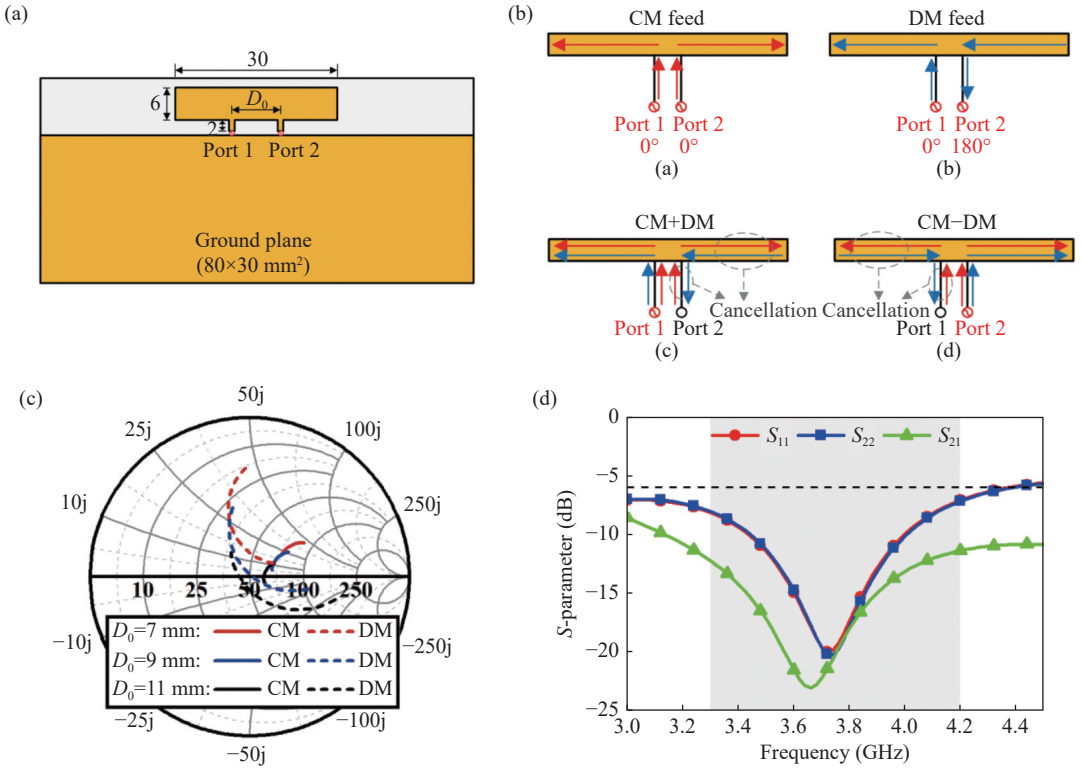

Figure 26 Self-decoupled antenna pair designed by the mode cancellation method [117]. (a) Antenna configuration; (b) Operating mechanism of the mode cancellation method; (c) Smith chart of CM and DM reflection coefficients; (d) Simulated *S*-parameters.

VI. Design of Compact, Wideband, and Wide-Angle-Scanning mm-Wave Arrays

The millimeter-wave (mm-wave) array design in mobile phones is usually based on phased-array antenna-in- package (AiP) modules for high-gain beam scanning. Because of the arbitrary posture of the smartphone in use, the array is usually required to have a wide-angle-scanning capability to ensure an effective connection range for communication [126]. Moreover, as the space for antenna design in mobile phones is very limited, compact and small mm-wave arrays are better [127], [128]. Thus, the key challenge in designing millimeter-wave arrays for mobile phones is to achieve small, wide-angle scanning across two broad bands (i.e., 24.25–29.50 GHz and 37.00–43.50 GHz) while maintaining compatibility with the smartphone industrial design (ID) and architecture of mobile phones.

Here, recent advances in the design of compact, wideband, wide-angle scanning mm-wave arrays for mobile phones are summarized. Figure 27 shows the expected spherical coverage of the beams of the mm-wave arrays for mobile phones [129]. Different expected beams can be realized by the array design of broadside and end-fire types. Here, we clearly summarize the characteristics and challenges of broadside array and end-fire array design. In addi-

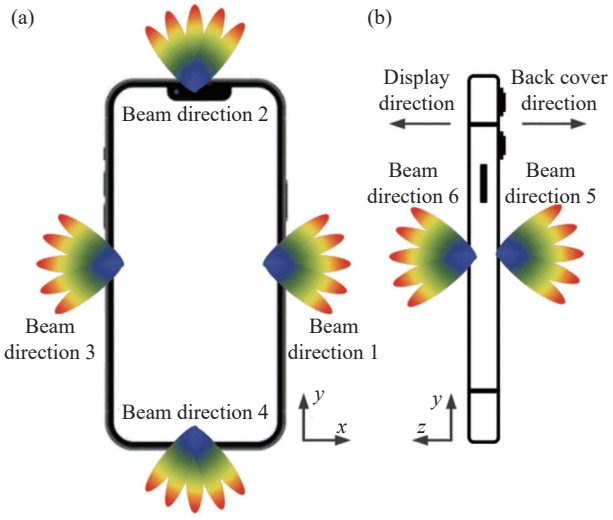

Figure 27 Diagram depicting the mm-wave array providing expected spherical coverage for mobile phones [129]. (a) Viewed from the front; (b) Viewed from the side.

tion, codesigns of mm-wave arrays with IDs and low-band antennas are also summarized.

1. Broadside array

For the broadside array, the maximum radiation direction is vertical to the array. As Figure 28(a) demonstrates, when the array is oriented horizontally with the main board, it enables the generation of the expected beams 5 and 6. Conversely, Figure 28(b) reveals that when the array is positioned vertically with the smartphone, it enables the achievement of the expected beams 1–4. However, because of the profile constraints of mobile phones, beams 1–4 are primarily achieved by employing end-fire arrays, which will be further explored in the next section. Moreover, broadside arrays are primarily utilized to achieve the expected beams 5 and 6.

The primary challenges in designing a broadside array lie in achieving superior performance for wide operating bandwidths, multiple operating bands, and wide-angle-scanning with size constraints. This section categorizes the broadside arrays into three segments: single-band, multi-band, and reconfigurable design. Moreover, this paper presents summarized solutions to the aforementioned challenges.

1) Single-band broadside array

The patch antenna, which is a prevalent element in broadside arrays, typically exhibits a narrow bandwidth [130]. Figure 29(a) portrays a common patch antenna with a limited 9% impedance bandwidth, and the proposed 1 × 8 array can achieve a beam scanning range of ±60° [131]. Figures 29(b)–(d) shows strategies such as slotting [132], parasitic patches [133], and parasitic branches [134] applied to enhance the bandwidth of the patch antenna to over 20% of the impedance bandwidth. Commonly, for mm-wave arrays in mobile phones, the elements are based on 0.5-wavelength resonance, taking 0.5-wavelength spacing. Wide-angle scanning can be realized when elements are numerous, but the array size is large for the mobile phones [135].

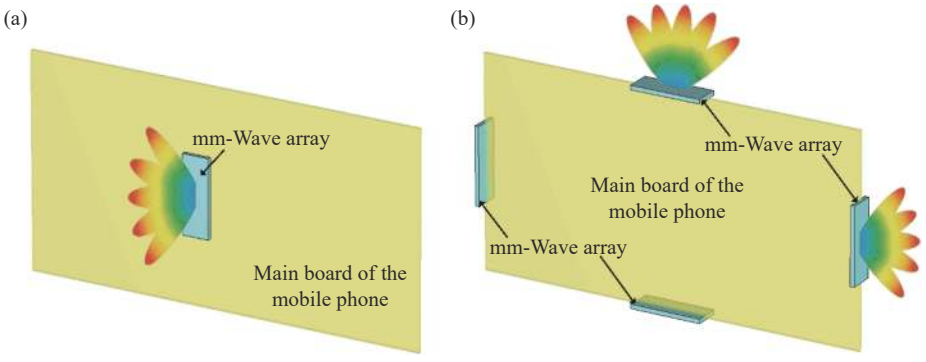

Figure 28 Concept sketch illustrating the broadside array (a) Oriented horizontally and (b) Oriented vertically with the mobile phone.

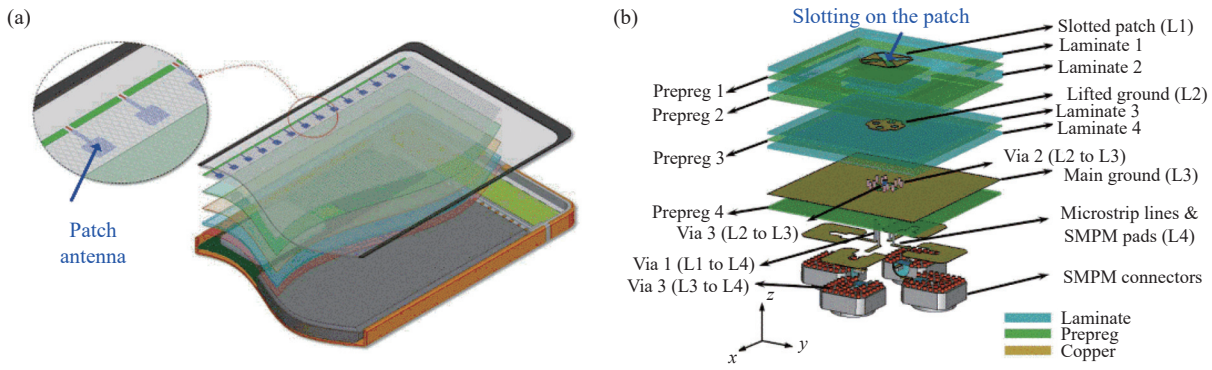

Figure 29 (to be continued)

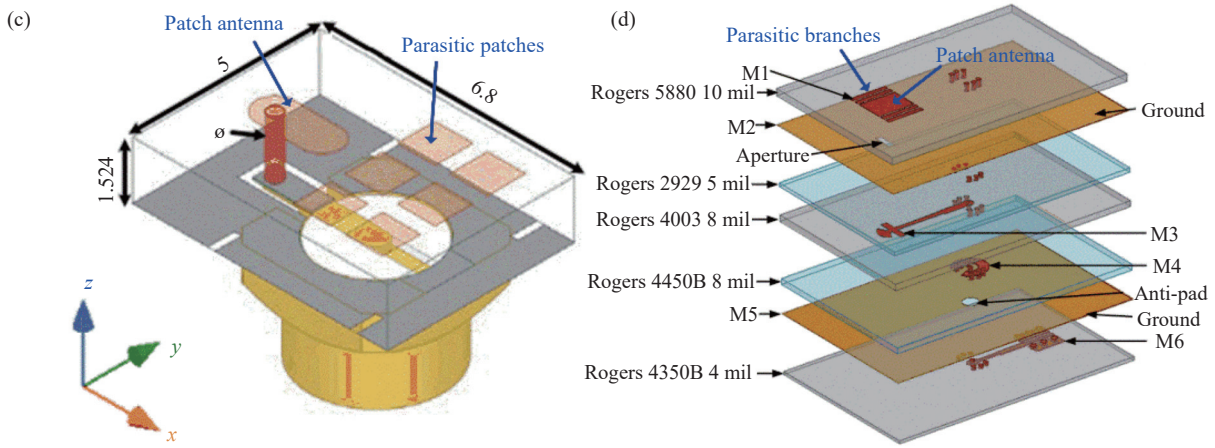

Figure 29 Typical designs of single-band broadside array. (a) Prevalent patch [131]; (b) Introducing slots on the patch [132]; (c) Implementing parasitic patches [133]; (d) Incorporating parasitic branches [134]. (continued)

For the 1 × 4 arrays usually deployed in mobile phones, the beam scanning range is limited, and generally, only ±45° scanning can be realized [136].

Notably, as shown in Figure 30(a), a compact array is proposed in [137] with a bandwidth of 25.5–27.5 GHz. The geometry of the element is shown in Figure 30(b). In con-

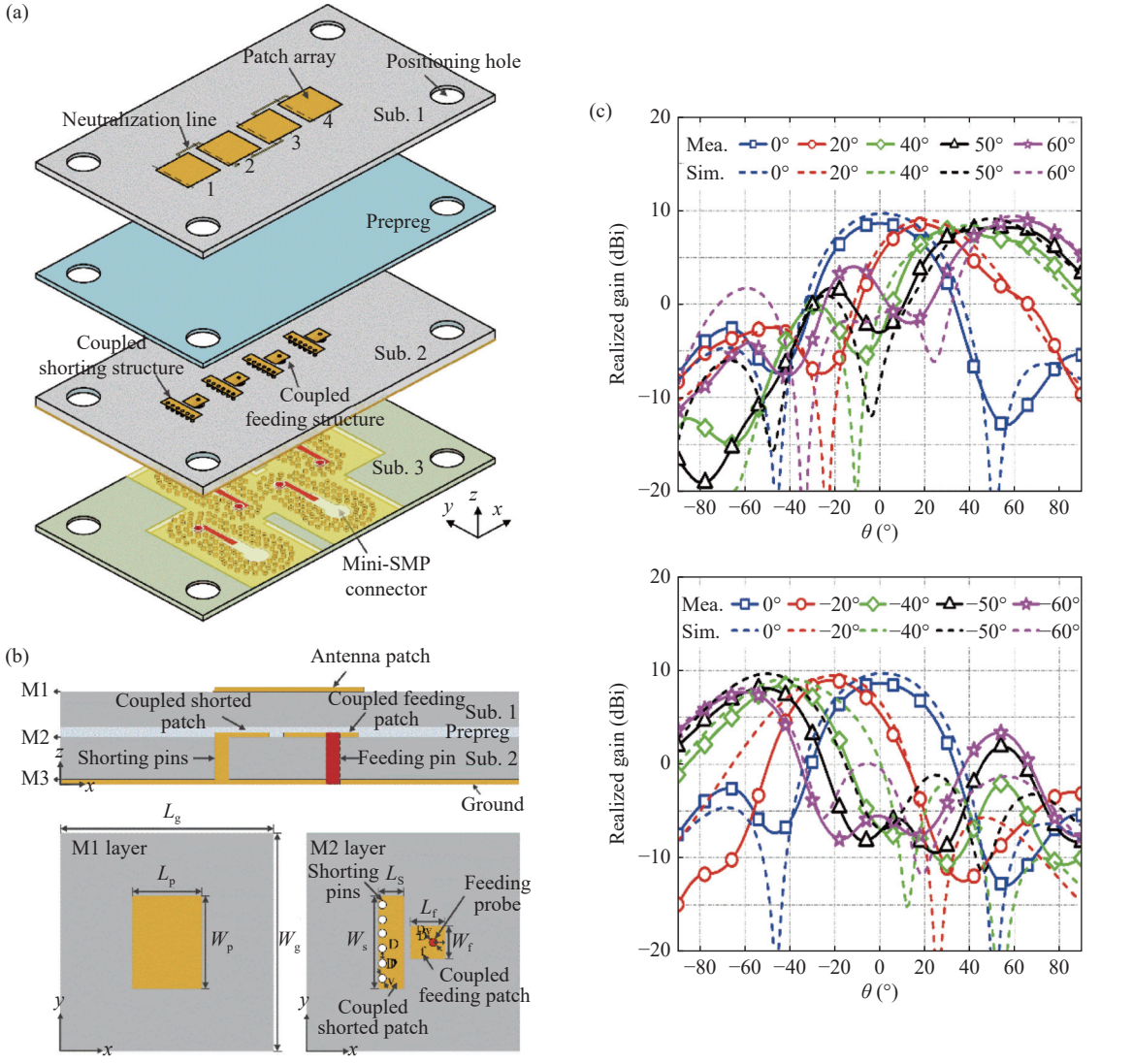

Figure 30 Compact and wide-angle scanning antenna design [137]. (a) Geometry of the array; (b) Geometry of the element; (c) Beam scanning radiation pattern.

trast to typical arrays with a 0.5-wavelength resonance element with 0.5-wavelength element spacing, the proposed array uses a 0.25-wavelength resonance coupled shorted patch with a small 0.3-wavelength element spacing to improve wide-angle scanning. Three neutralization lines are used to improve mutual coupling. Figure 30(c) shows that, the proposed 1 × 4 array can realize wide ±60° beam scanning with only a 1.3 dB scanning loss. Furthermore, the dual polarization can be achieved by orthogonal slot coupled feeding, and a 0.4-wavelength element spacing is used to improve the scanning range, as shown in [138]. A wide 3 dB beam scanning range of more than ±50° for both polarizations is achievable. The antennas shown in [137], [138] are smaller in size and have wider beam scanning ranges than the same type of single-band broadside arrays, which provides a promising application.

2) Multiband broadside array

As two wide bands (24.25–29.50 GHz and 37.00–43.50 GHz) need to be concurrently covered, extensive research has focused on mm-wave ultrawideband or multiband arrays. Achieving multiband antennas typically involves two approaches. A common approach is to assemble different structures that resonate at different frequencies [139], [140]. For instance, as shown in Figure 31(a), [140] introduces two pairs of dipole antennas, generating low-band and high-band radiation along co-polarized and cross-polarized directions, respectively. Another way to implement a multiband antenna is to adjust various modes of the same antenna structure to obtain different resonances [141]–[144]. As shown in Figure 31(b), the TM10 and TM20 modes of the patch are employed for dual-band resonance [143].

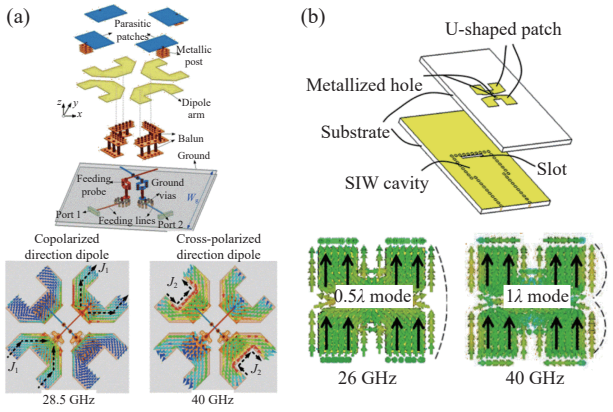

Figure 31 Multiband design. (a) By different resonant structures [140]; (b) By adjusting different resonant modes [143].

3) Reconfigurable broadside array

Recent designs utilizing reconfigurable methods to achieve beam scanning can be categorized into two kinds: those based on the excitation phase difference provided by shifter reconfigurable control and those based on direct pattern reconfigurable control. A phase shifter is often indispensable for controlling the array beam direction. The phase shifter provides the quantized phase, with each element taking the closest quantized phase instead of the ideal phase. The more quantized phase the phase shifter provides, the greater the cost. However, providing less quantized phase results in quantization phase error, which increases the sidelobe level and reduces the array gain [145].

In [146], a reconfigurable 1-bit array design is proposed as shown in Figure 32(a). Each element is fed by a slot on the ground. A 1-bit element with phase values of −π and 0 is achieved by selecting PIN diodes in different directions. A fixed phase is applied to mitigate the grating lobes, and the array can steer the beam from −34° to 35° without grating lobes. Additionally, to reduce the cost and ensure array performance, as shown in Figure 32(b), the antenna array introduces PIN-diode-controlled strips for direct pattern reconfigurable control, thus, direct beam tilting of ±50° is achieved [147].

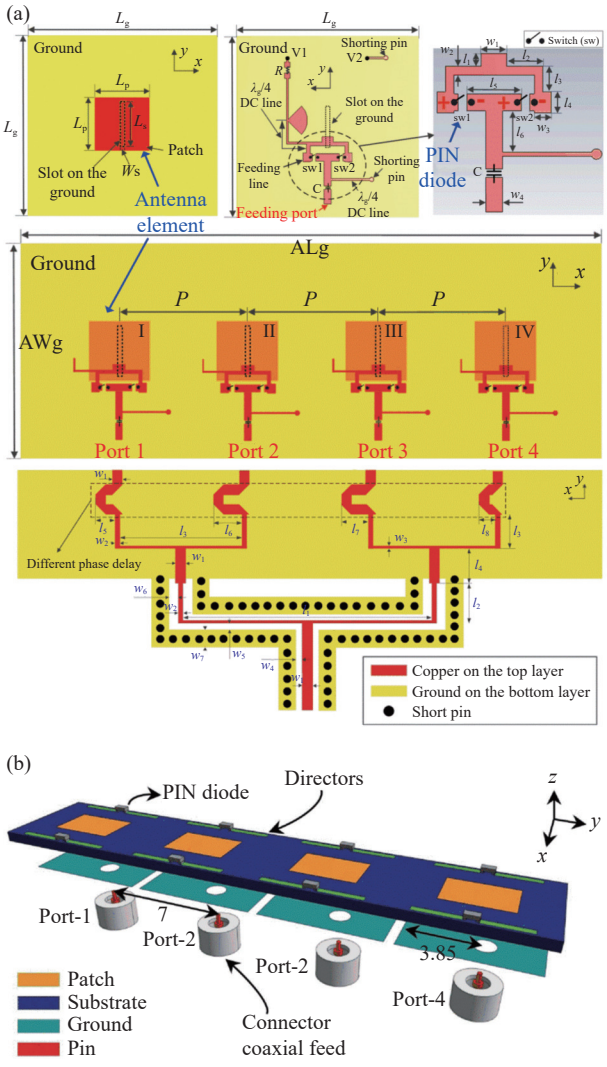

Figure 32 Reconfigurable design of (a) Control of the excitation phase difference[146] and (b) Direct control of the radiation pattern [147].

2. End-fire array

For the end-fire array, the maximum radiation direction is parallel to the array. Compared to the broadside arrays, end-fire arrays can be integrated directly into the PCB of a mo-

bile phone, which is particularly advantageous for mobile phones with special thin geometries. However, excellent performance is difficult to achieve with a thin profile, small clearance, dual polarization, and wide beam scanning. This section summarizes the typical designs for horizontally polarized, vertically polarized, and dual-polarized end-fire arrays.

1) Horizontal-polarized end-fire array

To provide an overview of the horizontally polarized end-fire array in mobile phones, Figure 33 illustrates the typical designs of several horizontally polarized end-fire arrays. As shown in Figure 33(a), in [148], the horizontally polarized magnetoelectric dipole is vertical to the system ground to achieve the horizontally polarized end-fire radiation. However, the array height must be sufficient for proper performance, impacting the smartphone thickness. As shown in Figure 33(b), a dipole antenna close to the system ground exhibits end-fire radiation with horizontal polarization [149]. Figure 33(c) shows that a patch antenna with a half-wavelength mode near the system ground can achieve horizontally polarized end-fire radiation [128]. Similarly, Figure 33(d) depicts an open-ended slot antenna with a horizontally polarized end-fire radiation pattern [150]. Notably, the monopole antenna and slot antenna need to occupy enough space to achieve good broadband performance.

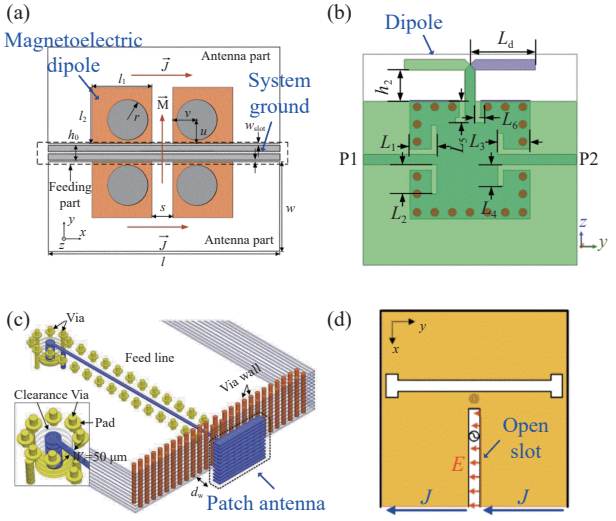

Figure 33 Typical designs of horizontal-polarized end-fire array. (a) Oriented vertically with the system ground [148]; (b) Dipole element [149]; (c) Patch element [128]; (d) Open slot element [150].

2) Vertical-polarized end-fire array

To provide a comprehensive overview of the vertically polarized end-fire array in mobile phones, Figure 34 illustrates several typical designs. Figure 34(a) shows that, the vertically polarized folded slot antenna moves vertically to the system ground to achieve vertically polarized end-fire radiation [151]. However, a critical drawback is that the profile must be sufficient for proper performance, which impacts the thinness and lightness of mobile phones. As depicted in Figure 34(b), the substrate-integrated waveguide (SIW) antenna element can be utilized to radiate the vertically polarized pattern [152]. For the dipole element [153] shown in Figure 34(c) and the monopole element [154] in Figure 34(d), vertical polarization with end-fire radiation can be achieved. For the dipole or monopole element, the profile of the smartphone should be substantial for a wide bandwidth.

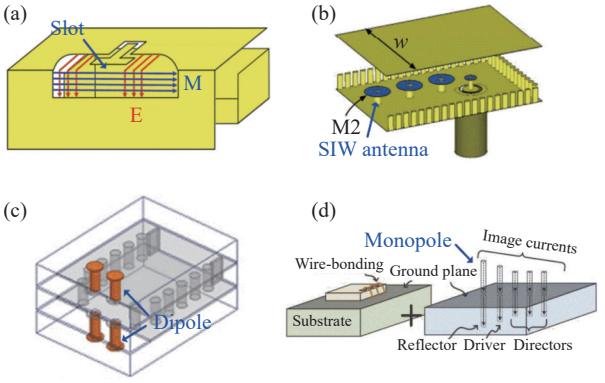

Figure 34 Typical designs of vertical-polarized end-fire array. (a) Slot antenna element [151]; (b) SIW antenna element [152]; (c) Dipole element [153]; (d) Monopole element [154].

3) Dual-polarized end-fire array

For instance, if the array is oriented vertically to the system ground, and the element has a dual-polarized radiation pattern, achieving a dual-polarized end-fire array becomes straightforward. This method is demonstrated in [155], as shown in Figure 35(a), where a smartphone features a vertically deployed dual-polarized slot antenna, resulting in a dual-polarized end-fire mm-wave array.

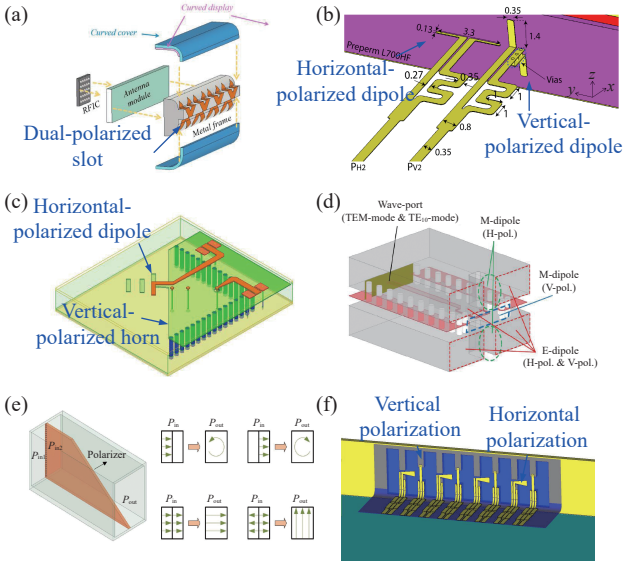

Figure 35 Typical designs of dual-polarized end-fire array. (a) Vertical deployment of the dual-polarized element [155]; (b) Horizontal-polarized and vertical-polarized dipole [156]; (c) Horizontal-polarized dipole with a vertical-polarized horn [157]; (d) Horizontal-polarized slot with a vertical-polarized horn [158]; (e) Two SIW horns with a polarizer [159]; (f) Dual-polarized slot antennas [160].

Moreover, by merging the horizontally polarized end-fire array with the vertically polarized array, a dual-polar-

ized array can also be achieved. Figure 35(b) shows that, a horizontal dipole with a vertical dipole element is employed to achieve a dual-polarized dipole array [156]. However, such a configuration requires a substantial profile to ensure optimal performance. To address the profile size, as shown in Figure 35(c), [157] achieved a low-profile dual-polarized end-fire array by combining a horizontally polarized dipole with a vertically polarized horn. However, such dual-polarized end-fire arrays typically require sufficient clearance for optimal performance.

Some efforts have been made to reduce clearance. As shown in Figure 35(d), a dual-polarized array without clearance is achieved by designing a horizontally polarized open slot and a vertically polarized open-ended waveguide radiation [158]. In addition, as shown in Figure 35(e), the proposed antenna achieves ±45° polarization by utilizing a modified SIW slot polarizer [159]. Moreover, [160] introduced the concept of exciting orthogonal slots simultaneously to realize a dual-polarized end-fire chain-slot array, as illustrated in Figure 35(f).

3. Codesign of mm-wave arrays with the ID and the low-band antennas

The existing broadside arrays and the end-fire arrays have demonstrated exceptional performance, covering the expected beams 1–6, as illustrated in Figure 27. However, considering the stringent specifications of mobile phones with full displays, curved displays, metal bezels, glass backs, etc., mm-wave arrays must match the industrial design. Therefore, the codesign of mm-wave arrays in mobile phones has been extensively researched, especially in conjunction with industrial design and low-band antennas. These codesign examples are summarized below.

1) Integration of the mm-wave array with a mobile phone

The integration of mm-wave arrays into the mobile phone of a smartphone is aesthetically and functionally critical. This integration optimizes space within the limited space of a mobile phone and ensures efficient placement of components. In addition, integration with a metal bezel helps mitigate beam blockage and maintain the performance of the millimeter-wave array. Therefore, considering the integration of mm-wave arrays with mobile phones is key to the deployment of mm-wave arrays.

In [161], the impact of the metal bezel on the radiation pattern was investigated. The obstruction caused by the metal bezel is more pronounced for horizontally polarized antennas than for vertically polarized antennas. As shown in Figure 36(a), the coupling metal strips are used to mitigate the blockage from the metal bezel [162]. Additionally, Figure 36(b) shows that slots on the metal bezel can be utilized to alleviate beam blockage [163]. As shown in Figure 36(c), direct radiation of the mm-wave array is allowed through a rectangular window in the metal bezel in [164]. This solution has been implemented in commercial 5G mobile terminals such as the Apple iPhone 12, which features a small mm-wave window [165]. Beyond mitigating the effects of the metal bezel, reference [166] explored the use of the metal bezel to design mm-wave leaky-wave arrays, as illustrated in Figure 36(d). Moreover, the mm-wave array

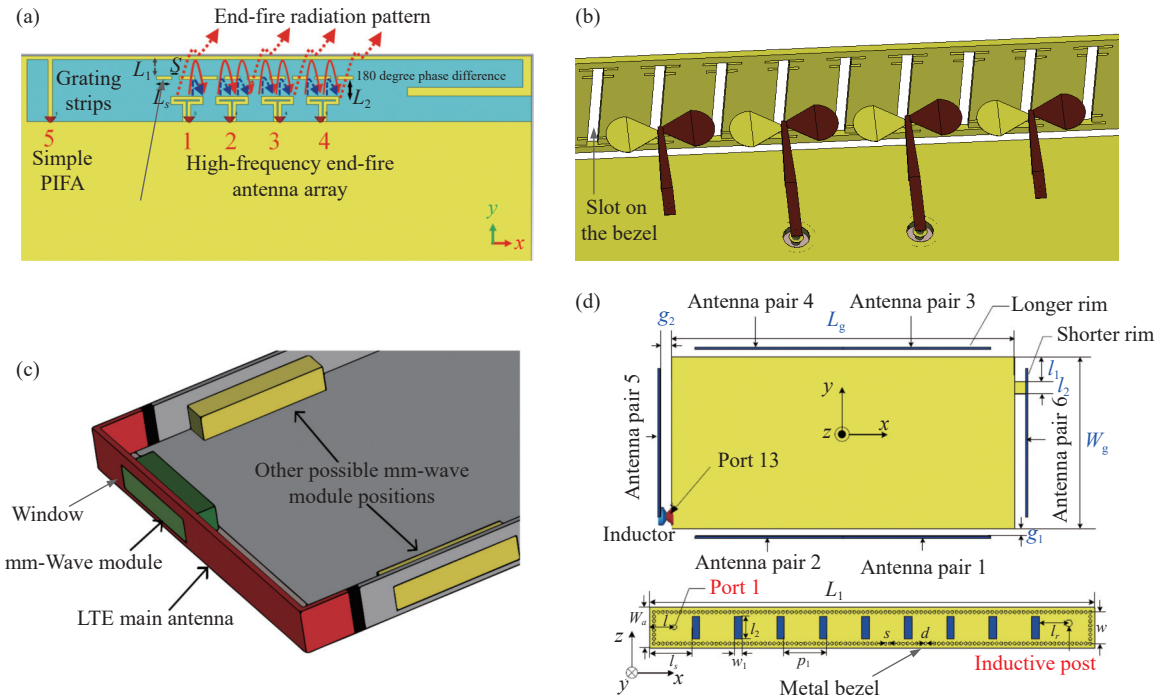

Figure 36 Typical integration designs with the metal bezel in smartphones. (a) Employing coupling metal strips to minimize blockage from the metal bezel [162]; (b) Utilizing slots for diminishing interference from the metal bezel [163]; (c) Employing a window to alleviate blockage effects from the metal bezel [164]; (d) Crafting the mm-wave array antenna directly into the metal-bezel design [166].

antenna can be directly implemented through slots on the metallic bezel [167], [168], effectively resolving blockage issues associated with the metal bezel.

As the mm-wave array is deployed on a mobile phone, the back cover and phone chassis might considerably affect the array performance where the array gain decreases greatly [128]. In [169], an ultra-thinned metasurface was proposed to reduce the negative effect from the back cover. In addition, to achieve mm-wave radiation in the display direction, an optically invisible mm-wave array antenna-on-display (AoD) with 88% optical transparency was studied in [131], [170]. Thus, the mm-wave array is directly implemented on the display.

2) mm-Wave array shared-aperture design with a low-band antenna

Considering that mm-waves coexist with low-band communications for a long period, mm-wave shared-aperture design with low band antennas is also important. This scheme will greatly save antenna design space and support multiband communication.

The application of the filter is a viable approach for shared-aperture design, as depicted in Figure 37(a). A low-band antenna is directly linked to a mm-wave antenna utilizing a low-pass and high-stop filter [171]. This scheme enables the design of the mm-wave and the low-band antenna to be near a single feeding port. As shown in Figure 37(b), the mm-wave slot array antenna is incorporated into the clearance of the low-band antenna [172].

To further minimize the space occupied by the shared-aperture design, the structure of the low-band antenna can be reused for mm-wave array design. As shown in Figure 37(c), in [173], the low-band antenna takes the form of a simple patch antenna, and the patch is configured as an SIW slot array for mm-waves. In addition to using the SIW structure, the higher-order mode of the low-band antenna can be directly employed to design the mm-wave array. As shown in Figure 37(d), in [174], the half-wavelength slot mode of the low band is excited multiple times to achieve a higher-order mode for the mm-wave.

Notably, as shown in Figure 38, a shared-aperture LTE and mm-wave antenna with enhanced mm-wave display direction radiation has been designed [129]. An interdigital coupling structure is applied to integrate the LTE antenna and mm-wave array in the same aperture. The attractive performance makes this design a promising candidate for use as a mm-wave array for modern mobile phones.

VII. Design of the Satellite Communication Antenna

As mentioned above, modern mobile flagship phones, such as the Huawei Mate 60, have introduced satellite communication capabilities [175]. Smartphones designed with satellite communication features can be utilized in special scenarios, such as emergencies and nonground communication, which are very large markets. In this section, before presenting the research progress on satellite communication antennas in modern mobile phones, conventional satellite phones with external antenna designs are briefly introduced. The external antenna influences the appearance of modern mobile phones, which is not preferable. To accommodate modern metal-bezel mobile phones, the preferable internal satellite communication antennas are summarized. Additionally, to solve the problems of the limited space of mobile phones and the large space occupied by a single satellite communication antenna, codesign methods for satellite communication antennas and cellular antennas are also summarized.

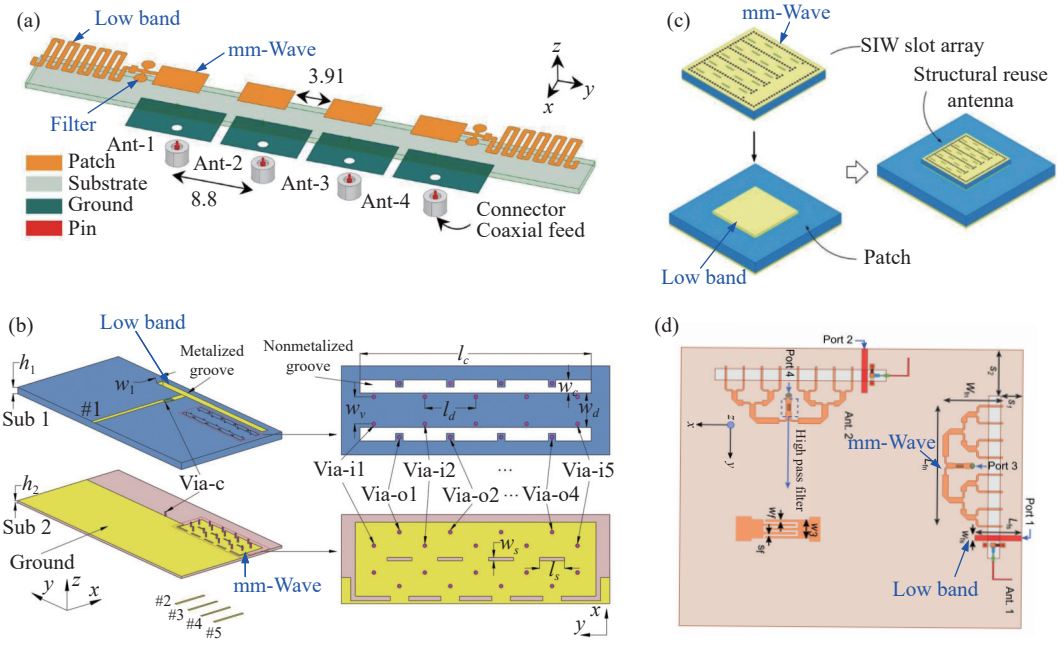

Figure 37 Typical shared-aperture designs. (a) Employing filter to integrate design [171]; (b) Using the clearance to deploy the mm-wave array [172]; (c) Utilizing the SIW to integrate design [173]; (d) Employing the higher order mode to integrate design [174].

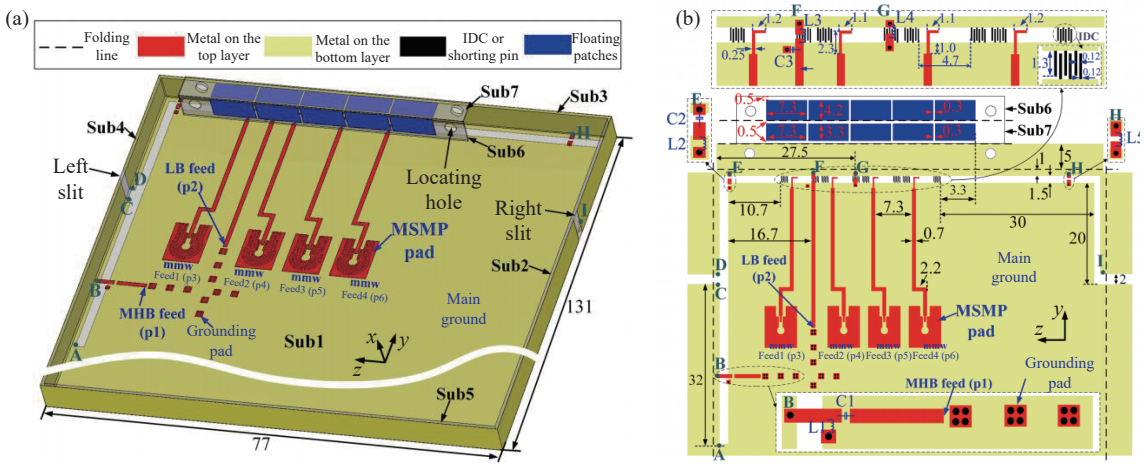

Figure 38 Shared-aperture design with display direction radiation [129]. (a) 3D view; (b) Front view.

1. Single satellite communication antenna

Traditional satellite phones usually adopt external antenna designs. Figure 39(a) illustrates the Iridium 9505a satellite phone with an external satellite antenna design [176]. Figure 39(b) shows the satellite communication antenna of this type of phone, which is mainly designed with a linearly polarized antenna [177]. Figure 40(a) illustrates the typical external CP satellite communication mobile phone Linyun YT1100 [178], which employs a helical antenna with CP radiation as shown in Figure 40(b) [179]. Compared with linearly polarized antennas, CP antennas reduce the polarization loss in satellite communication. However, external antennas severely affect the appearance of phones and are not favorable for modern mobile phones.

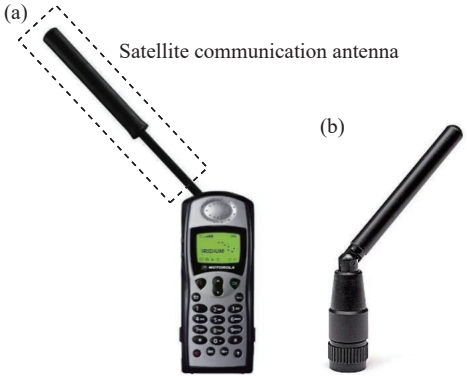

Figure 39 Typical external linearly polarized satellite communication mobile phone antennas. (a) Iridium 9505a satellite phone [176]; (b) Linearly polarized satellite communication antenna [177].

For modern mobile phones, internal satellite communication antennas have been designed to solve the appearance problems of traditional satellite phones. In [180]–[184], a ground-mode tuning technique was proposed for CP satellite communication antennas. A typical design is shown in Figure 41 [182]. As plotted in Figure 41(a), an antenna using a combination of an electric coupler and a magnetic coupler is placed on the ground of the mobile phone,

Figure 40 Typical external CP satellite communication mobile phone antenna. (a) Linyun YT1100 satellite phone [178]; (b) CP satellite communication antenna [179].

where these couplers can be coupled to excite the orthogonal mode 1 and mode 2, as shown in Figure 41(c). The addition of an inductor and a metal strip at the bottom of the antenna can adjust the phases, realizing a CP antenna. As shown in Figure 41(b), the 3:1 VSWR bandwidths cover 2.38–2.52 GHz, and the 6 dB axial ratio (AR) bandwidths are from 2.36–2.50 GHz. Because the many components on the ground in smartphones affecting the performance of the antenna, employing the ground mode is not suitable for practical applications.

In addition to broadside radiation, end-fire radiation is also preferable for modern mobile phones. [185]–[187] describe the use of an end-fire internal antenna for satellite communication. In [185], a CP satellite communication antenna is achieved in a folded mobile phone with the orthogonal structure of a direct-feed dipole and a parasitic dipole, as shown in Figure 42(a). As shown in Figure 42(b), the folded antenna achieves left-handed CP radiation along the $+z$-axis, which can be expected for satellite communication. In Figures 42(c) and (d), the −10 dB impedance bandwidths of the antenna in CP states are 2.44–2.58 GHz, and

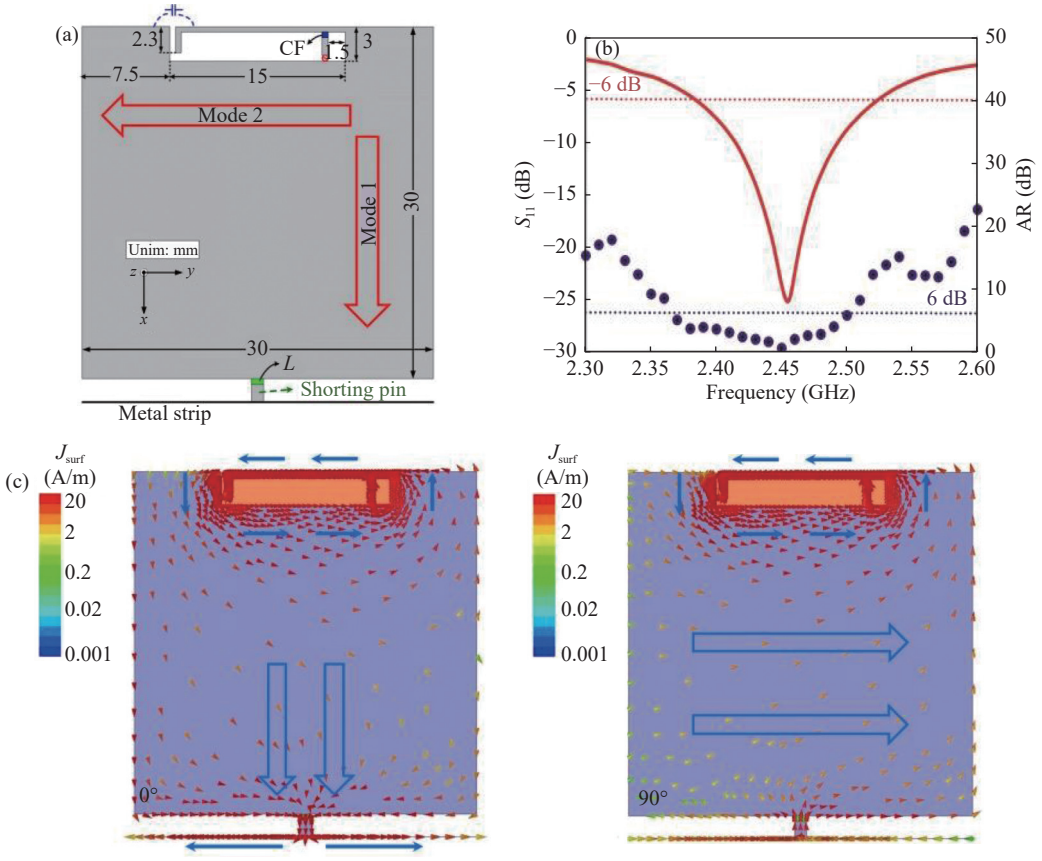

Figure 41 Typical design schematics of a CP satellite communication mobile antenna using the ground-mode tuning technique [182]. (a) Antenna structure; (b) S_{11} and AR; (c) Simulated surface-current distributions at 2.45 GHz at phases of 0° and 90°.

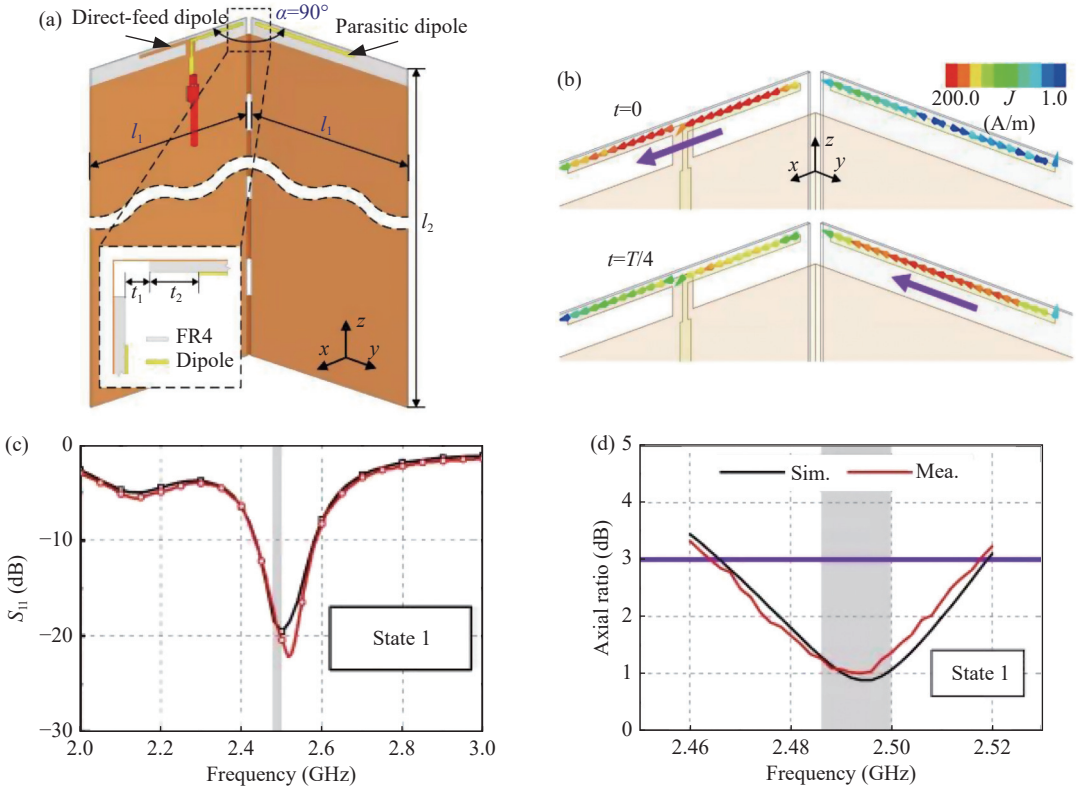

Figure 42 Circularly polarized folded mobile antenna for satellite communications [185]. (a) Antenna structure; (b) Simulated surface-current distributions at 2.49 GHz at phases of 0° and 90°; (c) S_{11}; (d) AR.

the 3 dB AR bandwidth is considerably wider than the impedance bandwidths. In [186], the folded dipole and loop modes of a rectangular loop antenna provide two orthogonal radiation patterns, enabling internal CP mobile antenna designs that can be expected to be used for satellite communications, as shown in Figure 43. As shown in Figure 43(b), the asymmetric feed simultaneously excites the horizontally polarized (HP) mode (folded dipole mode) and the vertical polarization (VP) mode (loop mode). Figures 43(c) and (d) show that the CP rectangular loop mobile antenna has −6 dB impedance bandwidths within 2.27–2.51 GHz and 3 dB AR bandwidths within 2.482–2.501 GHz.

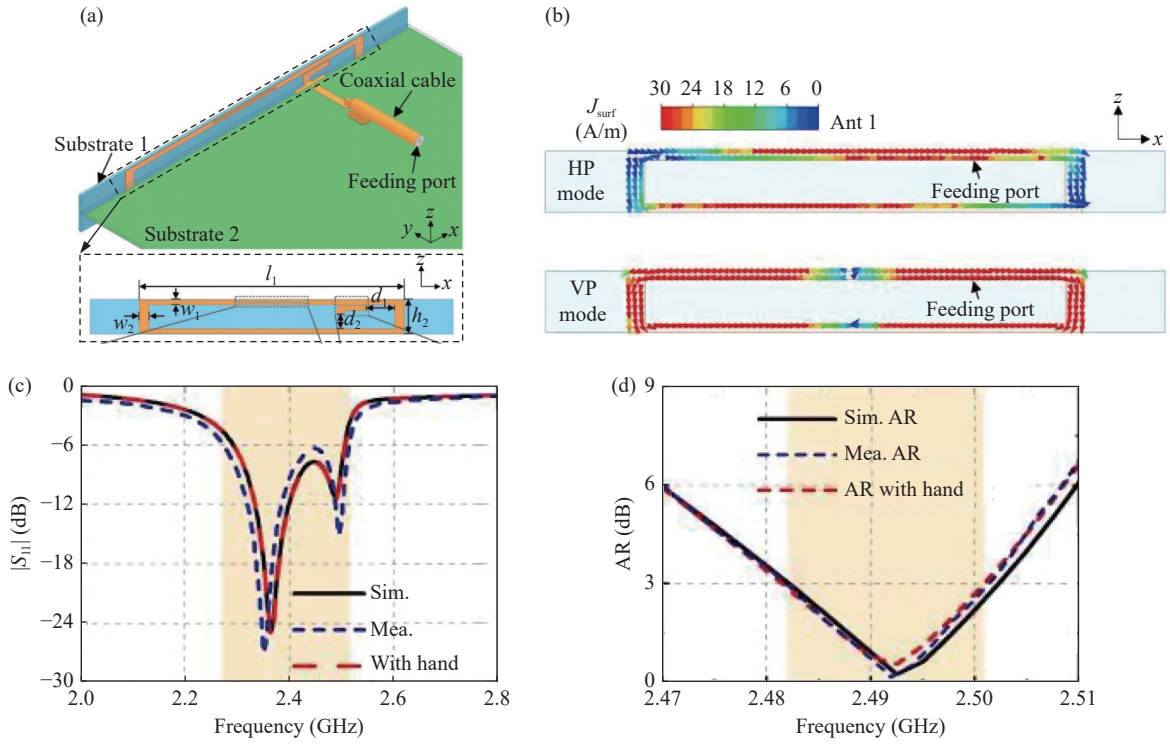

Figure 43 CP rectangular loop mobile antenna for satellite communications [186]. (a) Antenna structure; (b) Current distribution of the two orthogonal modes; (c) S_{11}; (d) AR.

In [187], two end-fire CP antennas were designed based on CM and DM theory. As shown in Figure 44(a), the orthogonal CM (PIFA mode) and DM (open-slot mode) are excited by adding a slot to the PIFA. As illustrated in Figure 44(b), the designed antenna resonates at 1.61 GHz. Figures 44(c) and (d) show that the designed PIFA antenna

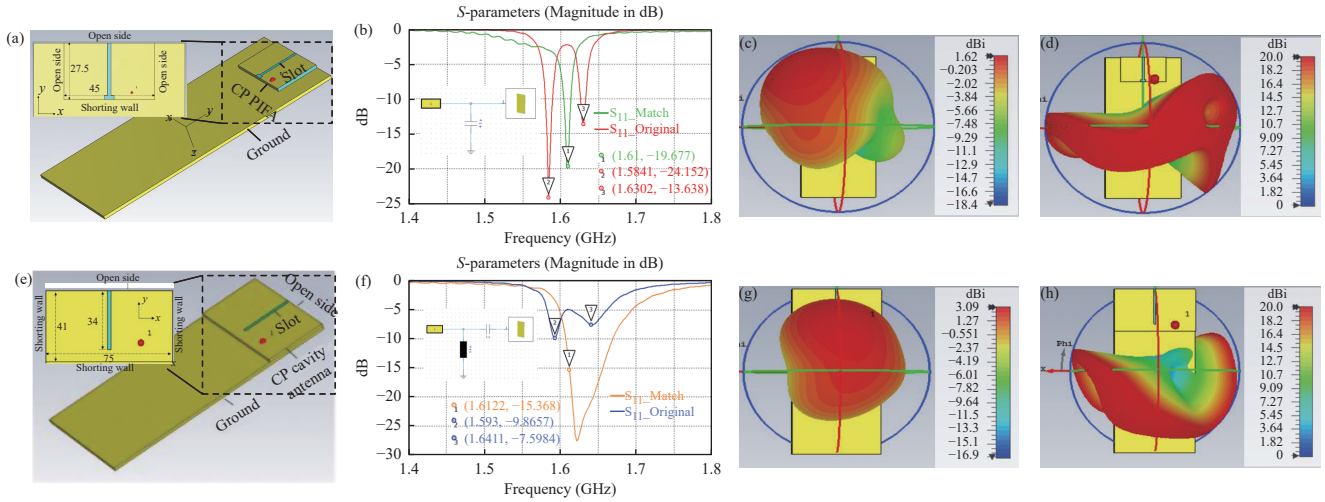

Figure 44 Two CP antenna based on the combination of CM and DM in a single mobile antenna [187]. (a) CP slotted PIFA; (b) *S*-parameters of the CP slotted PIFA; (c) Simulated radiation pattern of the CP slotted PIFA LHCP directivity at 1.61 GHz; (d) Simulated 3D plot of the CP slotted PIFA AR; (e) Slotted cavity antenna; (f) S-parameters of the slotted cavity antenna; (g) Simulated radiation pattern of the slotted cavity antenna LHCP directivity at 1.61 GHz; (h) Simulated 3D plot of the slotted cavity antenna AR.

has the characteristics of end-fire CP radiation. As shown in Figure 44(e), a slot is carved in the middle of the cavity antenna, and the orthogonal CM (TM1/2,1 cavity mode) and DM (open-slot mode) can be excited for CP radiation. Figure 44(f) shows that the slotted cavity resonates at 1.61 GHz. As shown in Figures 44(g) and (h), the slotted cavity antenna achieves end-fire CP radiation at 1.61 GHz, which should be useful in satellite communications.

2. Codesign of the satellite communication antenna and cellular antenna

The limited space for mobile antenna design and the large area occupied by a single satellite communication antenna have led to the codesign of satellite antennas and cellular antennas in mobile phones.

Figure 45 shows the codesign of the CP satellite communication antenna and cellular antenna [188]. In Figure 45(a) shows the antenna structure and the design process. The satellite communication antenna is a single CP antenna, which is composed of two orthogonal slot antennas and an inductor L1 with three short ends at points E, B, and D. The cellular antenna working in the LB band is a single LB antenna, which has two open ends at points E&A and one short end at point C. To realize the codesign in a smartphone, a pair of low-stop high-pass filters are added to points E and B. The filters can be equivalent to being open in the LB band of the single LB antenna and short in the S-band of the single CP antenna, realizing the codesign antenna (LB&CP Ant). Figure 45(c) indicates that the −6 dB impedance bandwidths of the LB&CP Ant are 698–962 MHz and 1980–2130 MHz. The 3 dB AR bandwidths are 2.06–2.1 GHz.

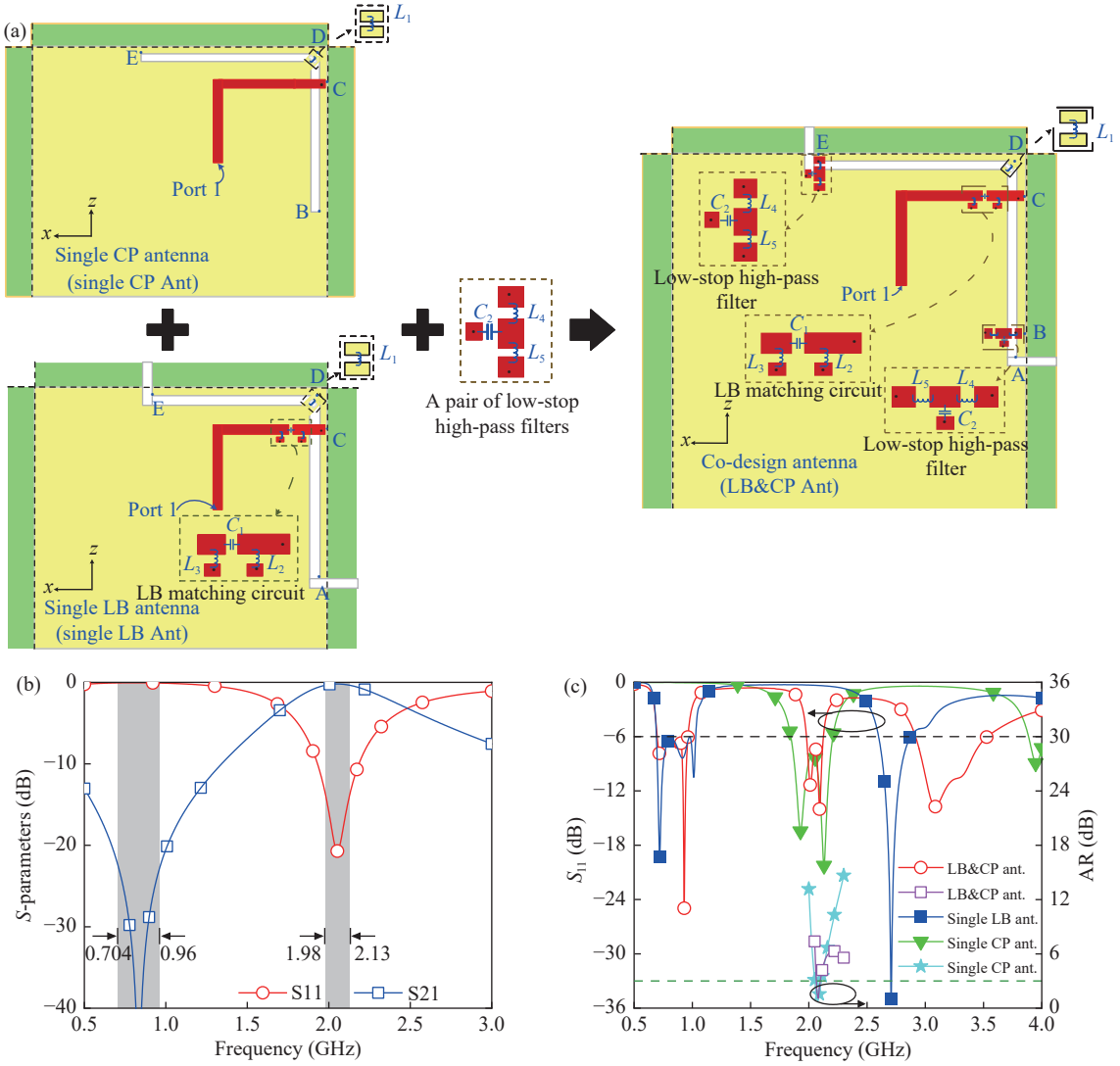

Figure 45 Codesign of the CP satellite communication antenna and cellular antenna in a single mobile antenna [188]. (a) Antenna structure and design process; (b) *S*-parameters of the low-stop high-pass filter; (c) S_{11} and AR of the codesign antenna.

Figure 46 shows the codesign of the wide end-fire beam satellite communication antenna and 4G LTE cellular antenna [189]. Figure 46(a) shows the design process of the codesign antenna. The satellite communication antenna is the floating dipole branch DC, which works in the 0.5-wavelength mode. A wide end-fire beam of the dipole an-

tenna is formed with the ground working as a reflector. To integrate the 4G LTE antenna, monopole branches and a low-stop high-pass filter are designed. Figure 46(b) shows that the −6 dB impedance bandwidths cover 701–973 MHz and 1640–2780 MHz. The radiation patterns in the *xoz*- and *yoz*- planes are shown in Figures 46(d) and (c), respectively. The orange-filled sections indicate that the antenna gain is greater than 0 dBi. Figure 46(d) and Figure 46(c) indicate that the end-fire beam width with a gain greater than 0 dBi is 195° in the *yoz*-plane and 88° in the *xoz*-plane, respectively.

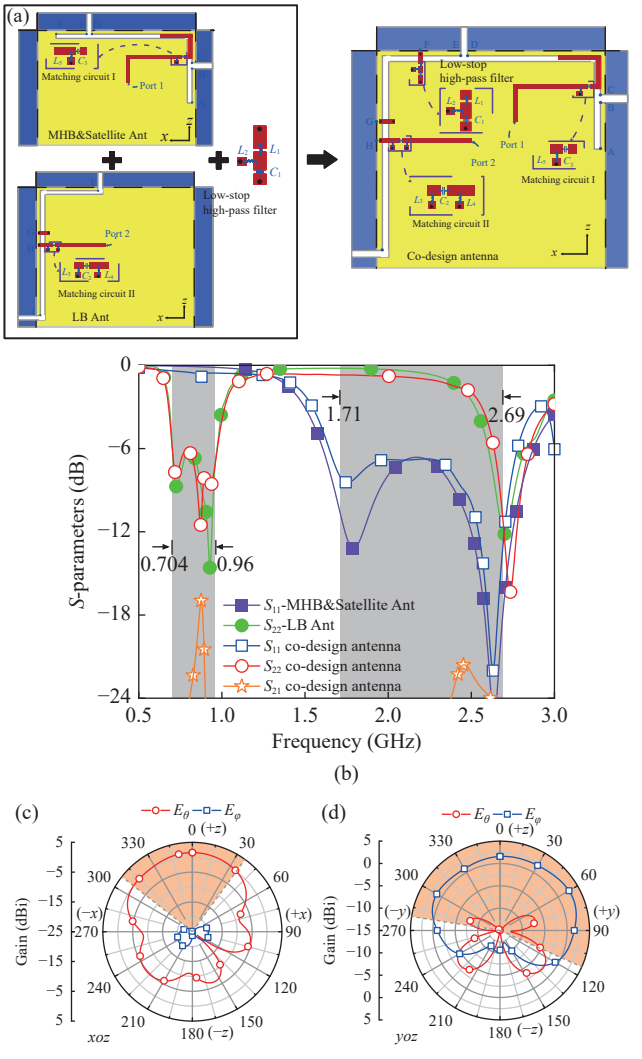

Figure 46 Codesign of the wide end-fire beam satellite communication antenna and 4G LTE cellular antenna in a single mobile antenna [189]. (a) Antenna structure and design process; (b) S-parameters of the codesign antenna; (c) Radiation pattern in the *xoz*-plane; (d) Radiation pattern in the *yoz*-plane.

3. Satellite antenna design for commercial mobile phones

In 2010, the world's first commercial smartphone with the function of direct phone-to-satellite communication was launched by the TerreStar Genus [190]. This plastic mobile phone, designed by TerreStar, could connect to the geosynchronous Earth orbit (GEO) satellite. The satellite antenna of the TerreStar Genus mobile phone is an internal PIFA, which is located at the upper right corner of the phone from the front view of [190]. In addition to the satellite band, this phone can also cover the 2G/3G, GPS, and WLAN/BT bands. After years of silence, in 2022, the Huawei Mate 50 series and Apple iPhone 14 series launched smartphones that support satellite message services. Since the realization of satellite SMS service does not require a high communication rate, it does not pose a considerable significant challenge for the design of mobile phone antennas. Then, in 2023, Huawei introduced a smartphone featuring the ability to make satellite voice calls [191]. Unlike the preceding product, the TerreStar Genus Huawei phone utilized a high-gain antenna integrated within an all-metal bezel to make connections to GEO satellites 36000 kilometers away, posing an even greater challenge in antenna design. Honor and Xiaomi swiftly followed suit with their own satellite phone-enabled smartphones in 2024. According to the current rapid development trend, we can boldly speculate that satellite communications will become a standard configuration of smartphones and bring considerable market value in the future.

VIII. Interaction Between Antennas and the Human Body

As mobile phones are usually used in proximity to the human body, interactions between mobile antennas and the human body are negligible. The effect of the human body on a mobile antenna is mainly quantified as the antenna efficiency drop, and the effect of a mobile antenna on the human body is mainly quantified as the SAR. The basic principle, test method, and several controlling SAR techniques are well documented in [7]. Additionally, in [192], the user effects on mobile antennas and the mitigation techniques are summarized for the different working frequency bands. Herein, we briefly summarize the recent research on the interactions between antennas and the human body as follows.

1. E-field distributions over a large volume

As the SAR is mainly calculated from the peak E-field in the human body, reducing the peak E-field is an efficient method for reducing the SAR. In [193], a novel antenna structure, which distributes the E-field over a large volume, exhibited an almost 50% lower maximum SAR than a patch antenna. Additionally, using multiple antenna elements with different feeding amplitudes and phases can also reduce the peak E-field and thus reduce the effects of the human band and SAR [194], [195]. As shown in Figure 47, a patch antenna with two feeding amplitudes and phases can achieve high antenna efficiency on a human hand.

2. Reverse current

In [196], the concept of reverse current was proposed to decrease the electric field radiated by an antenna at the air–tissue interface and, consequently, reduce the SAR of human tissues. As shown in Figure 48, with reverse current, the 10

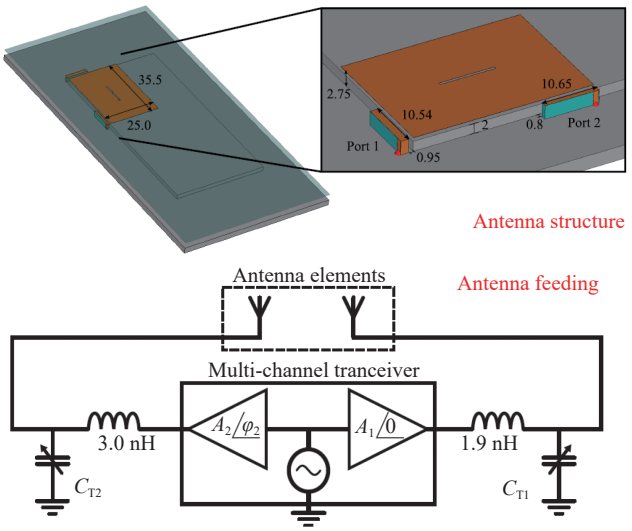

Figure 47 High antenna-on-hand efficiency with two feeding amplitude and phase [195].

g spatial average body SAR can decrease from 0.95 W/kg to 0.65 W/kg at 897.6 MHz [196]. Additionally, the concept of reverse current has also been applied to reduce the SAR for 5G MIMO antennas on mobile phones [197] and tablet devices [198].

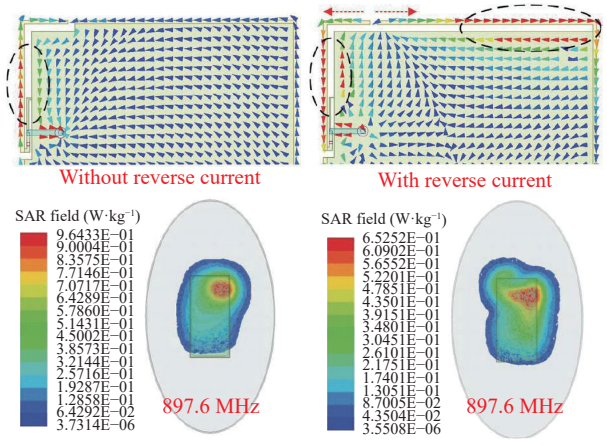

Figure 48 Reverse current to reduce the SAR [196].

3. Vertical E-field

In [199], the interaction principle of antenna radiation fields with nearby human bodies are analyzed by using electromagnetic boundary conditions. Under these boundary conditions, the horizontal E-field penetrates human tissue more easily than the vertical E-field does [199], as shown in Figure 49. Thus, mobile antennas with a vertical E-field have a higher on-body efficiency and lower SAR. As shown in Figure 50, a smartwatch antenna with a vertical E-field has a weak E-field in the human body, thus, the performance of an antenna with a vertical E-field is approximately 4 dB greater than that of an antenna with a horizontal E-field [200], [201]. Additionally, the vertical E-field method can also be applied to ear-bar TWS earphones, which can improve the antenna performance from 19.1% to 30.9% with a vertical E-field [202].

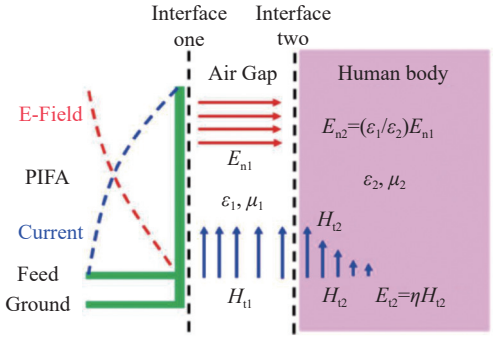

Figure 49 Interaction principle of the antenna radiation fields with a nearby human body [199].

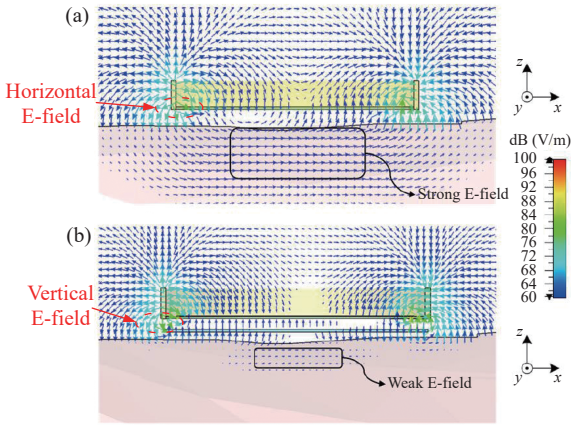

Figure 50 Horizontal and vertical E-field distributions of the smartwatch antenna on the human body [200]. (a) Horizontal E-filed; (b) Vertical E-field.

4. Characteristic modes of the PEC-lossy dielectric

In [203], the characteristic modes of a mobile antenna and human hand combination were analyzed to find the desired modes with good radiation properties. Thus, high antenna-on-hand efficiency is achieved with efficient excitation of these modes by the proper feeding method as shown in Figure 51. Additionally, the characteristic modes of composite PEC-lossy dielectric structures are calculated to achieve a low modal coupling coefficient to the human body, thus, a low-SAR antenna is achieved [204], [205]. In addition, shaping the radiation patterns has been proposed to reduce the effect of hand movement on a mobile antenna [206]. Reference [206] shows that the modes with less radiation in the boresight and backward directions are more robust to hands.

IX. Future of Antenna Design for Mobile Phones

As mobile communication technology continues to rapidly evolve and new applications, technologies, designs, and processes advance, the future of mobile phone antenna design will lean toward flexibility, integration, and intelli-

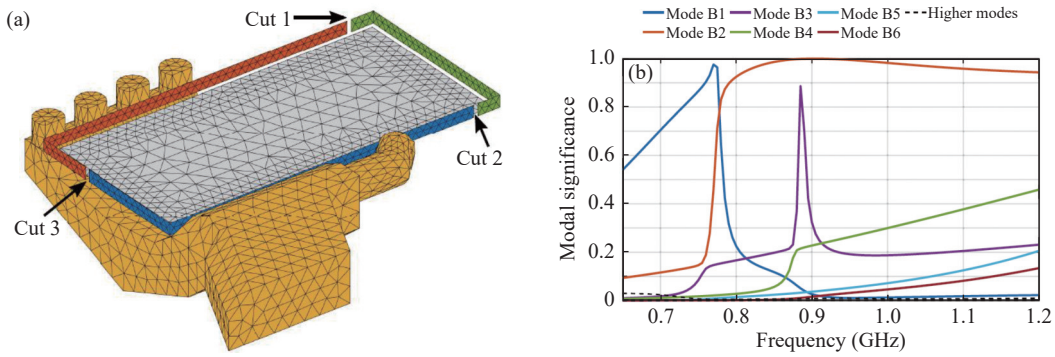

Figure 51 Characteristic modes of the mobile antenna and hand combination [203]. (a) Antenna structure; (b) Modal significances.

gence. The three key drivers of this evolution can be summarized as follows:

First, new user scenarios are driving mobile phone antenna innovation. The arrival of 5.5G and 6G will open up a range of new business scenarios, including augmented reality, cloud services, and holographic displays. These scenarios place extreme requirements on the communication traffic, communication delay, and communication reliability. To meet these challenges, next-generation mobile phone antenna design will shift toward higher frequency bands, wider bandwidths, and increased functionality. The communication band will transition from the millimeter wave to THz bands, allowing for increased communication bandwidth and data rates. However, higher-band antennas, will face more comprehensive design, process, and architecture challenges than traditional lower-band antennas. In terms of communication bandwidth, how to achieve wider antenna bandwidth and higher antenna efficiency within the ultimate design space remains a considerable challenge in mobile phone antenna design. Therefore, breakthroughs in antenna theory and system design should be sought in the future to address this issue. In terms of application scenarios, future mobile phone antennas will support a range of functions such as cellular communication, short-range communication, satellite communication, satellite navigation, and object perception. As the number of operating bands and antennas continues to increase, integrated antenna design will also undergo an important evolution in mobile phone antenna technology. Additionally, exploring more design space, such as on-screen antennas and back-cover antennas, will help alleviate the design pressure caused by the growing number of antennas.

Second, intelligence is driving mobile phone antenna innovation. The rapid development of artificial intelligence and large model technology is shaping communication intelligence as a key evolutionary direction for future 6G mobile communication. In the future, mobile phone antenna design will integrate with large-scale communication models, providing intelligent and flexible antenna configuration options that align with user usage scenarios. All antenna will be able to cooperate and support each other. In certain scenarios, all antennas can be aggregated to enhance antenna performance in a certain frequency band, solving the problems of weak signals and small throughput encountered in high-speed rail, subway, garage, and other scenarios, and facilitating full coverage without dead ends. Furthermore, the integration of artificial intelligence with mobile phone antenna design to achieve intelligent antenna design is also an important direction for the future evolution of mobile phone antenna technology.

Third, industrial design is driving mobile phone antenna innovation. The trend toward larger-screen mobile phones has led to the gradual evolution of the mobile phone form from a single straight screen to folding screens, scroll screens, flexible screens, and other new formats. However, the design of mobile phone antennas in these new forms presents considerable challenges, as the antenna needs to be carefully designed and flexibly reconstructed to achieve optimal performance in various states. As flexible wearable mobile phones will become more common in the future, the interaction between the antenna and the human body will further increase. Therefore, an antenna design with low human body absorption will be a key technology for future mobile phone antennas design. In addition, since the launch of the iPhone 4, the design concept of using metal frame slits as the main radiator of mobile phone antennas has remained prevalent, but with the pursuit of modern industrial aesthetics for mobile phone seamlessness, overcoming the traditional design of mobile phone antennas is also a problem and challenge.

X. Conclusion

In this review paper, the design challenges of mobile antennas for modern mobile phones are first described. Because metal-bezel mobile phones have become mainstream, antenna types suitable for metal-bezel mobile phones, including IFAs, slot antennas, loop antennas, and PIFAs, are studied according to their structures, modes, and potential bandwidths. Then, the commonly used methods of loading materials, meander lines, loading inductors, and matching circuits for reducing the antenna size and widening the antenna branch width, multiple modes and multiple branches, matching circuits, and reconfigurable methods for widening the bandwidth are clearly summarized. For the challenge of integration with high isolation, the commonly used methods of spatial layout, orthogonal mode, parasitic ele-

ment, decoupling network, neutralization line, and common mode and differential mode theory are carefully summarized. Recent progress on mm-wave arrays are summarized according to the categories of broadside arrays, endfire arrays, and the codesign of mm-wave arrays with industrial design and low-band antennas. Additionally, the recent progress on satellite communication antennas are summarized according to the categories of single satellite communication antennas and codesigns of the satellite communication antennas and cellular antennas. Recent new methods for determining the interaction between antennas and the human body include the use of E-field distributions over a large volume, reverse current, the vertical E-field, and the characteristic modes of PEC-lossy dielectrics. Finally, the future challenge of antenna design for mobile phones is briefly summarized. In summary, we hope this review paper can provide a systematic understanding of antenna design for modern mobile phones.

Acknowledgements

This work was supported by the National Natural Science Foundation of China (Grant Nos. 62101133, 62271279, 62271282), the Natural Science Foundation of Shanghai (Grant No. 21ZR1406800), and the Shanghai Rising Star Program (Grant No. 22QC1400100). The authors would like to thank Lin Shi, Wangxian Zhao, Xiaoxue Fan, Sisi Rao, and Huici Huang of Fudan University for their help in preparing the material.

References

[1] Defense Innovation Marketplace, "Emerging science and technology trends: 2016–2045," Available at: https://defenseinnovationmarketplace.dtic.mil/wp-content/uploads/2018/02/2016_SciTechReport_16June2016.pdf, 2023-11-5.

[2] International Data Corporation, "Worldwide smartphone forecast," Available at: https://www.idc.com/getdoc.jsp?containerId=prUS51430223, 2023-11-5.

[3] "Motorola DynaTAC phone," Available at: https://en.wikipedia.org/wiki/Motorola_DynaTAC, 2023-11-5.

[4] "Motorola MicroTAC phone," Available at: https://en.wikipedia.org/wiki/Motorola_MicroTAC, 2023-11-5.

[5] "Nokia 3210 phone," Available at: https://en.wikipedia.org/wiki/Nokia_3210, 2023-11-5.

[6] "iPhone 5 phone," Available at: https://en.wikipedia.org/wiki/IPhone_5, 2023-11-5.

[7] Z. J. Zhang, *Antenna Design for Mobile Devices*, 2nd ed., Wiley–IEEE Press, Piscataway, NJ, USA, 2017.

[8] B. S. Collins, "Handset antennas," in *Antennas for Portable Devices*, Z. N. Chen, Ed. Wiley, Hoboken, NJ, USA, 2007.

[9] Z. N. Ying, M. Ohtsuka, Y. Nishioka, *et al*., "Antennas for mobile terminals," in *Mobile Antenna System Handbook*, 3rd ed., Artech House, Norwood, MA, USA, 2008.

[10] H. Morishita, Y. Kim, and K. Fujimoto, "Design concept of antennas for small mobile terminals and the future perspective," *IEEE Antennas and Propagation Magazine*, vol. 44, no. 5, pp. 30–43, 2002.

[11] C. Rowell and E. Y. Lam, "Mobile-Phone antenna design," *IEEE Antennas and Propagation Magazine*, vol. 54, no. 4, pp. 14–34, 2012.

[12] Z. N. Ying, "Antennas in cellular phones for mobile communications," *Proceedings of the IEEE*, vol. 100, no. 7, pp. 2286–2296, 2012.

[13] H. Y. Wang, "Overview of future antenna design for mobile terminals," *Engineering*, vol. 11, pp. 12–14, 2022.

[14] W. B. Hong, "Solving the 5G mobile antenna puzzle: Assessing future directions for the 5G mobile antenna paradigm shift," *IEEE Microwave Magazine*, vol. 18, no. 7, pp. 86–102, 2017.

[15] User Equipment (UE) Radio Transmission and Reception; Part 2: Range 2 Standalone (Release 15), document TS38.101–2 v15.0. 0, 2018.

[16] K. Zhao, S. Zhang, Z. Ho, *et al*., "Spherical coverage characterization of 5G millimeter wave user equipment with 3GPP specifications," *IEEE Access*, vol. 7, pp. 4442–4452, 2019.

[17] 3GPP, "Solutions for NR to support non-terrestrial net-works (NTN)," V16.2. 0, 2023.

[18] J. Q. Zhu, Y. L. Ban, C. Y. D. Sim, *et al*., "NFC antenna with nonuniform meandering line and partial coverage ferrite sheet for metal cover smartphone applications," *IEEE Transactions on Antennas and Propagation*, vol. 65, no. 6, pp. 2827–2835, 2017.

[19] J. Q. Zhu, Y. L. Ban, R. M. Xu, *et al*., "Miniaturized dual-loop NFC antenna with a very small slot clearance for metal-cover smartphone applications," *IEEE Transactions on Antennas and Propagation*, vol. 66, no. 3, pp. 1553–1558, 2018.

[20] J. Q. Zhu, Y. L. Ban, R. M. Xu, *et al*., "A useful methodology to convert the smartphone metal cover into an antenna booster for NFC applications," *IEEE Transactions on Antennas and Propagation*, vol. 67, no. 7, pp. 4463–4473, 2019.

[21] Y. J. Zhang, Y. Li, M. Z. Hu, *et al*., "Dual-band circular-polarized microstrip antenna for ultrawideband positioning in smartphones with flexible liquid crystal polymer process," *IEEE Transactions on Antennas and Propagation*, vol. 71, no. 4, pp. 3155–3163, 2023.

[22] C. Z. Han, G. L. Huang, T. Yuan, *et al*., "A frequency-reconfigurable tuner-loaded coupled-fed frame-antenna for all-metal-shell handsets," *IEEE Access*, vol. 6, pp. 64041–64049, 2018.

[23] F. H. Chu and K. L. Wong, "Internal coupled-fed dual-loop antenna integrated with a USB connector for WWAN/LTE mobile handset," *IEEE Transactions on Antennas and Propagation*, vol. 59, no. 11, pp. 4215–4221, 2011.

[24] Q. X. Guo, R. Mittra, F. Lei, *et al*., "Interaction between internal antenna and external antenna of mobile phone and hand effect," *IEEE Transactions Antennas and Propagation*, vol. 61, no. 2, pp. 862–870, 2013.

[25] K. Payandehjoo and R. Abhari, "Compact multi-band PIFAs on a semi-populated mobile handset with tunable isolation," *IEEE Transactions on Antennas and Propagation*, vol. 61, no. 9, pp. 4814–4819, 2013.

[26] L. J. Chu, "Physical limitations of omni-directional antennas," *Journal of Applied Physics*, vol. 19, no. 12, pp. 1163–1175, 1948.

[27] W. Geyi, "Physical limitations of antenna," *IEEE Transactions on Antennas and Propagation*, vol. 51, no. 8, pp. 2116–2123, 2003.

[28] K. L. Wong, *Compact and Broadband Microstrip Antennas*. John Wiley & Sons, Inc, New York, NY, USA, 2002.

[29] Y. J. Ren, "Ceramic based small LTE MIMO handset antenna," *IEEE Transactions on Antennas and Propagation*, vol. 61, no. 2, pp. 934–938, 2013.

[30] J. Lee, J. Heo, J. Lee, *et al*., "Design of small antennas for mobile handsets using magneto-dielectric material," *IEEE Transactions on Antennas and Propagation*, vol. 60, no. 4, pp. 2080–2084, 2012.

[31] B. Y. Park, M. H. Jeong, and S. O. Park, "A magneto-dielectric handset antenna for LTE/WWAN/GPS applications," *IEEE Antennas and Wireless Propagation Letters*, vol. 13, pp. 1482–1485, 2014.

[32] Y. Li, Z. J. Zhang, J. F. Zheng, *et al*., "Compact heptaband reconfigurable loop antenna for mobile handset," *IEEE Antennas and Wireless Propagation Letters*, vol. 10, pp. 1162–1165, 2011.

[33] H. T. Chen, K. L. Wong, and T. W. Chiou, "PIFA with a meandered and folded patch for the dual-band mobile phone applica-

tion," *IEEE Transactions on Antennas and Propagation*, vol. 51, no. 9, pp. 2468–2471, 2003.
[34] K. L. Wong and S. C. Chen, "Printed single-strip monopole using a chip inductor for penta-band WWAN operation in the mobile phone," *IEEE Transactions on Antennas and Propagation*, vol. 58, no. 3, pp. 1011–1014, 2010.
[35] Y. L. Ban, C. L. Liu, J. L. W. Li, *et al*., "Small-size wideband monopole with distributed inductive strip for seven-band WWAN/LTE mobile phone," *IEEE Antennas and Wireless Propagation Letters*, vol. 12, pp. 7–10, 2013.
[36] C. J. Deng, Z. Xu, A. D. Ren, *et al*., "TCM-based bezel antenna design with small ground clearance for mobile terminals," *IEEE Transactions on Antennas and Propagation*, vol. 67, no. 2, pp. 745–754, 2019.
[37] Y. Liu, W. Cui, Y. T. Jia, *et al*., "Hepta-band metal-frame antenna for LTE/WWAN full-screen smartphone," *IEEE Antennas and Wireless Propagation Letters*, vol. 19, no. 7, pp. 1241–1245, 2020.
[38] L. W. Chen, Y. Huang, H. Y. Wang, *et al*., "A reconfigurable metal rim antenna with smallest clearance for smartphone applications," *IEEE Access*, vol. 10, pp. 112250–112260, 2022.
[39] D. W. Huang and Z. W. Du, "Eight-band antenna with a small ground clearance for LTE metal-frame mobile phone applications," *IEEE Antennas and Wireless Propagation Letters*, vol. 17, no. 1, pp. 34–37, 2018.
[40] K. L. Wong and L. Y. Chen, "Small-size LTE/WWAN tablet device antenna with two hybrid feeds," *IEEE Transactions on Antennas and Propagation*, vol. 62, no. 6, pp. 2926–2934, 2014.
[41] Y. Liu, Y. Luo, and S. X. Gong, "An antenna with a stair-like ground branch for octa-band narrow-frame mobile phone," *IEEE Antennas and Wireless Propagation Letters*, vol. 17, no. 8, pp. 1542–1546, 2018.
[42] X. Y. Tian and Z. W. Du, "Dual-feed shared-radiator metal-frame full-screen mobile phone antenna for GPS and LTE bands with a dual-function capacitor," *IEEE Transactions on Antennas and Propagation*, vol. 71, no. 10, pp. 8314–8319, 2023.
[43] Z. Q. Xu, Q. Q. Zhou, Y. L. Ban, *et al*., "Hepta-band coupled-fed loop antenna for LTE/WWAN unbroken metal-rimmed smartphone applications," *IEEE Antennas and Wireless Propagation Letters*, vol. 17, no. 2, pp. 311–314, 2018.
[44] Y. L. Ban, Z. X. Chen, Z. Chen, *et al*., "Reconfigurable narrow-frame antenna for heptaband WWAN/LTE smartphone applications," *IEEE Antennas and Wireless Propagation Letters*, vol. 13, pp. 1365–1368, 2014.
[45] H. D. Chen, H. W. Yang, and C. Y. D. Sim, "Single open-slot antenna for LTE/WWAN smartphone application," *IEEE Transactions on Antennas and Propagation*, vol. 65, no. 8, pp. 4278–4282, 2017.
[46] Y. Wang and Z. W. Du, "Wideband monopole antenna with less nonground portion for octa-band WWAN/LTE mobile phones," *IEEE Transactions on Antennas and Propagation*, vol. 64, no. 1, pp. 383–388, 2016.
[47] Q. G. Chen, H. W. Lin, J. P. Wang, *et al*., "Single ring slot-based antennas for metal-rimmed 4G/5G smartphones," *IEEE Transactions on Antennas and Propagation*, vol. 67, no. 3, pp. 1476–1487, 2019.
[48] H. Chen and A. P. Zhao, "LTE antenna design for mobile phone with metal frame," *IEEE Antennas and Wireless Propagation Letters*, vol. 15, pp. 1462–1465, 2016.
[49] J. W. Lian, Y. L. Ban, Y. L. Yang, *et al*., "Hybrid multi-mode narrow-frame antenna for WWAN/LTE metal-rimmed smartphone applications," *IEEE Access*, vol. 4, pp. 3991–3998, 2016.
[50] L. W. Zhang, Y. L. Ban, C. Y. D. Sim, *et al*., "Parallel dual-loop antenna for WWAN/LTE metal-rimmed smartphone," *IEEE Transactions on Antennas and Propagation*, vol. 66, no. 3, pp. 1217–1226, 2018.
[51] H. Xu, H. Y. Wang, S. Gao, *et al*., "A compact and low-profile loop antenna with six resonant modes for LTE smartphone," *IEEE Transactions on Antennas and Propagation*, vol. 64, no. 9, pp. 3743–3751, 2016.
[52] D. W. Huang, Z. W. Du, and Y. Wang, "Eight-band antenna for full-screen metal frame LTE mobile phones," *IEEE Transactions on Antennas and Propagation*, vol. 67, no. 3, pp. 1527–1534, 2019.
[53] L. Shi and Y. Wang, "Eliminating the radiation efficiency local minimum for high-efficiency octa-band mobile antenna in metal-bezel smartphone," *IEEE Transactions on Antennas and Propagation*, in press.
[54] C. J. Deng, Y. Li, Z. J. Zhang, *et al*., "A novel low-profile hepta-band handset antenna using modes controlling method," *IEEE Transactions on Antennas and Propagation*, vol. 63, no. 2, pp. 799–804, 2015.
[55] I. R. R. Barani and K. L. Wong, "Integrated inverted-f and open-slot antennas in the metal-framed smartphone for 2×2 LTE LB and 4×4 LTE M/HB MIMO operations," *IEEE Transactions on Antennas and Propagation*, vol. 66, no. 10, pp. 5004–5012, 2018.
[56] K. L. Wong and C. Y. Tsai, "Half-loop frame antenna for the LTE metal-casing tablet device," *IEEE Transactions on Antennas and Propagation*, vol. 65, no. 1, pp. 71–81, 2017.
[57] Y. Liu, J. K. Zhang, A. D. Ren, *et al*., "TCM-based hepta-band antenna with small clearance for metal-rimmed mobile phone applications," *IEEE Antennas and Wireless Propagation Letters*, vol. 18, no. 4, pp. 717–721, 2019.
[58] K. X. Liu, D. Yu, and H. Y. Wang, "Investigation on the radiation efficiency local minimum in open-slot and T-shaped antennas," *IEEE Transactions on Antennas and Propagation*, vol. 69, no. 9, pp. 5257–5268, 2021.
[59] W. X. Zhao and Y. Wang, "A shared-branch eleven-band mobile antenna with a 0.5-mm clearance for metal-bezel mobile phones covering all the 4G LTE and 5G NR bands," *IEEE Transactions on Antennas and Propagation*, vol. 72, no. 4, pp. 3748–3753, 2024.
[60] C. J. Deng, Y. Li, Z. J. Zhang, *et al*., "Planar Printed multi-resonant antenna for octa-band WWAN/LTE Mobile handset," *IEEE Antennas and Wireless Propagation Letters*, vol. 14, pp. 1734–1737, 2015.
[61] Y. Li, Z. J. Zhang, W. H. Chen, *et al*., "A switchable matching circuit for compact wideband antenna designs," *IEEE Transactions on Antennas and Propagation*, vol. 58, no. 11, pp. 3450–3457, 2010.
[62] Y. H. Yang, Z. Q. Zhao, W. Yang, *et al*., "Compact multimode monopole antenna for metal-rimmed mobile phones," *IEEE Transactions on Antennas and Propagation*, vol. 65, no. 5, pp. 2297–2304, 2017.
[63] Y. Liu, Y. M. Zhou, G. F. Liu, *et al*., "Heptaband inverted-F antenna for metal-rimmed mobile phone applications," *IEEE Antennas and Wireless Propagation Letters*, vol. 15, pp. 996–999, 2016.
[64] P. Y. Qiu and Q. Y. Feng, "Low-profile compact antenna for octa-band metal-rimmed mobile phone applications," *IEEE Transactions on Antennas and Propagation*, vol. 68, no. 1, pp. 54–61, 2020.
[65] Y. Li, Z. J. Zhang, J. F. Zheng, *et al*., "A compact hepta-band loop-inverted F reconfigurable antenna for mobile phone," *IEEE Transactions on Antennas and Propagation*, vol. 60, no. 1, pp. 389–392, 2012.
[66] M. Stanley, Y. Huang, H. Y. Wang, *et al*., "A novel reconfigurable metal rim integrated open slot antenna for octa-band smartphone applications," *IEEE Transactions on Antennas and Propagation*, vol. 65, no. 7, pp. 3352–3363, 2017.
[67] W. X. Zhao and Y. Wang, "A reconfigurable antenna with one slit and a small clearance for nona-band metal-bezel mobile phones," *IEEE Transactions on Antennas and Propagation*, vol. 71, no. 9, pp. 7172–7183, 2023.
[68] C. Z. Han, S. M. Liao, K. D. Hong, *et al*., "A frequency-reconfigurable antenna with 1-mm nonground portion for metal-frame and full-display screen handset applications using mode control method," *IEEE Access*, vol. 7, pp. 48037–48045, 2019.

[69] Chow-Yen-Desmond Sim, Gang-Yan Fan, and Yu-Hsuan Lin, "Compact Size Printed Reconfigurable Antenna Design with Slotted Ground Structure", *2019 8th Asia-Pacific Conference on Antennas and Propagation (APCAP)*, Incheon, Korea, pp.567-568, 2019.

[70] S. R. Yang and Q. L. Yang, "A reconfigurable LTE full-band antenna for smartphones with high screen-to-body ratio," *IEEE Antennas and Wireless Propagation Letters*, vol. 21, no. 6, pp. 1075–1079, 2022.

[71] F. de Flaviis, L. Jofre, J. Romeu, *et al., Multiantenna Systems for MIMO Communications*. Morgan & Claypool Publishers, San Rafael, CA, USA, 2008.

[72] S. S. Alja'afreh, Y. Huang, L. Xing, *et al*., "A low-profile and wideband PILA-based antenna for handset diversity applications," *IEEE Antennas and Wireless Propagation Letters*, vol. 14, pp. 923–926, 2015.

[73] K. Wang, R. A. M. Mauermayer, and T. F. Eibert, "Contour-integrated dual-band compact antenna elements and arrays for low-profile mobile terminals," *IEEE Transactions on Antennas and Propagation*, vol. 63, no. 7, pp. 3305–3311, 2015.

[74] Y. X. Li, C. Y. D. Sim, Y. Luo, *et al*., "High-isolation 3.5 GHz eight-antenna MIMO array using balanced open-slot antenna element for 5G smartphones," *IEEE Transactions on Antennas and Propagation*, vol. 67, no. 6, pp. 3820–3830, 2019.

[75] D. Q. Liu, H. J. Luo, M. Zhang, *et al*., "An extremely low-profile wideband MIMO antenna for 5G smartphones," *IEEE Transactions on Antennas Propagation*, vol. 67, no. 9, pp. 5772–5780, 2019.

[76] X. M. Chen, J. L. Wang, and L. Chang, "Extremely low-profile dual-band microstrip patch antenna using electric coupling for 5G mobile terminal applications," *IEEE Transactions on Antennas and Propagation*, vol. 71, no. 2, pp. 1895–1900, 2023.

[77] X. Zhao, S. P. Yeo, and L. C. Ong, "Decoupling of inverted-F antennas with high-order modes of ground plane for 5G mobile MIMO platform," *IEEE Transactions on Antennas and Propagation*, vol. 66, no. 9, pp. 4485–4495, 2018.

[78] X. Wang, Z. H. Feng, and K. M. Luk, "Pattern and polarization diversity antenna with high isolation for portable wireless devices," *IEEE Antennas and Wireless Propagation Letters*, vol. 8, pp. 209–211, 2009.

[79] C. F. Ding, X. Y. Zhang, C. D. Xue, *et al*., "Novel pattern-diversity-based decoupling method and its application to multielement MIMO antenna," *IEEE Transactions on Antennas and Propagation*, vol. 66, no. 10, pp. 4976–4985, 2018.

[80] K. K. Kishor and S. V. Hum, "A two-port chassis-mode MIMO antenna," *IEEE Antennas and Wireless Propagation Letters*, vol. 12, pp. 690–693, 2013.

[81] H. Li, Z. T. Miers, and B. K. Lau, "Design of orthogonal MIMO handset antennas based on characteristic mode manipulation at frequency bands below 1 GHz," *IEEE Transactions on Antennas and Propagation*, vol. 62, no. 5, pp. 2756–2766, 2014.

[82] C. J. Deng, Z. H. Feng, and S. V. Hum, "MIMO mobile handset antenna merging characteristic modes for increased bandwidth," *IEEE Transactions on Antennas and Propagation*, vol. 64, no. 7, pp. 2660–2667, 2016.

[83] J. F. Qian, S. Gao, B. Sanz-Izquierdo, *et al*., "Mutual coupling suppression between two closely placed patch antennas using higher-order modes," *IEEE Transactions on Antennas and Propagation*, vol. 71, no. 6, pp. 4686–4694, 2023.

[84] Z. Y. Li, Z. W. Du, M. Takahashi, *et al*., "Reducing mutual coupling of MIMO antennas with parasitic elements for mobile terminals," *IEEE Transactions on Antennas and Propagation*, vol. 60, no. 2, pp. 473–481, 2012.

[85] Y. Wang and Z. W. Du, "A printed dual-antenna system operating in the GSM1800/GSM1900/UMTS/LTE2300/LTE2500/2.4-GHz WLAN bands for mobile terminals," *IEEE Antennas and Wireless Propagation Letters*, vol. 13, pp. 233–236, 2014.

[86] J. W. Sui, C. X. Huang, and Y. F. Cheng, "Multi-element fully decoupled inverted-F antennas for mobile terminals," *IEEE Transactions on Antennas and Propagation*, vol. 70, no. 11, pp. 10076–10085, 2022.

[87] S. W. Su, C. T. Lee, and Y. W. Hsiao, "Compact two-inverted-F-antenna system with highly integrated π-shaped decoupling structure," *IEEE Transactions on Antennas and Propagation*, vol. 67, no. 9, pp. 6182–6186, 2019.

[88] A. F. Zhang, K. P. Wei, Q. Guan, *et al*., "Compactly placed high-isolated antenna pair with independent control of decoupling amplitude and phase," *IEEE Transactions on Antennas and Propagation*, vol. 71, no. 3, pp. 2814–2819, 2023.

[89] M. Z. Hu and Y. Li, "Wideband back cover microstrip antenna with multiple shorting vias for mobile 5G MIMO applications," *IEEE Transactions on Antennas and Propagation*, vol. 71, no. 10, pp. 8290–8295, 2023.

[90] Y. L. Ban, S. Yang, Z. Chen, *et al*., "Decoupled planar WWAN antennas with T-shaped protruded ground for smartphone applications," *IEEE Antennas and Wireless Propagation Letters*, vol. 13, pp. 483–486, 2014.

[91] S. Wang and Z. W. Du, "A multiband dual-antenna system with a folded fork-shaped ground branch and folded asymmetric U-shaped slots for smartphone applications," *IEEE Antennas and Wireless Propagation Letters*, vol. 14, pp. 1626–1629, 2015.

[92] S. Wang and Z. W. Du, "A dual-antenna system for LTE/WWAN/WLAN/WiMAX smartphone applications," *IEEE Antennas and Wireless Propagation Letters*, vol. 14, pp. 1443–1446, 2015.

[93] S. C. Chen, Y. S. Wang, and S. J. Chung, "A decoupling technique for increasing the port isolation between two strongly coupled antennas," *IEEE Transactions on Antennas and Propagation*, vol. 56, no. 12, pp. 3650–3658, 2008.

[94] Y. Chen, C. Z. Hua, Y. L. Lu, *et al*., "A bandwidth-enhanced tunable decoupling method for compact mobile terminal antennas," *IEEE Transactions on Antennas and Propagation*, vol. 70, no. 8, pp. 6455–6468, 2022.

[95] M. Li, L. J. Jiang, and K. L. Yeung, "Novel and efficient parasitic decoupling network for closely coupled antennas," *IEEE Transactions on Antennas and Propagation*, vol. 67, no. 6, pp. 3574–3585, 2019.

[96] L. Y. Zhao, L. K. Yeung, and K. L. Wu, "A coupled resonator decoupling network for two-element compact antenna arrays in mobile terminals," *IEEE Transactions on Antennas and Propagation*, vol. 62, no. 5, pp. 2767–2776, 2014.

[97] H. Makimura, K. Nishimoto, T. Yanagi, *et al*, "Novel decoupling concept for strongly coupled frequency-dependent antenna arrays," *IEEE Transactions on Antennas and Propagation*, vol. 65, no. 10, pp. 5147–5154, 2017.

[98] L. Y. Zhao and K. L. Wu, "A dual-band coupled resonator decoupling network for two coupled antennas," *IEEE Transactions on Antennas and Propagation*, vol. 63, no. 7, pp. 2843–2850, 2015.

[99] Z. T. Wang and Q. Wu, "A novel decoupling feeding network for circularly polarized patch arrays using orthogonal mode decomposition," *IEEE Transactions on Antennas and Propagation*, vol. 71, no. 2, pp. 1448–1457, 2023.

[100] A. Diallo, C. Luxey, P. Le Thuc, *et al*., "Study and reduction of the mutual coupling between two mobile phone PIFAs operating in the DCS1800 and UMTS bands," *IEEE Transactions on Antennas and Propagation*, vol. 54, no. 11, pp. 3063–3074, 2006.

[101] Y. Wang and Z. W. Du, "A wideband printed dual-antenna system with a novel neutralization line for mobile terminals," *IEEE Antennas and Wireless Propagation Letters*, vol. 12, pp. 1428–1431, 2013.

[102] Y. Wang and Z. W. Du, "A wideband printed dual-antenna with three neutralization lines for mobile terminals," *IEEE Transactions on Antennas and Propagation*, vol. 62, no. 3, pp. 1495–1500, 2014.

[103] Y. L. Ban, Z. X. Chen, Z. Chen, *et al*., "Decoupled hepta-band antenna array for WWAN/LTE smartphone applications," *IEEE An-*

tennas and Wireless Propagation Letters, vol. 13, pp. 999–1002, 2014.

[104] S. Wang and Z. W. Du, "Decoupled dual-antenna system using crossed neutralization lines for LTE/WWAN smartphone applications," *IEEE Antennas and Wireless Propagation Letters*, vol. 14, pp. 523–526, 2015.

[105] Y. Wang and Z. W. Du, "Octaband WWAN/LTE dual-antenna system decoupled by two neutralization lines with inductors for smart phones," *International Journal of Antennas and Propagation*, vol. 2021, article no. 1609263, 2021.

[106] L. Chang and H. Y. Wang, "Miniaturized wideband four-antenna module based on dual-mode PIFA for 5G 4×4 MIMO applications," *IEEE Transactions on Antennas and Propagation*, vol. 69, no. 9, pp. 5297–5304, 2021.

[107] L. B. Sun, H. G. Feng, Y. Li, *et al*., "Compact 5G MIMO mobile phone antennas with tightly arranged orthogonal-mode pairs," *IEEE Transactions on Antennas and Propagation*, vol. 66, no. 11, pp. 6364–6369, 2018.

[108] L. B. Sun, H. G. Feng, Y. Li, *et al*., "Tightly arranged orthogonal mode antenna for 5G MIMO mobile terminal," *Microwave and Optical Technology Letters*, vol. 60, no. 7, pp. 1751–1756, 2018.

[109] H. Xu, S. S. Gao, H. Zhou, *et al*., "A highly integrated MIMO antenna unit: Differential/common mode design," *IEEE Transactions on Antennas and Propagation*, vol. 67, no. 11, pp. 6724–6734, 2019.

[110] Z. Xu and C. J. Deng, "High-isolated MIMO antenna design based on pattern diversity for 5G mobile terminals," *IEEE Antennas and Wireless Propagation Letters*, vol. 19, no. 3, pp. 467–471, 2020.

[111] L. Chang, Y. F. Yu, K. P. Wei, *et al*., "Polarization-orthogonal co-frequency dual antenna pair suitable for 5G MIMO smartphone with metallic bezels," *IEEE Transactions on Antennas and Propagation*, vol. 67, no. 8, pp. 5212–5220, 2019.

[112] A. D. Ren, Y. Liu, and C. Y. D. Sim, "A compact building block with two shared-aperture antennas for eight-antenna MIMO array in metal-rimmed smartphone," *IEEE Transactions on Antennas and Propagation*, vol. 67, no. 10, pp. 6430–6438, 2019.

[113] C. Z. Han, L. Xiao, Z. Chen, *et al*., "Co-located self-neutralized handset antenna pairs with complementary radiation patterns for 5G MIMO applications," *IEEE Access*, vol. 8, pp. 73151–73163, 2020.

[114] L. Chang, Y. F. Yu, K. P. Wei, *et al*., "Orthogonally polarized dual antenna pair with high isolation and balanced high performance for 5G MIMO smartphone," *IEEE Transactions on Antennas and Propagation*, vol. 68, no. 5, pp. 3487–3495, 2020.

[115] H. Y. Piao, Y. N. Jin, and L. Y. Qu, "A compact and straightforward self-decoupled MIMO antenna system for 5G applications," *IEEE Access*, vol. 8, pp. 129236–129245, 2020.

[116] L. B. Sun, Y. Li, Z. J. Zhang, *et al*., "Wideband 5G MIMO antenna with integrated orthogonal-mode dual-antenna pairs for metal-rimmed smartphones," *IEEE Transactions on Antennas and Propagation*, vol. 68, no. 4, pp. 2494–2503, 2020.

[117] L. B. Sun, Y. Li, Z. J. Zhang, *et al*., "Self-decoupled MIMO antenna pair with shared radiator for 5G smartphones," *IEEE Transactions on Antennas and Propagation*, vol. 68, no. 5, pp. 3423–3432, 2020.

[118] L. B. Sun, Y. Li, Z. J. Zhang, *et al*., "Antenna decoupling by common and differential modes cancellation," *IEEE Transactions on Antennas and Propagation*, vol. 69, no. 2, pp. 672–682, 2021.

[119] L. B. Sun, Y. Li, and Z. J. Zhang, "Wideband decoupling of integrated slot antenna pairs for 5G smartphones," *IEEE Transactions on Antennas and Propagation*, vol. 69, no. 4, pp. 2386–2391, 2021.

[120] L. B. Sun, Y. Li, and Z. J. Zhang, "Decoupling between extremely closely spaced patch antennas by mode cancellation method," *IEEE Transactions on Antennas and Propagation*, vol. 69, no. 6, pp. 3074–3083, 2021.

[121] L. B. Sun, Y. Li, and Z. J. Zhang, "Wideband integrated quad-element MIMO antennas based on complementary antenna pairs for 5G smartphones," *IEEE Transactions on Antennas and Propagation*, vol. 69, no. 8, pp. 4466–4474, 2021.

[122] J. D. Hu, W. Q. Zhang, Y. Li, *et al*., "Compact co-polarized PIFAs for full-duplex application based on CM/DM cancellation theory," *IEEE Transactions on Antennas and Propagation*, vol. 69, no. 11, pp. 7103–7110, 2021.

[123] W. Q. Zhang, Y. Li, K. P. Wei, *et al*., "A two-port microstrip antenna with high isolation for Wi-Fi 6 and Wi-Fi 6E applications," *IEEE Transactions on Antennas and Propagation*, vol. 70, no. 7, pp. 5227–5234, 2022.

[124] A. F. Zhang, K. P. Wei, Y. W. Hu, *et al*., "High-isolated coupling-grounded patch antenna pair with shared radiator for the application of 5G mobile terminals," *IEEE Transactions on Antennas and Propagation*, vol. 70, no. 9, pp. 7896–7904, 2022.

[125] A. F. Zhang, K. P. Wei, and Z. J. Zhang, "Multiband and wideband self-multipath decoupled antenna pairs," *IEEE Transactions on Antennas and Propagation*, vol. 71, no. 7, pp. 5605–5615, 2023.

[126] I. Syrytsin, S. Zhang, G. F. Pedersen, *et al*., "Statistical investigation of the user effects on mobile terminal antennas for 5G applications," *IEEE Transactions on Antennas and Propagation*, vol. 65, no. 12, pp. 6596–6605, 2017.

[127] L. B. Sun, Y. F. Hou, Y. Li, *et al*., "An Open Cavity Leaky-Wave Antenna With Vertical-Polarization Endfire Radiation," *IEEE Transactions on Antennas and Propagation*, vol. 67, no. 5, pp. 3455–3460, 2019.

[128] W. B. Hong, K. H. Baek, and S. Ko, "Millimeter-wave 5G antennas for smartphones: Overview and experimental demonstration," *IEEE Transactions on Antennas and Propagation*, vol. 65, no. 12, pp. 6250–6261, 2017.

[129] Y. Wang and F. Xu, "Shared aperture 4G LTE and 5G mm-wave antenna in mobile phones with enhanced mm-wave radiation in the display direction," *IEEE Transactions on Antennas and Propagation*, vol. 71, no. 6, pp. 4772–4782, 2023.

[130] Y. Q. Zhang, W. C. Yang, Q. Xue, *et al*., "Broadband dual-polarized differential-fed filtering antenna array for 5G millimeter-wave applications," *IEEE Transactions on Antennas and Propagation*, vol. 70, no. 3, pp. 1989–1998, 2022.

[131] J. Park, S. Y. Lee, J. Kim, *et al*., "An optically invisible antenna-on-display concept for millimeter-wave 5G cellular devices," *IEEE Transactions on Antennas and Propagation*, vol. 67, no. 5, pp. 2942–2952, 2019.

[132] J. C. Chen, M. Berg, K. Rasilainen, *et al*., "Broadband cross-slotted patch antenna for 5G millimeter-wave applications based on characteristic mode analysis," *IEEE Transactions on Antennas and Propagation*, vol. 70, no. 12, pp. 11277–11292, 2022.

[133] C. Y. D. Sim, J. Jr. Lo, and Z. N. Chen, "Design of a broadband millimeter-wave array antenna for 5G applications," *IEEE Antennas and Wireless Propagation Letters*, vol. 22, no. 5, pp. 1030–1034, 2023.

[134] T. Zhang, L. M. Li, M. Xie, *et al*., "Low-cost aperture-coupled 60-GHz-phased array antenna package with compact matching network," *IEEE Transactions on Antennas and Propagation*, vol. 65, no. 12, pp. 6355–6362, 2017.

[135] R. J. Mailloux, *Phased Array Antenna Handbook*, 2nd ed., Artech House, Norwood, MA, USA, 2005.

[136] Qualcomm, "QTM545 mmWave antenna module," Accessed at: https://www.qualcomm.com/products/technology/modems/rf/qtm545-mmwave-antenna-module, 2022-07-19.

[137] X. X. Fan and Y. Wang, "Compact millimeter-wave array with wide-angle scanning for mobile phones," *IEEE Transactions on Antennas and Propagation*, vol. 71, no. 8, pp. 6983–6988, 2023.

[138] X. X. Fan and Y. Wang, "Compact wide-beam scanning dual-polarized mmWave array for mobile terminals," *IEEE Antennas and Wireless Propagation Letters*, vol. 23, no. 2, pp. 763–767, 2024.

[139] D. S. Huang, G. H. Xu, J. Wu, *et al*., "A microstrip dual-split-ring antenna array for 5G millimeter-wave dual-band applications," *IEEE Antennas and Wireless Propagation Letters*, vol. 21, no. 10,

pp. 2025–2029, 2022.
[140] S. J. Yang, S. F. Yao, R. Y. Ma, *et al*., "Low-profile dual-wideband dual-polarized antenna for 5G millimeter-wave communications," *IEEE Antennas and Wireless Propagation Letters*, vol. 21, no. 12, pp. 2367–2371, 2022.
[141] T. Hong, Z. M. Zhao, W. Jiang, *et al*., "Dual-band SIW cavity-backed slot array using TM_{020} and TM_{120} modes for 5G applications," *IEEE Transactions on Antennas and Propagation*, vol. 67, no. 5, pp. 3490–3495, 2019.
[142] R. Lu, C. Yu, Y. W. Zhu, *et al*., "Millimeter-wave dual-band dual-polarized SIW cavity-fed filtenna for 5G applications," *IEEE Transactions on Antennas and Propagation*, vol. 70, no. 11, pp. 10104–10112, 2022.
[143] W. Y. Sun, Y. Li, L. Chang, *et al*., "Dual-band dual-polarized microstrip antenna array using double-layer gridded patches for 5G millimeter-wave applications," *IEEE Transactions on Antennas and Propagation*, vol. 69, no. 10, pp. 6489–6499, 2021.
[144] S. Zhang, I. Syrytsin, and G. F. Pedersen, "Compact beam-steerable antenna array with two passive parasitic elements for 5G mobile terminals at 28 GHz," *IEEE Transactions on Antennas and Propagation*, vol. 66, no. 10, pp. 5193–5203, 2018.
[145] J. D. Hu, Y. Li, and Z. J. Zhang, "A novel reconfigurable miniaturized phase shifter for 2-D beam steering 2-bit array applications," *IEEE Microwave and Wireless Components Letters*, vol. 31, no. 4, pp. 381–384, 2021.
[146] Y. Wang, F. Xu, Y. Q. Jin, *et al*., "Low-cost reconfigurable 1 bit millimeter-wave array antenna for mobile terminals," *IEEE Transactions on Antennas and Propagation*, vol. 70, no. 6, pp. 4507–4517, 2022.
[147] S. Islam, M. Zada, and H. Yoo, "Low-profile P-I-N-diode-controlled bezel fit radiation-pattern reconfigurable antenna arrays for 5G smartphones," *IEEE Transactions on Antennas and Propagation*, vol. 71, no. 8, pp. 6470–6480, 2023.
[148] J. X. Yin, Q. Wu, C. Yu, *et al*., "Broadband endfire magnetoelectric dipole antenna array using SICL feeding network for 5G millimeter-wave applications," *IEEE Transactions on Antennas and Propagation*, vol. 67, no. 7, pp. 4895–4900, 2019.
[149] C. X. Mao, M. Khalily, P. Xiao, *et al*., "High-gain phased array antenna with endfire radiation for 26 GHz wide-beam-scanning applications," *IEEE Transactions on Antennas and Propagation*, vol. 69, no. 5, pp. 3015–3020, 2021.
[150] L. B. Sun, Y. Li, and Z. J. Zhang, "Wideband dual-polarized endfire antenna based on compact open-ended cavity for 5G mm-wave mobile phones," *IEEE Transactions on Antennas and Propagation*, vol. 70, no. 3, pp. 1632–1642, 2022.
[151] J. Park, H. Seong, Y. N. Whang, *et al*., "Energy-efficient 5G phased arrays incorporating vertically polarized endfire planar folded slot antenna for mmWave mobile terminals," *IEEE Transactions on Antennas and Propagation*, vol. 68, no. 1, pp. 230–241, 2020.
[152] J. Zhang, M. O. Akinsolu, B. Liu, *et al*., "Design of zero clearance SIW endfire antenna array using machine learning-assisted optimization," *IEEE Transactions on Antennas and Propagation*, vol. 70, no. 5, pp. 3858–3863, 2022.
[153] J. X. Wang, Y. J. Li, J. H. Wang, *et al*., "A low-profile vertically polarized magneto-electric monopole antenna with a 60% bandwidth for millimeter-wave applications," *IEEE Transactions on Antennas and Propagation*, vol. 69, no. 1, pp. 3–13, 2021.
[154] H. Kim, T. H. Jang, and C. S. Park, "60-GHz compact vertically polarized end-fire monopole-based Yagi antenna-in-package for wideband mobile communication," *IEEE Access*, vol. 10, pp. 111077–111086, 2022.
[155] X. Y. Xia, C. Yu, F. Wu, *et al*., "Millimeter-wave phased array antenna integrated with the industry design in 5G/B5G smartphones," *IEEE Transactions on Antennas and Propagation*, vol. 71, no. 2, pp. 1883–1888, 2023.
[156] R. Montoya Moreno, J. Ala-Laurinaho, A. Khripkov, *et al*., "Dual-polarized mm-wave endfire antenna for mobile devices," *IEEE Transactions on Antennas and Propagation*, vol. 68, no. 8, pp. 5924–5934, 2020.
[157] Y. W. Hsu, T. C. Huang, H. S. Lin, *et al*., "Dual-polarized quasi yagi–uda antennas with endfire radiation for millimeter-wave MIMO terminals," *IEEE Transactions on Antennas and Propagation*, vol. 65, no. 12, pp. 6282–6289, 2017.
[158] K. Sun, B. N. Wang, T. M. Yang, *et al*., "Dual-polarized millimeter-wave endfire array based on substrate integrated mode-composite transmission line," *IEEE Transactions on Antennas and Propagation*, vol. 70, no. 1, pp. 341–352, 2022.
[159] X. Y. Xia, F. Wu, C. Yu, *et al*., "Millimeter-wave ±45° dual linearly polarized end-fire phased array antenna for 5G/B5G mobile terminals," *IEEE Transactions on Antennas and Propagation*, vol. 70, no. 11, pp. 10391–10404, 2022.
[160] R. Montoya Moreno, J. Kurvinen, J. Ala-Laurinaho, *et al*., "Dual-polarized mm-wave endfire chain-slot antenna for mobile devices," *IEEE Transactions on Antennas and Propagation*, vol. 69, no. 1, pp. 25–34, 2021.
[161] R. Rodriguez-Cano, S. Zhang, K. Zhao, *et al*., "Reduction of main beam-blockage in an integrated 5G array with a metal-frame antenna," *IEEE Transactions on Antennas and Propagation*, vol. 67, no. 5, pp. 3161–3170, 2019.
[162] M. M. Samadi Taheri, A. Abdipour, S. Zhang, *et al*., "Integrated millimeter-wave wideband end-fire 5G beam steerable array and low-frequency 4G LTE antenna in mobile terminals," *IEEE Transactions on Vehicular Technology*, vol. 68, no. 4, pp. 4042–4046, 2019.
[163] R. Rodriguez-Cano, S. Zhang, K. Zhao, *et al*., "mm-Wave beam-steerable endfire array embedded in a slotted metal-frame LTE antenna," *IEEE Transactions on Antennas and Propagation*, vol. 68, no. 5, pp. 3685–3694, 2020.
[164] J. Kurvinen, H. Kähkönen, A. Lehtovuori, *et al*., "Co-designed mm-wave and LTE handset antennas," *IEEE Transactions on Antennas and Propagation*, vol. 67, no. 3, pp. 1545–1553, 2019.
[165] IFIXIT, "iPhone 12 and 12 pro teardown," Accessed at: https://www.ifixit.com/Teardown/iPhone+12+and+12+Pro+Teardown/137669, 2021. (in Chinese)
[166] H. Li, M. Wu, Y. B. Cheng, *et al*., "Leaky-wave antennas as metal rims of mobile handset for mm-wave communications," *IEEE Transactions on Antennas and Propagation*, vol. 69, no. 7, pp. 4142–4147, 2021.
[167] R. S. Malfajani, F. B. Ashraf, and M. S. Sharawi, "A 5G enabled shared-aperture, dual-band, in-rim antenna system for wireless handsets," *IEEE Open Journal of Antennas and Propagation*, vol. 3, pp. 1013–1024, 2022.
[168] B. Yu, K. Yang, C. Y. D. Sim, *et al*., "A novel 28 GHz beam steering array for 5G mobile device with metallic casing application," *IEEE Transactions on Antennas and Propagation*, vol. 66, no. 1, pp. 462–466, 2018.
[169] J. Jung, W. Lee, G. Lee, *et al*., "Ultra-thinned metasurface-embedded smartphone antenna-in-package for millimeter-wave 5G/6G coverage enhancement," *IEEE Transactions on Antennas and Propagation*, vol. 71, no. 10, pp. 7766–7781, 2023.
[170] J. Park, J. Choi, and W. Hong, "Systematically integrated phased-array antenna configuration to enhance beam coverage efficiencies of millimeter-wave 5G mobile devices," in *Proceedings of 2020 International Workshop on Antenna Technology*, Bucharest, Romania, pp. 1–4, 2020.
[171] S. Islam, M. Zada, and H. Yoo, "Highly compact integrated sub-6 GHz and millimeter-wave band antenna array for 5G smartphone communications," *IEEE Transactions on Antennas and Propagation*, vol. 70, no. 12, pp. 11629–11638, 2022.
[172] X. H. Ding, Q. H. Zhang, W. W. Yang, *et al*., "A dual-band antenna for LTE/mmWave mobile terminal applications," *IEEE Transactions on Antennas and Propagation*, vol. 71, no. 3, pp. 2826–2831, 2023.

[173] J. F. Zhang, Y. J. Cheng, Y. R. Ding, *et al*., "A dual-band shared-aperture antenna with large frequency ratio, high aperture reuse efficiency, and high channel isolation," *IEEE Transactions on Antennas and Propagation*, vol. 67, no. 2, pp. 853–860, 2019.

[174] M. Ikram, E. Al Abbas, N. Nguyen-Trong, *et al*., "Integrated frequency-reconfigurable slot antenna and connected slot antenna array for 4G and 5G mobile handsets," *IEEE Transactions on Antennas and Propagation*, vol. 67, no. 12, pp. 7225–7233, 2019.

[175] "Huawei mate 60 phone," Available at: https://consumer.huawei.com/cn/phones/mate60/.

[176] "Iridium-9505a phone," Available at: https://www.satellitephone-store.com/catalog/sale/details/iridium-9505a-satellite-phone-kit-1.

[177] "Linearly polarized satellite communication antenna," Available at: https://www.2j-antennas.com/antennas/gnss.

[178] "Linyun YT1100 satellite phone," Available at: https://item.jd.com/100043776921.html.

[179] "Wide beam omnidirectional CP antenna," Available at: https://item.jd.com/10076573657150.html.

[180] W. J. Liao, J. T. Yeh, and S. H. Chang, "Circularly polarized chip antenna design for GPS reception on handsets," *IEEE Transactions on Antennas and Propagation*, vol. 62, no. 7, pp. 3482–3489, 2014.

[181] S. H. Chang and W. J. Liao, "A novel dual band circularly polarized GNSS antenna for handheld devices," *IEEE Transactions on Antennas and Propagation*, vol. 61, no. 2, pp. 555–562, 2013.

[182] L. Y. Qu, Z. Zahid, H. H. Kim, *et al*., "Circular polarized ground radiation antenna for mobile applications," *IEEE Transactions on Antennas and Propagation*, vol. 66, no. 5, pp. 2655–2660, 2018.

[183] L. Y. Qu and H. Kim, "A novel single-feed dual-element antenna using phase compensation and magnitude regulation to achieve circular polarization," *IEEE Transactions on Antennas and Propagation*, vol. 66, no. 10, pp. 5098–5108, 2018.

[184] H. Y. Piao, G. H. Dong, and L. Y. Qu, "Circularly polarized antenna using ground-mode tuning technique for small-sized IoT devices," *Journal of Electromagnetic Waves and Applications*, vol. 33, no. 8, pp. 1042–1051, 2019.

[185] X. P. Zhang, K. P. Wei, Y. Li, *et al*., "A polarization reconfigurable antenna for satellite communication in foldable smartphone," *IEEE Transactions on Antennas and Propagation*, vol. 71, no. 12, pp. 9938–9943, 2023.

[186] Z. Y. Cao, L. Chang, Y. Li, *et al*., "Compact mobile terminal antenna With Endfire Circularly polarized beam for satellite communications," *IEEE Transactions on Antennas and Propagation*, vol. 71, no. 12, pp. 9980–9985, 2023.

[187] L. Sun and H. Wang, "Circularly-polarized antenna design in mobile phones by the combination of common and differential modes," in *Proceedings of the ICMMT*, 2023.

[188] S. S. Rao and Y. Wang, "Shared-aperture design of the cellular antenna and satellite communication antenna with circular polarization in S-band for metal-bezel smartphones," *IEEE Transactions on Antennas and Propagation*, vol. 72, no. 5, pp. 3938–3949, 2024.

[189] S. Rao and Y. Wang, "Design of octa-band mobile antenna with a wide end-fire beam in S-band for 4G LTE and satellite communication in metal-bezel smartphone," *IEEE Trans. Antennas Propag*., in press.

[190] X. W. Zhao, "Internal PIFA performance evaluations for a satellite-terrestrial handset," *Microwave Journal*, vol. 53, no. 8, article no. 84,86,88,90,92, 2010.

[191] L. Sun, L. Ke, and H. Wang, "An electronic device," *Patent*, 117117470, CN, 2023-11-24. (in Chinese)

[192] R. Khan, A. A. Al-Hadi, and P. J. Soh, "Recent advancements in user effect mitigation for mobile terminal antennas: A review," *IEEE Transactions on Electromagnetic Compatibility*, vol. 61, no. 1, pp. 279–287, 2019.

[193] H. Varheenmaa, A. Lehtovuori, P. Ylä-Oijala, *et al*., "Low-SAR back cover mobile antenna," *IEEE Open Journal of Antennas and Propagation*, vol. 3, pp. 1154–1160, 2022.

[194] R. Luomaniemi, A. Lehtovuori, J. Ilvonen, *et al*., "Extremely low-profile tunable multiport handset antenna," *IEEE Transactions on Antennas and Propagation*, vol. 70, no. 2, pp. 911–921, 2022.

[195] M. Ali Jamshed, T. W. C. Brown, and F. Héliot, "Dual antenna coupling manipulation for low SAR smartphone terminals in talk position," *IEEE Transactions on Antennas and Propagation*, vol. 70, no. 6, pp. 4299–4306, 2022.

[196] H. H. Zhang, G. G. Yu, Y. Liu, *et al*., "Design of low-SAR mobile phone antenna: Theory and applications," *IEEE Transactions on Antennas and Propagation*, vol. 69, no. 2, pp. 698–707, 2021.

[197] H. H. Zhang, G. G. Yu, X. Z. Liu, *et al*., "Low-SAR MIMO antenna array design using characteristic modes for 5G mobile phones," *IEEE Transactions on Antennas and Propagation*, vol. 70, no. 4, pp. 3052–3057, 2022.

[198] Y. X. Fang, Y. Liu, Y. T. Jia, *et al*., "5G SAR-reduction MIMO antenna with high isolation for full metal-rimmed tablet device," *IEEE Transactions on Antennas and Propagation*, vol. 70, no. 5, pp. 3846–3851, 2022.

[199] H. Y. Wang, "Analysis of electromagnetic energy absorption in the human body for mobile terminals," *IEEE Open Journal of Antennas and Propagation*, vol. 1, pp. 113–117, 2020.

[200] Z. S. Xu and Y. Wang, "Design of dual-band antenna for metal-bezel smartwatches with circular polarization in GPS band and low wrist effect," *IEEE Transactions on Antennas and Propagation*, vol. 71, no. 6, pp. 4651–4662, 2023.

[201] Z. S. Xu and Y. Wang, "Design of triple-band antenna for metal-bezel smartwatches with circular polarization in both GPS L5/L1 bands," *IEEE Transactions on Antennas and Propagation*, vol. 72, no. 3, pp. 2926–2931, 2024.

[202] H. C. Huang, Y. Wang, and J. Luo, "Analysis and design of compact and high-performance ear-bar TWS earphone antenna with characteristic mode analysis," *IEEE Transactions on Antennas and Propagation*, vol. 71, no. 9, pp. 7091–7101, 2023.

[203] R. Luomaniemi, P. Yla-Oijala, A. Lehtovuori, *et al*., "Designing hand-immune handset antennas with adaptive excitation and characteristic modes," *IEEE Transactions on Antennas and Propagation*, vol. 69, no. 7, pp. 3829–3839, 2021.

[204] H. H. Zhang, X. Z. Liu, G. S. Cheng, *et al*., "Low-SAR four-antenna MIMO array for 5G mobile phones based on the theory of characteristic modes of composite PEC-lossy dielectric structures," *IEEE Transactions on Antennas and Propagation*, vol. 70, no. 3, pp. 1623–1631, 2022.

[205] H. H. Zhang, L. F. Gong, X. Z. Liu, *et al*., "Design of low-SAR and high on-body efficiency tri-band smartwatch antenna utilizing the theory of characteristic modes of composite PEC-lossy dielectric structures," *IEEE Transactions on Antennas and Propagation*, vol. 71, no. 2, pp. 1913–1918, 2023.

[206] H. Li, M. Wu, W. C. Li, *et al*., "Reducing hand effect on mobile handset antennas by shaping radiation patterns," *IEEE Transactions on Antennas and Propagation*, vol. 69, no. 8, pp. 4279–4288, 2021.

Yan Wang received the B.S. degree (Hons.) in electronic information science and technology from the University of Electronic Science and Technology of China, Chengdu, China, in 2011, and the Ph.D. degree in electronic engineering from Tsinghua University, Beijing, China, in 2016. In September 2016, he joined Huawei Technology Ltd., Shanghai, China, as a Senior Antenna Engineer. In January 2020, he joined VIVO Shanghai Research Center, Shanghai, China, as an Antenna Director and Antenna Expert. Since February 2021, he has been with Fudan Uni-

versity, where he is currently a tenure-tracked Associate Professor. His current research interests include antenna theory and design, especially the antenna technology for mobile devices, base stations, and radar. Dr. Wang serves as an Associate Editor for *IET Electronic Letters*, and a reviewer for *IEEE Transactions on Antennas and Propagation* and *IEEE Antennas and Wireless Propagation Letters*.
(Email: yanwang_fd@fudan.edu.cn)

Libin Sun received the B.S. degree from Xidian University, Xi'an, China, in 2016, and the Ph.D. degree in electronic engineering from Tsinghua University, Beijing, China, in 2021.

Since 2021, he has been selected for the Huawei Top Minds Project and is currently working for the Device Business Group, Huawei Technologies Co. Ltd., Shanghai, as an Antenna Expert and Team Leader. He has authored or co-authored over 20 academic papers and applied for over 30 international and Chinese patents. His current research interests include antenna design and electromagnetic theory, particularly in mobile phone antennas, MIMO antennas, antenna decoupling techniques, satellite antennas, millimeter-wave antennas, and the interaction between antennas and the human body. Dr. Sun was a recipient of the Elsevier World Top 2% Scientist Award in 2023, ESI Highly Cited Papers Award, Top Reviewer Award for *IEEE Transactions on Antennas and Propagation* in 2019/2021/2022/2023, the Honorable Mention in 2020 IEEE AP-S Student Paper Competition, the Principal Scholarship (Highest Honor) of Tsinghua University in 2020, and the Top Ten Patent Award of Huawei Device Business Group in 2024. He currently serves as the Associate Editor of *IET Electronics Letters* and actively contributes to more than 25 international academic journals as a reviewer, such as the *IEEE Transactions on Antennas and Propagation*, *IEEE Transactions on Microwave Theory and Techniques*, *IEEE Transactions on Vehicular Technology*, *IEEE Transactions on Components, Packaging and Manufacturing Technology*, *IEEE Internet of Things Journal*, *IEEE Sensors Journal*, *IEEE Antennas and Wireless Propagation Letters*, *IEEE Open Journal of Antennas and Propagation*, *IEEE Access*, *IET Microwaves*, *Antennas & Propagation*, *Electromagnetic Science*, etc.
(Email: sunlibin0624@163.com)

Zhengwei Du received the B.S., M.S. and Ph.D. degrees from the University of Electronic Science and Technology of China, Chengdu, China, in 1992, 1995 and 1998, respectively. Since 1998, he has been with Tsinghua University, Beijing, China, as a Postdoctoral Fellow (February 1998 to October 1999), Research Assistant (November 1999 to July 2000), Associate Professor (August 2000 to December 2006), and currently, Full Professor. His main research interests include antennas, propagation, and electromagnetic compatibility / electromagnetic interference (EMC/EMI).
(Email: zwdu@tsinghua.edu.cn)

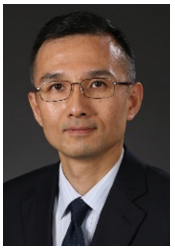

Zhijun Zhang received the B.S. and M.S. degrees from the University of Electronic Science and Technology of China, Chengdu, China, in 1992 and 1995, respectively, and the Ph.D. degree from Tsinghua University, Beijing, China, in 1999. In 1999, he was a Postdoctoral Fellow with the Department of Electrical Engineering, The University of Utah, Salt Lake City, UT, USA, where he was appointed as a Research Assistant Professor, in 2001. In May 2002, he was an Assistant Researcher with the University of Hawaii at Manoa, Honolulu, HI, USA. In November 2002, he joined Amphenol T&M Antennas, Vernon Hills, IL, USA, as a Senior Staff Antenna Development Engineer and was then promoted to the position of Antenna Engineer Manager. In 2004, he joined Nokia Inc., San Diego, CA, USA, as a Senior Antenna Design Engineer. In 2006, he joined Apple Inc., Cupertino, CA, USA, as a Senior Antenna Design Engineer and was then promoted to the position of Principal Antenna Engineer. Since August 2007, he has been with Tsinghua University, where he is a Professor in the Department of Electronic Engineering. He is the author of *Antenna Design for Mobile Devices* (Wiley, first edition 2011, second edition 2017). Dr. Zhang served as an Associate Editor for *IEEE Transactions on Antennas and Propagation* (2010–2014) and *IEEE Antennas and Wireless Propagation Letters* (2009–2015).
(Email: zjzh@tsinghua.edu.cn)